

UNIVERSITÀ DI PISA
DOTTORATO DI RICERCA IN INGEGNERIA DELL'INFORMAZIONE

A PORTABLE, INTELLIGENT, CUSTOMIZABLE DEVICE
FOR HUMAN BREATH ANALYSIS

DOCTORAL THESIS

Author
Danila Germanese

Tutor (s)

Prof. Luigi Landini
Prof. Francesco Marcelloni
Dott. Ovidio Salvetti

Reviewer (s)

Prof. Dermot Diamond
Prof. Claudia Manfredi
Prof. Ruggero Micheletto

The Coordinator of the PhD Program

Prof. Marco Luise

Pisa, May 2018

XXX Cicle

"Considerate la vostra semenza:
fatti non foste a viver come bruti,
ma per seguir virtute e canoscenza"

Dante Alighieri, La Divina Commedia, Inferno, Canto XXVI

Acknowledgements

THE time to write these phrases of thanksgiving has come. It means that three long and intense years have passed. It has been a period of hard work and intense learning, both from a scientific and personal standpoint.

For this purpose, firstly I would like to express my sincere gratitude to my tutors. Thanks to Prof. Francesco Marcelloni for his time, patient and his useful support. I Would thank Prof. Luigi Landini for his helpful suggestions and advice. To Dr. Ovidio Salvetti, I am grateful for the continuous support, for every encouragement and immense knowledge. His guidance helped me in all the time of research and writing of this thesis.

Besides my tutors, I would also thank the coordinator of the PhD Program, prof. Marco Luise, who impeccably guided us, his PhD students, in this three years.

My sincere thanks to my external reviewers Prof. Dermot Diamond, Prof. Claudia Manfredi and Prof. Ruggero Micheletto. Thank you in advance for your time, your precious suggestions and comments.

A special thanks to Dr. Mario D'Acunto, who have guided and supported me since the beginning of this work. Thank for encouraging my work and for helping me to grow as a researcher.

I am also grateful to Dr. Maurizia Brunetto, Director of Hepatology Unit of the University Hospital of Pisa, and her staff, Dr. Veronica Romagnoli and Dr. Antonio Salvati in particular. You gave me the opportunity to add value to my reasearch. Your knowledge, your expertise and your kindness have been invaluable.

My thanks also goes to SEMEOTICONS group, and in particular to Dr. Sara Colantonio (Project Coordinator), Dr. Giuseppe Coppini (Scientific Coordinator), Dr. Aurora Morales (Clinical Coordinator) and Dr. Emanuele Pagliei (COSMED s.r.l.) for giving

me the precious opportunity to join their team. Thank you for your ideas, for stimulating discussion, and for your invaluable suggestions. Without your collaboration it would not be possible to conduct this research.

Ringraziamenti

IL momento di scrivere queste parole di ringraziamento è arrivato. Ciò significa che tre anni di duro lavoro sono passati. Sono stati tre anni intensi, di continuo apprendimento, non solo dal punto di vista scientifico ma anche a livello personale.

A questo proposito, desidero innanzitutto esprimere la mia sincera gratitudine ai miei supervisori.

Ringrazio il Prof. Francesco Marcelloni per la sua disponibilità, la sua gentilezza e il suo valido supporto.

Grazie al Prof. Luigi Landini per i suoi preziosi suggerimenti e consigli.

Al Dott. Ovidio Salvetti vanno i miei ringraziamenti per il continuo supporto, scientifico e morale, che mi ha guidato in tutte le fasi del lavoro di ricerca e nella scrittura di questa Tesi.

Oltre ai miei supervisori, desidero ringraziare anche il Coordinatore del PhD Program, il Prof. Marco Luise, che ha ci ha accompagnato e guidato in maniera impeccabile in questo percorso.

La mia più sincera gratitudine va ai miei revisori, il Prof. Dermot Diamond, la Prof.ssa Claudia Manfredi e il Prof. Ruggero Micheletto. Grazie in anticipo per aver la vostra disponibilità, e per il tempo prezioso che dedicherete alla revisione di questo manoscritto.

Un ringraziamento speciale al Dott. Mario D'Acunto, che mi ha accompagnata e supportata fin dall'inizio del mio lavoro di ricerca. Grazie per il tuo punto di vista sempre ottimista, per i tuoi consigli, e per avermi aiutato a crescere come ricercatrice.

Ringrazio di cuore la Dott.ssa Maurizia Brunetto, primario dell' Unità Operativa di Epatologia dell' Azienda Ospedaliero Universitaria Pisana e tutto il suo staff, la Dott.ssa Veronica Romagnoli e il Dott. Antonio Salvati in particolare, per avermi dato l'opportunità di collaborare con loro e dare un ulteriore valore aggiunto al mio lavoro

di ricerca. Di valore inestimabile la vostra disponibilità, la vostra gentilezza e la vostra competenza.

I miei ringraziamenti vanno a tutto il partenariato del progetto europeo SEMEOTI-CONS, ed in particolare alla Dott.ssa Sara Colantonio (coordinatrice del progetto), al Dott. Giuseppe Coppini (coordinatore scientifico), alla Dott.ssa Aurora Morales (coordinatrice clinica) e al Dott. Emanuele Pagliei (di COSMED s.r.l.) per avermi dato l'opportunità di essere parte del loro team. Grazie per avermi fornito molteplici spunti di riflessione e punti di vista, nonchè preziosi consigli. Senza di voi tutto questo non sarebbe stato possibile.

Desidero inoltre ringraziare tutti i colleghi del Laboratorio Segnali e Immagini del CNR di Pisa, che hanno, in un modo o in altro, condiviso con me questo percorso. A Massimo Magrini, Paolo Paradisi e Marco Righi, parte del Wize Sniffer team di SEMEOTICONS, grazie infinite per il vostro prezioso contributo e supporto, specialmente nelle fasi iniziali di questo lavoro. Ho imparato molto da voi e per questo ve ne sono grata.

Al Dott. Antonio Benassi va un ringraziamento speciale per aver creduto in me sin da subito. Grazie per la gentilezza, per la disponibilità, per il sostegno ed i preziosi consigli, sempre mirati. E' stato, in questi anni, e sarà, per me, un punto di riferimento.

A Claudia Caudai, Sara Colantonio (che ho già ringraziato prima in quanto vera Boss di SEMEOTICONS), Daniela Giorgi (Mara!) e Mariantonietta Pascali: che dire? Facciamo che innanzitutto vi ringrazio, di vero cuore, per avermi supportata e sopportata! E poi, mi faccio un augurio: *da grande*, mi auguro di essere...voi. Mi auguro di avere la resilienza e la forza di Claudia, la sensibilità e il coraggio di Sara, la sicurezza e la determinazione di Daniela, la passione e la positività di Mariantonietta.

Davide, Gabriele, Marchino, Tampe: Il mio Dottorato non sarebbe stato lo stesso senza di voi. Ma questo lo sapete già, no? Anche nelle giornate più grigie e tempestose, mi avete strappato una risata. Grazie per avermi reso tutto più leggero, e per aver smorzato con la vostra... come definirlo... ironia (?) le mie più sferzanti polemiche!

Non posso, infine, non essere grata a Riccardo Leone, Massimo Martinelli, Francesca Pardini per il supporto tecnico.

Last but not least (mai!): i miei amici, i miei genitori, mia sorella e la mia famiglia. A tutti i miei amici con i quali ho conviso le immense soddisfazioni che riserva un Dottorato di Ricerca, ma anche i giorni più difficili: grazie mille.

Non sarei andata molto lontano, poi, senza il costante appoggio e supporto dei miei genitori, di mia sorella Gaia e di mia nonna. Insieme a voi e grazie a voi ho raggiunto quest'altro traguardo, o nuovo punto di partenza.

Antonio, compagno di vita, a te va il mio ringraziamento più grande. Mi hai saputo incoraggiare, consolare, lodare, rimproverare. Ma, se vogliamo, i consigli più preziosi me li hai dati silenziosamente: la passione che metti nel tuo di lavoro, la tua tenacia, la tua testardaggine, il tuo saperti rialzare dopo una caduta, il tuo non arrenderti sono stati per me linfa, e più significativi di mille parole. Grazie.

Summary

BREATH analysis allows for monitoring the metabolic processes that occur in human body in a non-invasive way. Comparing with other traditional methods such as blood test, breath analysis is harmless to not only the subjects but also the personnel who collect the samples.

However, despite its great potential, only few breath tests are commonly used in clinical practice nowadays. Breath analysis has not gained a wider use yet. One of the main reasons is related to standard instrumentation for gas analysis. Standard instrumentation, such as gas chromatography, is expensive and time consuming. Its use, as well as the interpretation of the results, often requires specialized personnel. E-nose systems, based on gas sensor array, are easier to use and able to analyze gases in real time, but, although cheaper than a gas chromatograph, their cost remains high.

During my research activity, carried on at the Signals and Images Laboratory (SiLab) of the Institute of Information Science and Technology (ISTI) of the National Research Council (CNR), I design and developed the so called *Wize Sniffer (WS)*, a device able to accurately analyze human breath composition and, at the same time, to overcome the limitations of existing instrumentation for gas analysis.

The idea of the *Wize Sniffer* was born in the framework of SEMEiotic Oriented Technology for Individual's CardiOmetabolic risk self-assessmeNt and Self-monitoring (SEMEOTICONS, www.semeoticons.eu) European Project, and it was designed for detecting, in human breath, those molecules related to the noxious habits for cardio-metabolic risk. The clinical assumption behind the *Wize Sniffer* lied in the fact that harmful habits such as alcohol consumption, smoking, unhealthy diet cause a variation in the concentration of a set of molecules (among which carbon monoxide, ethanol, hydrogen, hydrogen sulfide) in the exhaled breath. Therefore, the goal was to realize a portable and easy-to-use device, based on cheap electronics, to be used by anybody at their home.

The main contributions of my work were the following:

- design and development of a portable, low cost, customizable, easy to use device, able to be used in whichever context of use: I succeeded in this with using cheap commercial discrete gas sensors and an Arduino board, wrote the software and

calibrated the system;

- development of a method to analyze breath composition and understand individual's cardio-metabolic risk; I also validated it with success on real people.

Given such good outcomes, I wanted the *Wize Sniffer* took a further step forward, towards the diagnosis in particular. The application field regarded the chronic liver impairment, as the studies which involve e-nose systems in the identification of liver disease are still few. In addition, the diagnosis of liver impairment often requires very invasive clinical test (biopsy, for instance).

In this *proof-of-concept* study, the *Wize Sniffer* showed good diagnosis-oriented properties in discriminating the severity of liver disease (absence of disease, chronic liver disease, cirrhosis, hepatic encephalopathy) on the base of the detected ammonia.

Sommario

L'ANALISI dell' espirato permette di identificare l'impronta metabolica di un individuo, la quale può contenere preziose informazioni sul suo stato di salute. Il punto forte dell'analisi dell' espirato è la sua non invasività: rispetto alle tecniche diagnostiche standard, spesso invasive (basti pensare all'analisi del sangue), questa metodica è priva di rischi sia per il soggetto che viene sottoposto al test, sia per chi preleva il campione di esalato. Tuttavia, nonostante il suo grandissimo potenziale, sono pochi i *breath test* comunemente utilizzati nella pratica clinica. Purtroppo, l'analisi dell' espirato non vede ancora un'ampia diffusione in ambito clinico-diagnostico. Tra le ragioni principali, c'è quella legata alla strumentazione standard. Lo strumento considerato *gold standard* per l'analisi dei gas, e quindi anche dell' espirato umano, è la gas cromatografia. Essa è una tecnica molto costosa sia in termini di denaro che di tempo richiesto per l'analisi di ciascun campione. Inoltre, l'utilizzo di tale strumentazione, come anche l'interpretazione dei risultati, è appannaggio di personale esperto. I nasi elettronici, basati su array di sensori di gas, sono più semplici da utilizzare e permettono di analizzare i gas in tempo reale. Il loro costo, seppur inferiore a quello di un gas cromatografo, rimane tuttavia, in molti casi, elevato.

L'obiettivo della mia attività di ricerca (condotta presso il Laboratorio Segnali e Immagini, SiLab, dell' Istituto di Scienza e Tecnologie dell' Informazione, ISTI, del Consiglio Nazionale delle Ricerche, CNR) è stato quello di progettare e sviluppare il *Wize Sniffer*, un dispositivo in grado di analizzare la composizione dell' esalato umano superando i limiti dello stato dell'arte.

L'idea del *Wize Sniffer* è nata nell'ambito del progetto europeo SEMEOTICONS (SEMEiotic Oriented Technology for Individual's CardiOmetabolic risk self-assessmeNt and Self-monitoring, www.semeoticons.eu), per monitorare le abitudini nocive per il rischio cadio-metabolico mediante l'analisi della composizione dell' espirato. L'ipotesi clinica alla base del *Wize Sniffer* è che abitudini dannose quali assunzione di alcol, fumo, dieta squilibrata, provocano una variazione nelle concentrazioni di molecole quali etanolo, monossido di carbonio, idrogeno, acido solfidrico, presenti nel nostro esalato. I principali contributi del mio lavoro di Tesi sono stati i seguenti:

- progetto e sviluppo di un dispositivo portatile, a basso costo, dal design modulare,

facile da utilizzare e adattabile a diversi contesti di utilizzo;

- sviluppo di un metodo per la valutazione del rischio cardio-metabolico del soggetto a partire dall'analisi della composizione del suo esalato.

Visti i risultati raggiunti, ho infine cercato di capire se, da strumento di *auto-monitoraggio dello stile di vita*, il *Wize Sniffer* possa essere spinto verso la diagnosi. Il campo di applicazione è quello della malattia di fegato, dal momento che sono ancora pochi gli studi che sfruttano l'analisi dell'esalato, e i nasi elettronici in particolare, per la diagnosi delle epatopatie croniche. Inoltre, per la diagnosi dell'epatopatia sono molto spesso richiesti test diagnostici invasivi (biopsie, ad esempio).

Da questo studio di fattibilità sono emerse buone proprietà diagnostiche del *Wize Sniffer* nel discriminare i diversi stadi della malattia di fegato (assenza di malattia, epatopatia cronica, cirrosi, encefalopatia epatica) sulla base dell'ammoniaca rilevata.

List of publications

International Journals

1. Colantonio, S., Coppini, G., Germanese, D., Giorgi, D., Magrini, M., Marraccini, P., Martinelli, M., Morales, A., Pascali, M.A., Raccichini, G., Righi, M. and Salvetti O. (2015, October). A Smart Mirror to Promote a Healthy Lifestyle. *Biosystems Engineering*. (Vol. 138, pp. 33-43). Elsevier.
2. Germanese, D., Righi, M., Benassi, A., D'Acunto, M., Leone, R., Magrini, M., Paradisi, P., Puppi, D. and Salvetti O. (2017, January). A Low Cost, Portable Device for Breath Analysis and Self-monitoring, the Wize Sniffer. *De Gloria A. (eds) Applications in Electronics Pervading Industry, Environment and Society. ApplePies 2016. Lecture Notes in Electrical Engineering*. (Vol. 409, pp. 51-57).
3. Henriquez, P., Matuszewski, B.J., Andreu-Cabedo, Y., Bastiani, L., Colantonio, S., Coppini, G., D'Acunto, M., Favilla, R., Germanese, D. et al. (2017, July). Mirror mirror on the wall... an unobtrusive intelligent multisensory mirror for well-being status self-assessment and visualisation. *IEEE Transactions on Multimedia*. (Vol. 19, pp. 1467-1481)
4. Germanese, D., D'Acunto, M., Magrini, M., Righi, M. and Salvetti O. (2017, August). Cardio-metabolic Diseases Prevention by Self-monitoring the Breath. *Sensors and Transducers Journal*. (Vol. 215, pp. 19-26)
5. Germanese, D., D'Acunto, M., Righi, M., Magrini, M. and Salvetti O. (2017). The Wize Sniffer Knows What You Did: Prevent Cardio-Metabolic Risk by Analyzing Your Breath. *Int. J. on Advances in Life Sciences*. (Vol. 9, pp. 198-207)

International Conferences/Workshops with Peer Review

1. D'Acunto M., Benassi A., Chiellini F., Germanese D., Ishak R., Magrini M., Pagliei E., Paradisi P., Righi M. and Salvetti O. (2014, March). Wize Sniffer: a new portable device for selective olfaction. *Proceeding of BIOSTEC 2014 - 7th*

-
- International Joint Conference on Biomedical Engineering Systems and Technologies. Special Session SUPERHEAL 2014 (Angers, France, 3-6 March 2014). (pp. 577 - 582)*
2. Andreu-Cabedo Y., Castellano P., Colantonio S., Coppini G., Favilla R., Germanese D., Giannakakis G., Giorgi D., Larsson M., Marraccini P., Martinelli M., Matuszewski B., Milanic M., Pascali M., Padiaditis M., Raccichini G., Randeberg L., Salvetti O. and Stromberg T. (2015, July). Mirror mirror on the wall. . . an intelligent multisensory mirror for well-being self-assessment. *Proceeding of ICME 2015 - International Conference on Multimedia and Expo (Turin, Italy, 29 June - 3 July 2015), IEEE*
 3. Colantonio S., Germanese D., Moroni D., Giorgi D., Pascali M. A., Righi M., Coppini G., Morales M., Chiarugi F., Padiaditis M., Larsson M., Stromberg T., Henriquez P., Matuszewski B. J., Milanic M. and Randeberg L. (2015, October). SEMEOTICONS – reading the face code of cardio-metabolic risk. *Proceeding of IWCIM 2015 - International Workshop on Computational Intelligence for Multimedia Understanding (Prague, Czech Republic, 29-30 October 2015), IEEE*
 4. Germanese D., D’Acunto M. and Salvetti O. (2016, February). Design of a breath analysis device for self-monitoring and remote health-care. *Proceeding of BIOSTEC 2016 - 9th International Joint Conference on Biomedical Engineering Systems and Technologies - Doctoral Consortium (Roma, Italy, 21-23 February 2016). (pp. 9 - 14.) SciTePress.*
 5. Germanese D., Righi M., Magrini M., Guidi M., D’Acunto M. and Salvetti O. (2016, July). A device for self-monitoring breath analysis. *Proceeding of SENSORDEVICES 2016 - The Seventh International Conference on Sensor Device Technologies and Applications (Nice, France, 24-28 July 2016). (pp. 77 - 82) IARIA.*
 6. Germanese D., D’Acunto, M., Magrini M., Righi M. and Salvetti O. (2017, May). A Low Cost Technology-based Device for Breath Analysis and Self-monitoring. *Proceeding and Best Paper Award of SIGNAL 2017- The Second International Conference on Advances in Signal, Image and Video Processing (Barcellona, Spain, 21-25 May 2017).(pp. 8 - 13). IARIA.*
 7. Germanese D., D’Acunto, M., Magrini M., Righi M. and Salvetti O. (2017, May). Self-monitoring the Breath for the Prevention of Cardio-metabolic Risk. *Proceeding of SENSORDEVICES 2017- The Eighth International Conference on Sensor Devices Technologies and Applications (Rome, Italy, 9-14 September 2017).(pp. 96 - 101). IARIA.*

Others

1. D’Acunto M. and Germanese D. (2014). Wize Sniffer 1.0: development of a new portable device designed for selective olfaction. *Technical report.*
2. Germanese, D., Benassi, A., D’Acunto, M., Leone, R., Magrini, M., Paradisi, P., Righi, M. and Salvetti O. (2015). A low cost and portable device for home care breath sensing. *Technical report.*

-
3. D'Acunto M., Germanese D., Magrini M., Paradisi P., Righi M., Pagliei E. and Gimeno M. (2015) SEMEOTICONS - Gas sensors for breath analysis. *SEMEiotic Oriented Technology for Individual's CardioMetabolic risk self-assessmeNt and Self-monitoring. Project Report.*
 4. D'Acunto M., Germanese D., Magrini M., Paradisi P., Puppi D., Righi M., Pagliei E. and Gimeno M. (2015) SEMEOTICONS - Design and integration of the Wise Sniffer. *SEMEiotic Oriented Technology for Individual's CardioMetabolic risk self-assessmeNt and Self-monitoring. Project Report.*
 5. Colantonio S., Germanese D., Righi M., Martinelli M., Coppini G., Morales M., Chiarugi F., Padiaditis M., Stromberg T., Randeberg L. and Vitali I. (2015) SEMEOTICONS - Revised specification of system requirements and functionalities. *SEMEiotic Oriented Technology for Individual's CardioMetabolic risk self-assessmeNt and Self-monitoring. Project Report.*
 6. Colantonio S., Germanese D., Martinelli M., Righi M., Coppini G., Chiarugi F., Padiaditis M., Stromberg T., Bjorgan A., Henriquez P., Matuszewski B. J., Nicoletta A., Vitali I., Miliarakis A. and Assimakopoulou C. (2015) SEMEOTICONS - Final specification of system requirements and functionalities. *SEMEiotic Oriented Technology for Individual's CardioMetabolic risk self-assessmeNt and Self-monitoring. Project Report.*
 7. Colantonio S., Giorgi D., Germanese D., Pascali M. A., Coppini G. and Favilla R. (2015) SEMEOTICONS - Data analysis and fusion strategies. *SEMEiotic Oriented Technology for Individual's CardioMetabolic risk self-assessmeNt and Self-monitoring. Project Report.*
 8. Germanese, D., Righi, M., D'Acunto, M., Chiellini, F., Guidi, M., Magrini, M., Paradisi, P., and Puppi, D. (2015). Criticality of human breath detection with a portable device I: nanotechniques for improving sensing materials. *Technical report.*
 9. Germanese, D., Righi, M., D'Acunto, M., Magrini, M., Paradisi, P. and Guidi, M. (2016). Criticality of human breath detection with a portable device II: data analysis. *Technical report.*
 10. Righi, M., Germanese, D., Magrini, M., D'Acunto, M., Paradisi, P. and Guidi, M. (2016). Criticality of human breath detection with a portable device III: integration with other devices for health care and self-monitoring. *Technical report.*
 11. Germanese, D., Righi, M., D'Acunto, M., Magrini, M., Paradisi, P. and Guidi, M. (2016). Towards the Wise Sniffer 1.1: a functional gas sensor for breath analysis. *Technical report.*
 12. Benassi, A., Germanese, D., Magrini, M., Martinelli, M., Reggiannini, M., Righi, M. (2016). Sistema di monitoraggio, prevenzione e allarme in acqua e in aria. *Technical report.*
 13. Banterle F., Barsocchi P., Candela L., Carlini E., Carrara F., Cassarà P., Ciancia V., Cintia P., Dellepiane M., Esuli A., Gabrielli L., Germanese D., Girardi M.,

Girolami M., Kavalionak H., Lonetti F., Lulli A., Moreo Fernandez A., Moroni D., Nardini F. M., Monteiro De Lira V. C., Palumbo F., Pappalardo L., Pascali M. A., Reggiannini M., Righi M., Rinzivillo S., Russo D., Siotto E. and Villa A. (2016) *ProgettISTI 2016. Technical report.*

14. Martinelli M., Germanese D., Pascali M. A., Mazzarisi A., Henriquez P. and Vitali I. (2016) SEMEOTICONS - Software Integration and Wize Mirror user manual. *SEMEiotic Oriented Technology for Individual's CardioMetabolic risk self-assessment and Self-monitoring. Project Report.*

Contents

1	Introduction	1
1.1	Contributions	3
2	Why analyse the breath?	6
2.1	Introduction	6
2.2	Physiological basis of breath molecules	7
2.3	Current status of breath analysis in clinical practice	10
2.4	Techniques for breath analysis	13
2.4.1	Gas chromatography (GC)	14
2.4.2	Proton-transfer reaction-mass spectrometry (PTR-MS)	15
2.4.3	Laser adsorption spectroscopic- based approaches	15
3	Why electrify the...nose? Gas sensors and Electronic-nose systems for breath analysis	16
3.1	Introduction	16
3.2	Gas sensors	17
3.2.1	Conductivity sensors	18
3.2.2	Piezoelectric sensors	22
3.2.3	Optical sensors	23
3.2.4	Metal-oxide-semiconductor field-effect transistor (MOSFET) sensors	25
3.2.5	Electrochemical gas sensors	26
3.3	Gas sensors and e-noses for breath analysis	26
4	The Wize Sniffer	33
4.1	The aim of the research	33
4.2	Detected molecules	34
4.3	Hardware	36
4.3.1	The core of the WS: the gas sampling chamber and the gas sensor array	38
4.3.2	The corrugated tube, the heat and moisture filter and the flow-meter	47

Contents

4.3.3	The sampling pump and the CO_2 and O_2 gas sensors	49
4.3.4	The signal conditioning module and Arduino board	50
4.3.5	The final hardware configuration	50
4.4	Data processing	53
4.4.1	Data pre-processing	53
4.4.2	Data analysis	54
4.4.3	Data handling: development of a Graphical User Interface (GUI)	58
5	WS validation: self-monitoring the breath for the prevention of cardio-metabolic risk	61
5.1	Introduction	61
5.2	The data acquisition campaign	61
5.3	Results and discussion	64
6	Towards the diagnosis: detection of ammonia in the breath of patients suffering from liver impairment	67
6.1	Introduction	67
6.2	The liver disease and its progression: from chronic hepatitis to hepatic encephalopathy	68
6.3	The data acquisition campaign	69
6.4	Statistical data analysis and results	71
7	Conclusions	78
	Bibliography	80

CHAPTER 1

Introduction

Since the time of Hippocrates, medical practitioners have recognized that the presence of human diseases changes the odours released from the body and breath [1]: the fruity-smelling breath underlines the presence of diabetes; the stale beer-like odour of the skin is typical of the persons with tuberculosis; the butcher's – like smell of the skin suggests yellow fever, etc.

The modern breath analysis started in 1971, when Linus Pauling demonstrated that breath is a mixture of more than 200 volatile molecules at the levels of part per million (ppm), part per billion (ppb), or lower.

Human breath is composed of nitrogen (75%), oxygen (13%), water vapor (6%) and carbon dioxide (5%). The remaining 1% is composed of a series of volatile organic compounds (VOCs) that are produced endogenously as part of our normal (or disease-related) metabolism, travel via the blood, participate to alveolar exchanges, and are peculiar for each individual.

Therefore, it is correct to think that every one of us has his/her own breath-print, which can tell a lot about the state of health.

Breath analysis allows for monitoring the metabolic processes that occur in human body in a non-invasive way. Comparing with other traditional methods such as blood test, breath analysis is harmless to not only the subjects but also the personnel who collect the samples. A brief overview of breath analysis and its current status in clinical practice is reported in **chapter 2**.

However, despite its great potential, only few breath tests are commonly used in clinical practice nowadays. Breath analysis has not gained a wider use yet.

Some of the main reasons are:

- lack of standard procedures to collect breath sampling [2–5]. This inevitably leads to an incompatibility among breath data, which hardly can be shared among physi-

cians and scientists all over the world;

- presence of multiple influencing factors [6–10], such as surrounding air, respiration rate, heart rate, posture, etc., that lead to strong inter-variability and intra-variability of breath composition;
- lack of a one-to-one correlation between breath biomarkers and diseases. Many studies aimed at assessing the physiological basis of breath molecules [1, 3, 10–16], thus understanding their possible correlation with certain diseases. Nevertheless, the same VOC can be considered as biomarkers for two or more different diseases, as well as the same pathological condition may have many breath biomarkers.
- reasons related to standard instrumentation for gas analysis. Standard instrumentation, such as gas chromatography, is expensive and time consuming. Its use, as well as the interpretation of the results, often requires specialized personnel [6, 17]. E-nose systems, based on gas sensor array, are easier to use and able to analyse gases in real time, but, although cheaper than a gas chromatograph, their cost remains high. An overview of the existing gas sensing technologies and the current status of e-nose systems in clinical practice is reported in **chapter 3**.

Another important issue should be considered: the greater demands on improvements in effectiveness, speed, smartness and lower costs of biomedical instruments for daily healthcare applications [18], resulting from increasing limitations of healthcare financial resources as a consequence of budgetary cuts.

During my PhD program, my aim was to design and develop a device able to accurately analyse human breath composition and, at the same time, to overcome the limitations of existing instrumentation for gas analysis.

In this regard, my work was focused on the design and development of the so called *Wize Sniffer (WS)*, whose strengths were the following [19, 20]:

- ability to analyse a set of breath molecules in real time;
- modular and customizable design, in order to easily change the gas sensors according to the molecules to be detected;
- portability, in order to promote its use not only in laboratory settings, but also in home environment, for instance;
- use of low-cost technology, in order to encourage its purchase;
- ease of use, also for non-specialized personnel;

The idea of the *Wize Sniffer* was born in the framework of SEMEiotic Oriented Technology for Individual's CardiOmetabolic risk self-assessmeNt and Self-monitoring (SEMEOTICONS) European Project, and it was designed for detecting, in human breath, those molecules related to the noxious habits for cardio-metabolic risk.

The clinical assumption behind the *Wize Sniffer* lied in the fact that harmful habits such as alcohol consumption, smoking, unhealthy diet cause a variation in the concentration of a set of molecules (among which carbon monoxide, ethanol, hydrogen, hydrogen

sulfide) in the exhaled breath. The more dangerous the habits are, the larger the variations in breath composition and the higher the cardio-metabolic risk.

A description of my research activity, the developed technological approaches and the used data analysis methods are reported in **chapter 4**.

The *Wize Sniffer* is based on an array of six semiconductor-based gas sensors placed in a gas sampling box (subsection 4.3.1). Breath gases reach the gas sampling box by flowing through a plastic, corrugated tube. A heat and moisture (HME) filter, made of hygroscopic material, absorb the water vapor present in exhaled breath. A flow-meter allow for monitoring user's flow rate and for calculating user's exhaled volume (subsection 4.3.2). A sampling pump injects, at a fixed rate, the sampled exhaled gases to other two sensors which have faster response time and work in *flowing-regime* (subsection 4.3.3). In order to facilitate sensors recovery time, a flushing pump is placed on one side of sampling chamber. After each breath test, the pump can be switched on in order to "purge" the chamber with ambient air and recovery sensors baseline. A signal pre-conditioning module (subsection 4.3.4) stabilizes sensor raw signals and transfer them to the controller board, which executes a pre-processing of the data (subsection 4.4.1). A further processing step allows for understanding user's cardio-metabolic risk from the analysis of his/her breath composition (subsection 4.4.2).

1.1 Contributions

Despite its great potential, breath analysis is not widely used in clinical practice: the high costs for standard analytical instrumentation (i.e., gas chromatograph-mass spectrometer), the need for specialized personnel able to read the results and the lack of standardized protocols to collect breath samples, set limits to its exploitation. My goal was to realize the *Wize Sniffer* (WS), a portable light and simple device for breath analysis based on cheap electronics to be used by anybody at their home. I succeeded in this by using cheap commercial gas sensors an Arduino board, wrote the software, calibrated the system and tested it with success on real people.

The challenges I faced with were the followings:

- the design of the core of the *Wize Sniffer*. In particular,
 - The requirement of modularity led me to design a core composed of three distinct modules: an array of Taguchi semiconductor-based gas sensor housed in a gas sampling box, a pre-conditioning module and a widely employed open source controller, an Arduino Mega2560. The gas sampling box can be easily customized, by changing the gas sensors according to the volatile molecules to be detected. I programmed the board Arduino Mega2560 to execute a real-time pre-processing of sensors raw data: i) sensors output sampling, ii) humidity drift compensation, iii) feature extraction. Also, a monitoring of exhaled volume was implemented in order to evaluate the quality of each breath test.
 - The fundamental requirement of low-cost led me to use Taguchi gas sensors (<http://www.figaro.co.jp/en/>), which show long term stability and reproducibility, great chemical stability of the sensing material, short reaction and

recovery time. In addition, they are small, compact and inexpensive. On the other hand, they are affected by multiple factors, such as temperature, humidity, cross-sensitivity. The effect of each of them was taken into account, managed and countered: a heating voltage in the sensors measurement circuit was integrated, in order to keep them at a constant temperature; a filter, made of hygroscopic material, was integrated on *Wize Sniffer* mouthpiece, in order to absorb the majority of the water vapour present in exhaled breath, and a Sensirion SHT11 into the gas sampling box in order to monitor the variations in humidity into the box itself and compensate, during the data processing, the resulting sensors drift; finally, feature extraction and pattern recognition techniques allowed for counteracting sensors cross-sensitivity, whose mechanism remains difficult to be understood [21].

- the aim of making the *Wize Sniffer* able to be used in whichever context of use: in home environment, for instance, as a localized self-monitoring tool (from user's point of view), and, at the same time, as a remote monitoring tool (from medical doctor's point of view). The combination of a localized monitoring tool and data transmission methods may provide a means of extending the effective range within which medical doctors can provide services and offer clinical support. For this purpose, an Arduino Ethernet module was integrated in order to implement a Telnet Server and send breath data to a remote personal computer by means of an internet connection.
- with the view to developing an easy-to-use device, my idea was to provide the user with a clear, easily interpretable result not only by expert personnel. The clinical assumption behind the *Wize Sniffer* lied in the fact that the noxious habits for cardio-metabolic risk affect the breath composition causing a change in the concentration of a set of molecules. My idea was to exploit higher-order data reduction techniques and regressive methods¹ to make the *Wize Sniffer* able to understand user's cardio-metabolic risk on the base of his/her noxious habits identified by the analysis of his/her breath composition in a swift and computationally inexpensive way. Therefore, by means of such data analysis approach, the clinical assumption was confirmed. Not only, a relationship between breath composition and cardio-metabolic risk was found, beyond the state of art, and a clear, easily interpretable outcome was provided to the user [22, 23].

The technological and data analysis methods were validated by carrying on a data acquisition campaign which involved 169 subjects and which is described in (**chapter 5**).

To sum up, the main contributions were the following:

- **development of a portable, low cost, customizable, easy to use device, able to be used in whichever context of use;**
- **evaluation of individual's cardio-metabolic risk from the analysis of his/her breath composition.**

¹both implemented in MATLAB R2014a environment

Given the good outcomes from the validation campaign, I wanted the *Wize Sniffer* took a step forward, towards the diagnosis in particular. The application field regarded the chronic liver impairment, as the studies which involve e-nose systems in the identification of liver disease are still few. In addition, the diagnosis of liver impairment often requires very invasive clinical test (biopsy, for instance).

I carried on a *proof-of-concept* study, with 64 subject involved, in order to evaluate the discriminative, diagnosis-oriented properties of the *Wize Sniffer*. The aim was to detect ammonia in the breath of the subjects and evaluate the ability of the *Wize Sniffer* in discriminating the severity of liver disease (absence of disease, chronic liver disease, cirrhosis, hepatic encephalopathy) on the base of the detected ammonia. The study, the statistical data analysis and the future perspectives of the *Wize Sniffer* are described in **chapter 6**.

Chapter 7 concludes the Thesis: the contributions beyond the state of art are summarized, and the results are discussed.

CHAPTER 2

Why analyse the breath?

2.1 Introduction

The field of breath analysis is as old as the one of medicine. Since the time of Hippocrates, classical medicine has used the sense of smell as an indicator of human diseases [1]: the fruity-smelling breath underlined the presence of diabetes; the stale beer-like odour of the skin was typical of the persons with tuberculosis; the butcher's – like smell of the skin suggested yellow fever, etc. Therefore, early medical practitioners recognized that the presence of human diseases changed the odours released from the body and breath.

In 1784, for the first time, Lavoisier and Laplace identified the presence of carbon dioxide in human exhaled breath [24]. The foundations for the modern alcohol testing were laid by Anstie, which isolated, in 1874, ethanol from the breath. However, it is commonly recognized that the modern breath analysis started in 1971, when Linus Pauling demonstrated that breath is a mixture of more than 200 volatile molecules at the levels of part per million (ppm), part per billion (ppb), or lower [25].

For its unobtrusiveness and its inherent safety, breath analysis may play a key role in health care diagnostics. Breath analysis may be used to detect disease, monitor disease progression, or monitor a therapy. Comparing with other traditional methods such as blood test, breath analysis is non-invasive, real-time, and harmless to not only the subjects but also the personnel who collect the samples.

Human breath is composed of nitrogen (75%), oxygen (13%), water vapour (6%) and carbon dioxide (5%). The remaining 1% is composed of a series of volatile organic compounds (VOCs) that are peculiar for each individual. Therefore, it is correct to think that every one of us has his/her own breath-print, which can tell a lot about the state of health.

Breath is the product of the composition of inspiratory air, molecules deriving from

2.2. Physiological basis of breath molecules

ingested food and beverages or from dermal adsorption (exogenous molecules), and all the volatile substances in the blood which are produced endogenously as part of our normal (or disease-related) metabolism and participate to alveolar exchanges according to their types, concentrations, volatilities and rates of diffusion. In addition, also cells in the mouth, upper airways, and gastro-intestinal tract contribute volatile molecules to the breath.

The major VOCs in healthy subjects' breath are isoprene (12-580 ppb), acetone (1.2-1,880 ppb), ethanol (13-1,000 ppb), and other alcohols. Minor components include pentane, aldehydes and ketones [26].

Here, an overview of the studies that aimed to assess the biochemical pathways of breath molecules and their possible correlation with certain diseases is provided. In addition, a summary of the standard gas analysis techniques is reported.

2.2 Physiological basis of breath molecules

Many studies aimed at assessing the physiological basis of breath molecules, thus understanding their possible correlation with certain diseases. Table 2.1 summarizes some of the molecules present in human breath and also reports their typical concentrations.

Table 2.1: *Some of the molecules found in human breath and their typical concentrations.*

Molecule	Physiological basis	Concentration
Oxygen	Cellular metabolism	13.6%-16%.
Carbon dioxide	Cellular metabolism	4%
Acetone	Decarboxylation of acetoacetate	ppm
Carbon monoxide	Production catalyzed by heme oxygenase	2-4 ppm
Methane	Gut bacteria	ppm
Hydrogen	Gut bacteria	9.1-30ppm
Acetaldehyde	Ethanol metabolism	ppb
Pentane	Lipid peroxidation	ppb
Isoprene	Cholesterol biosynthesis	ppb
Ethane	Lipid peroxidation	ppb
Ethylene	Lipid peroxidation	ppb
Other hydrocarbons	Lipid peroxidation/metabolism	ppb
Nitric oxide	Production catalyzed by nitric oxide synthase	ppb
Carbon disulfide	Gut bacteria	ppb
Methanol	Metabolism of fruit	ppb
Carbonyl sulfide	Gut bacteria	ppb
Ammonia	Protein metabolism	ppb
Ethanol	Gut bacteria	ppb
Methanethiol	Methionine metabolism	ppb
Methylamine	Protein metabolism	ppb

Exhaled air has a decreased amount of **oxygen** (O_2) and an increased amount of **carbon dioxide** (CO_2). These amounts can be considered as a measure of the metabolism. They show how much oxygen is retained within the body for use by the cells and how much carbon dioxide is produced as a by-product of cellular metabolism [27]. In particular, carbon dioxide is produced as a waste product when energy is released during certain metabolic reactions of cellular respiration. As it moves from cells into surrounding body fluids and blood, most of the carbon dioxide reacts with water to form a weak acid (carbonic acid). This acid ionizes, releasing hydrogen ions (H^+) and bicarbonate

ions (HCO_3^-) which blood carries to the respiratory organs. There, the chemical reactions reverse, and carbon dioxide gas is produced, eventually to be exhaled.

An increase of CO_2 can be due to different factors, such as physical activity. There is a decrease in case of hypothermia, for instance. Also in presence of most forms of lung diseases and some forms of congenital heart disease (for example, cyanotic lesions that result in a bluish-grey discolouration of the skin and in a lack of O_2 in the body), there is a decrease of CO_2 exhaled. Also individual's breathing rate influences the level of CO_2 in blood and, as a consequence, in exhaled gas. Breathing that is too slow causes respiratory acidosis (that results in an increase of CO_2 partial pressure in blood, which may cause hypertension, build up of heart rate), while breathing that is too rapid leads to hyperventilation, which may cause respiratory alkalosis (that results in decrease of CO_2 in blood; so, it can no longer fulfill its role of vasodilator, resulting in arrhythmias, extra systoles). A way to monitor the carbon dioxide concentration (or partial pressure) is capnography. The max value of capnogram corresponds to the end of the tidal volume of exhaled breath and the steady-state concentration of each breath (see section 2.3).

Acetone is produced by hepatocytes via decarboxylation of excess Acetyl-CoA. Its high volatility makes it easily detectable in breath, urine and skin. Breath acetone increases in patients with uncontrolled diabetes mellitus. Other studies found higher level of breath acetone also in over-weighted and obese children with non-Alcoholic Fatty Liver Disease [1,3]. Acetone concentration in human breath can also be an indicator of congestive heart failure and cardiac index [11]. Given the several sources that can lead to a variation in breath acetone levels, it can hardly be considered as a biomarker for a single precise disease. Nonetheless, taking together with other standard clinical parameters, it can provide useful information about the individual's state of health.

Carbon monoxide (CO) is usually detected to assess smoking status [12]. CO in non-smokers is between 0.6 and 4.9 ppm (mean 2.1ppm); CO in smokers increases up to 30-40ppm. An increase of CO leads haemoglobin to carry less oxygen through the vessels, because CO usurps the space in haemoglobin that normally carries oxygen, forming carboxyhaemoglobin [28]. However, increased levels may be due also to airway inflammation in asthma and in chronic obstructive pulmonary disease (COPD) [13].

Hydrogen (H_2) is related to the carbohydrates breakdown in the oral cavity and in the intestine tract. Indeed, bacteria in the gut metabolize the carbohydrates to low-molecular species, such as carbon dioxide, alcohols and hydrogen, which are exhaled in the breath [12]. Hydrogen breath tests are used in order to evaluate lactose and fructose malabsorption syndromes and small intestinal bacterial overgrowth (SIBO). Higher levels of hydrogen was found also in coeliac patients [10]. Breath hydrogen levels vary within a day and from day to day; fasting levels range between 0.3 and 34.1ppm (mean 9.1ppm). Breath hydrogen concentration may decrease in case of hyperventilation. Cigarette smoke, in contrast, may increase its values [12].

Ethane and **pentane** are biomarker for oxidative stress. They are generated from $\omega 3$ and $\omega 6$ fatty acids respectively, which are the basic components of membrane cells. In vitro studies have demonstrated that ethane and pentane are generated when cell cultures are exposed to reactive oxygen species (ROS) [14]. Hydrocarbons show low solubility in blood, then they are exhaled within few minutes of their formation in tissues and may be useful to evaluate the oxidative damage in the body [3]. As per-

oxidation and other reaction of ROS are basic mechanisms of inflammatory processes, their values increase in patients with asthma, COPD, obstructive sleep apnoea and acute respiratory distress syndrome (ARDS). Also smoking causes a rise in value of breath ethane and pentane.

Isoprene is formed along the pathway of cholesterol synthesis [3]. Isoprene can be considered as a marker of cellular damage and cellular repair. Decreasing concentrations of isoprene can be found in patients with ARDS, due to some impairment of membrane repair mechanisms in alveolar cells. Analogue mechanism may occur in case of patients with chronic heart failure. Nevertheless, reduced breath isoprene may be due also to a reduced cardiac output in this patients. In [11] exhaled isoprene concentrations show a correlation with cardiac output. Isoprene has been studied also in other diseases, among which lung cancer [1]. In patients suffering from this disease breath isoprene levels show a decreased concentration. Breath isoprene is age dependent; in men is higher than in women.

Nitric Oxide (*NO*) is produced by different type of cells in the respiratory tract, such as inflammatory, epithelial, vascular endothelial cells and airways nerves [1]. *NO* modulates the endothelium vasodilatation. *NO* is an example of an exhaled biomarker which has reached clinical practice: by monitoring *NO* levels in breath, asthma can be diagnosed and managed. Higher level of *NO* were also found in patients with unstable COPD [13], which is characterized by a generalized inflammation that causes airways obstruction and breath shortness. Variation in breath *NO* were observed also in patients with cystic fibrosis, systemic sclerosis, hepatopulmonary syndrome and primary ciliary dyskinesia.

Concentrations of volatile **sulfur-containing compounds** in healthy subjects' blood are very low. The body uses sulfur compounds in order to neutralize the action of free radicals. Their levels increase in case of impairment of liver function. Among the sulfur-containing volatile molecules, hydrogen sulfide is considered as a vascular relaxant agent, as it has a therapeutic effect in various cardiovascular diseases [3].

Ammonia NH_3 is a metabolic product of amino-acids de-amination [3]. Its levels in healthy subjects' breath are 425-1800ppb (mean 960ppb). It is toxic in high concentrations, indeed it is converted in urea by the liver. In chronic liver impairment, significant levels of ammonia appear in the blood as the removal of ammonia through conversion to urea is compromised due to an impairment of liver function [15]. Elevated breath ammonia may be due also to uremia, which is an inability of the kidneys to effectively filter the blood, resulting in a build- up of nitrogen based compounds. It may be also correlated also to helicobacter Pylori.

Breath **ethanol** is commonly associated with alcoholic beverages intake. Nevertheless, ethanol may have other endogenous sources (even though ethanol concentrations in breath normally are lower than ethanol levels found in subjects' breath after alcoholic drinks ingestion). For instance, ethanol may derive from intestinal gut flora such as bacteria or fungi. In some studies ethanol was correlated also with obesity. Its levels in healthy subjects' breath are 0-3.9ppm (mean 0.62ppm) [16].

2.3 Current status of breath analysis in clinical practice

The previously cited study are just a small part of the widely documented works regarding breath analysis.

However, despite its great potential, only few breath tests (listed in Table 2.2 and referring to [6]) are commonly used in clinical practice nowadays. Breath analysis has not gained a wider use yet [6]. Some of the main reasons are as follows:

Table 2.2: *Breath tests commonly used in clinical practice.*

Detected breath molecule	Clinical application
carbon dioxide	capnography
carbon monoxide	neonatal jaundice
ethanol	blood ethanol levels (law enforcement)
hydrogen	detection of disaccharidase deficiency, evaluation of gastrointestinal transit time, monitoring of bacterial overgrowth, evaluation of intestinal stasis
nitric oxide	asthma therapy
hydrogen	detection of h. pylori infection

- Lack of standard procedures to collect breath sampling.
There are not standard guidelines to sample the breath. Standard protocols should be generated to make breath samples collected and analysed in different sites comparable. In practice, three methods of sampling are used [2, 3]:
 - alveolar (end-tidal) sampling: the expired gas is collected when the plateau of CO_2 capnogram is reached (see Figure 2.1). Such method is used if only systemic volatile biomarkers are to be assessed;
 - mixed expiratory air sampling: it corresponds to a whole breath sample, and it is used if substance concentrations in the airways are of interest;
 - time-controlled sampling, which corresponds to a part of exhaled air sampled after the start of expiration. Such method shows large variations of samples composition because of wide variations of individual breathing manoeuvres

However, a controlled identification of respiratory phases should be performed, especially to avoid dilution by dead space air in the case of mixed expiratory air or to prevent large variations in the case of time-controlled sampling.

Ideally, standard guidelines should be defined for the collection of single mixed-breath samples, for the collection and analysis of end-tidal breath samples, for methods of breath collection that involve breath holding, etc.

In [4] Salvo and co-workers present a prototype of breath sampler that is able to automatically collect end-tidal or dead space air fraction, even if the subject hyperventilates. The result is achieved by real time measurement of exhaled CO_2 and expiratory flow both during the inspiratory and expiratory phase. A suitable software allow for controlling a valve and for selecting the desired breath fraction.

In [5], Di Francesco and co-workers present a CO_2 -triggered breath sampler based on Fowler's method to distinguish pure dead space air and pure alveolar air. In 1948 Fowler defined dead space as the volume of conducting airway as far as

2.3. Current status of breath analysis in clinical practice

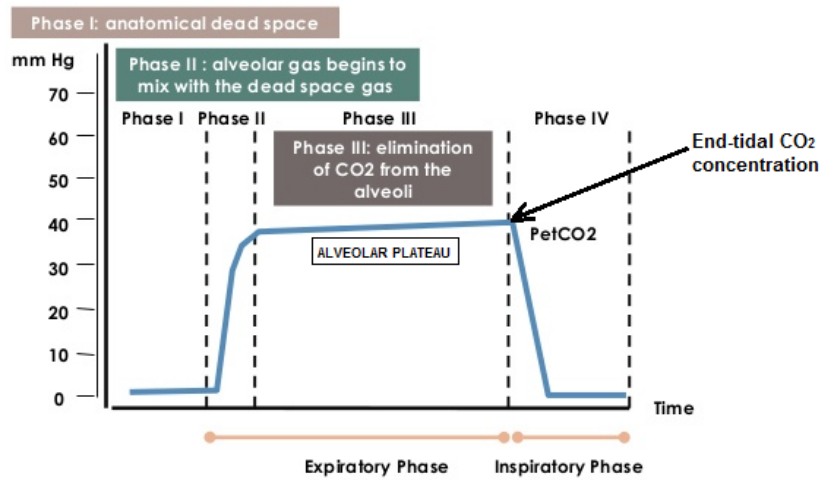


Figure 2.1: Capnography is the monitoring of the concentration or partial pressure of carbon dioxide in the respiratory gases. It is usually presented as a graph of expiratory CO_2 (measured in millimetres of mercury, "mmHg") plotted against time.

the location where a large change in gas composition occurs. He also proposed a method to identify it. Referring to the capnogram shown in Figure 2.1, in the expiratory phase, the volume of dead space air and alveolar air may be distinguished. According to Fowler's method, the volume for which the shaded areas *a* and *b* in the capnogram are equivalent (see Figure 2.2) represents the ideal transition point between dead space and alveolar air.

Once standard procedures will be defined, also standard units of measure and normal concentration ranges (as a function of gender for instance, or as a function of age) can be generated.

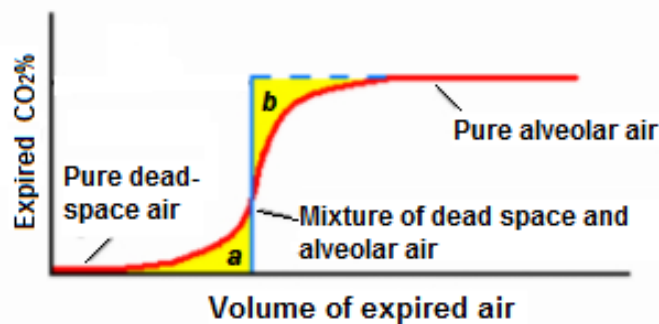


Figure 2.2: Fowler's method, as explained in [5].

- Presence of multiple influencing factors.
The definition of precise guidelines to collect breath sample would be useful also to avoid a series of factors that influence the breath composition such as:
 - Surrounding air [6, 7]: many molecules that have clinical relevance often are present also in ambient air. Currently there is not a standard method which

Chapter 2. Why analyse the breath?

provides for a subtraction of background air levels. This is due to the fact that there are no data regarding how long it takes for a subject to reach the steady state with environmental air. The lung take approximately 4 minutes, but the entire body may take hours or days according to the type of molecule. Influencing compounds may derive also from fragrances, cosmetic, cleaning agents, toothpaste.

- Volume of air inhaled before exhaling [7]: inhaling a high quantity of air before exhaling may dilute the alveolar air leading to a decrease in endogenous VOCs concentration.
- Respiration rate and heart rate [7, 8]: lower breathing flow rate allow the endogenous VOCs for better diffusing from the alveoli to the periphery of lungs and then from diffusing in exhaled air. Controlled breathing would prevent hyperventilation, which often occurs when the subjects are asked to breathe spontaneously.
- Posture [8, 9]: differences in pre-expiratory gas concentrations occur in the lungs and areas with different gas concentrations vary their contribution to the total expired gas. Gravitational gradient of pleural pressures may cause vertical differences in regional pre-expiratory gas concentrations, and, if vertically distributed lung regions empty sequentially and at a variable rate, gravity-determined differences in the distributions of inspired gases may cause changes in breath composition.
- Inter-variability and intra-variability [7, 8, 10]: VOCs concentrations vary depending on food intake, general health of subject, physical conditions. This suggests that intra- and inter- subject variability in exhaled VOCs is significant. Intra-individual variability may be also a consequence of several uncontrolled sampling-related parameters, such as exhalation flow rate, volume of exhalation, breath holding, etc. [7].

As an example of inter-variability, Table 2.3 (from [8]) shows variations in some biomarkers according to the gender. Men, for instance, exhales higher levels of carbon monoxide and sulfur-containing molecules compared with women. Also pregnancy may also be responsible for a breath profile alterations [29].

What is shown in Figure 2.3 (from [8]) can be considered as both an example of inter-variability and an example of intra-variability. Breath ethanol shows variation not only among the study subjects, but also for each individual, before and after lunch.

Table 2.3: Gender differences in biomarkers. Values are means \pm SD. A value of $p < 0.05$ was considered to be statistically significant

Molecule	Women	Men	p-value
Oxygen, %	97.7 \pm 0.5	96.5 \pm 0.8	0.004
Carbon monoxide, ppm	3.0 \pm 0.5	4.0 \pm 0.7	0.01
Sulfur-containing molecules, ppb	94.8 \pm 29.2	135.0 \pm 24.6	0.016
Nitric oxide, ppb	28.4 \pm 29.9	26.8 \pm 22.3	not significant

- Lack of a one-to-one correlation between breath biomarkers and diseases. In order to assess the physiological meaning of each breath molecule and exploit

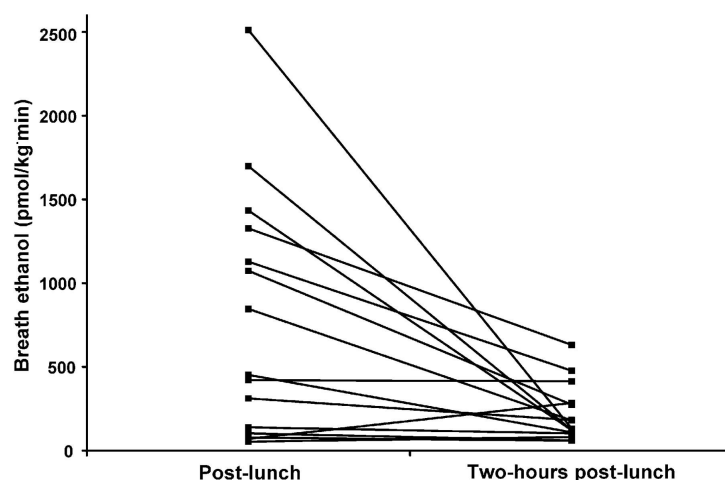


Figure 2.3: Breath ethanol concentrations collected from subjects directly after lunch and 2 h after lunch. In 13 of 16 subjects, breath ethanol concentrations increased during the post-lunch period and decreased 2 h after lunch.

its potential as a disease biomarker, the biochemical pathways of generation must be known. Unfortunately, biochemical pathways have been investigated only for a small number of VOCs [3]. Moreover, the same VOC can be considered as biomarkers for two or more different diseases, as well as the same pathological condition may have many breath biomarkers.

- Reasons related to standard instrumentation.
Standard instrumentation, such as gas chromatography (GC, which is described in more detail in the section 2.4), is expensive, time consuming, bulky. Its use, as well as the interpretation of the results, often requires specialized personnel [6,17]. These issues discourage the enthusiasm for clinical applications of breath analysis.

As W. Miekisch and his colleagues wrote in [3], “introducing breath analysis into clinical practice will be the challenge of today and tomorrow”.

Success will occur only with a strong cooperation among experts from different fields: engineers, instrument makers, clinicians, breath analysis experts, chemists.

2.4 Techniques for breath analysis

Several techniques are employed to detect gaseous molecules. They can be categorized into three main group:

- Methods based on gas chromatography coupled with mass-spectrometry (GC-MS), or other MS-based approaches;
- Laser adsorption spectroscopic- based approaches;
- Chemical sensors.

Here, the first two techniques are briefly described. A separate chapter (chapter 3), will be dedicated to the gas sensors and their use in clinical field.

2.4.1 Gas chromatography (GC)

Gas chromatography is the most common method employed to analyse human breath composition, usually in combination with flame ionization detection (FID) or MS, or ion-mobility spectrometry, (IMS). A gas chromatographic system includes:

- A regulated carrier gas source, which moves the sample through the GC. The carrier gas must be pure: contaminants may react with the sample or the column, create spurious peaks, etc.
- An inlet, which works at 200 °C, acts as a vaporizer for liquid samples. The inlet introduces the vaporized sample into the carrier gas stream. The most common inlets are injection ports and sampling valves.
- A column, in which the time separation occurs. Since the column type is selected by the user, many different analyses can be performed using the same equipment. Most separations are highly temperature-dependent, so the column is placed in a well-controlled oven.
- A detector, which responds to the components as they occur by changing its electrical output. The output from the detector becomes the chromatogram.
- Data interpretation. The list of times and sizes must be converted to component names and amounts. This is done by comparison to times and responses of known samples (calibration samples).

The sample is injected onto the head of the column. Separation in the column can be performed by exploiting different detection systems:

- **Thermal conductivity (TCD):** it operates on thermal conductivity differences. All gases conduct heat, but hydrogen and helium are the best thermal conductors. When one of these is used as the carrier gas, anything else that may be present causes a decrease in the thermal conductivity of the gas stream. This change can be measured and used to create a chromatogram.
- **Flame ionization (FID):** it responds to everything that creates ions in a flame, that means, all organic compounds. In fact, GC-FID is one of the most widely used system for human breath analysis [30]. The carrier gas from the column mixes with hydrogen and is burned in air. The FID uses two electrodes, one of which is often the jet where the flame burns, and a polarizing voltage to collect the ions from the flame. When a component appears, the collected current rises. After amplification, the current creates the chromatogram. In [31] Phillips and Greenberg assessed exhaled endogenous isoprene by using a GC-FID.
- **Electron capture (ECD):** A radioactive isotope, usually ^{63}Ni , in the detector cell emits beta particles. These collide with carrier gas to create showers of low energy free electrons. Two electrodes and a polarizing voltage collect the electrons as a current. Some molecules can capture low-energy electrons to form negative ions. When such a molecule enters the cell, some of the electrons are captured and the collected current decreases. After processing, this signal creates the chromatogram.

- **Mass selective (MSD):** it identifies components from mass spectra; its principles relies on the difference in mass-to-charge ratio (m/z). When combined with GC, it is the most powerful identification tool able to identify the separated species, as for instance in [32].

2.4.2 Proton-transfer reaction-mass spectrometry (PTR-MS)

PTR-MS is a promising technique for breath analysis as it allows for on-line and multiple measurements [30]. In addition, it does not requires pre-concentration and/or separation of breath samples.

PTR-MS principle relies on protonation of the chemical species, coming from a transfer from protonated water. A PTR-MS instrument consists of an ion source that is directly connected to a drift tube and an analysing system (quadrupole mass analyser or time-of-flight mass spectrometer). Almost all VOC's have proton affinities greater than water, hence there is complete transfer. In fact, the technique is particularly advantageous for breath analysis as large volumetric contributions from N_2 , O_2 , CO_2 and water do not interfere with measurement. Like MS, species identification is done purely on an m/z ratio.

Commercially available PTR-MS instruments have a response time of about 100ms and reach a detection limit in the single digit part-per- trillion (ppt) region, as described in [10]. Nevertheless, PTR-MS characterized molecules on the base of their m/z ratio, without any chemical identification. This problem can be overcome by coupling a PTR-MS system with a GC.

2.4.3 Laser adsorption spectroscopic- based approaches

It is a high resolution technique which allow for detecting specific molecular species at very low concentrations. In addition, gases can be measured in real time and without the need for pre-concentration or any sort of sample pre-treatment [30]. The gas sample is interrogated by a laser beam, which can be absorbed by the molecular species of interest. The detector measures the absorbed amount of laser radiation, thus quantifying the gas concentration.

Why electrify the...nose? Gas sensors and Electronic-nose systems for breath analysis

3.1 Introduction

Faster and cheaper than a gas chromatograph – mass spectrometer, e-nose systems may overcome the shortcomings of the standard technologies for gas sensing.

The term "electronic nose" was introduced in the scholarly literature in the early 1980s [33], when Persaud and Dodd developed the first e-nose in 1982. In August 1991, an advanced research workshop was organized in Reykjavik, Iceland, which accelerated interest in the field.

Since then, this kind of devices attempts to emulate the human olfactory system by using an array of gas sensors and a specific signal processing [34, 35]. In Figure 3.1, adapted from [34], the working principle of an electronic nose is represented.

In a typical electronic nose, the chemical input typically is sampled through a tube into a small chamber housing the electronic sensor array. The tube may be made of plastic or stainless steel. Then, the gas sensors behave as olfactory receptors. The sensor array consists of two or more sensors with partially overlapping sensitivities. Their number depend on the volatile molecules to be detected. The odour sample causes a reversible physical and/or chemical change in sensors' sensing material, which result in electrical signals. Interface electronics performs an analogue to digital conversion of such signals and a first pre-conditioning and pre-processing. Due to the nature of the partially overlapping sensitivity of the gas sensors, pattern recognition techniques are usually used for gas molecules discrimination. The most common pattern recognition techniques aim to emulate olfactory cortex. They include principal component analysis (PCA), feature weighting, artificial neural network (ANN), cluster analysis, classification algorithms, and discriminant function analysis.

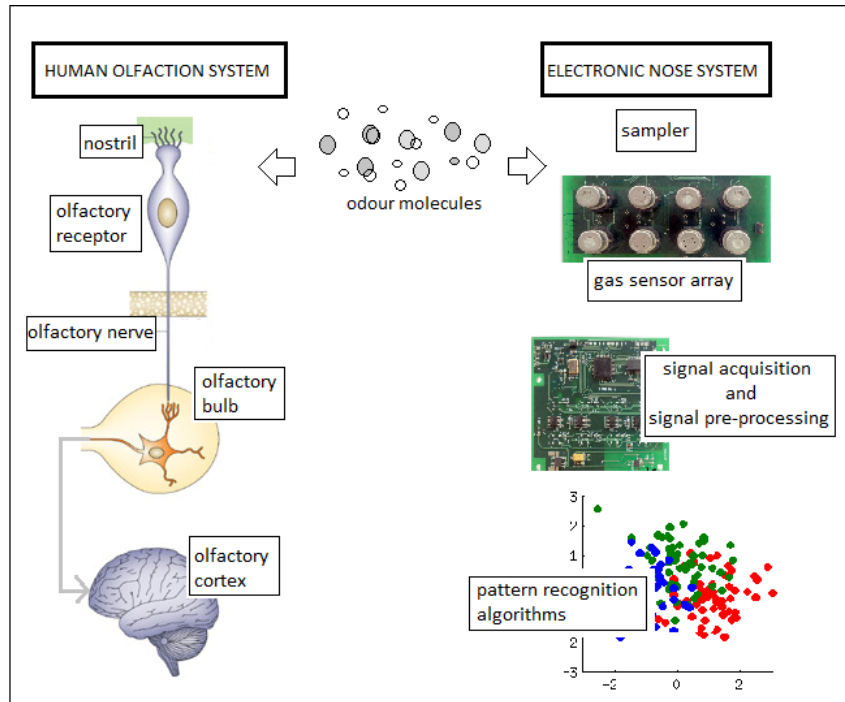


Figure 3.1: How e-nose device attempt to mimicry human olfactory system.

The output of an electronic nose may be the identity of the odorant, an estimate of the concentration of the odorant, or the characteristic properties of the odour as might be perceived by a human [33]. What is important is that the pattern of response across the sensors is distinct for different odorants. The pattern of response across all sensors in the array is used to identify and/or characterize the odour

Finally, a washing gas (such as N_2) is applied to the array for a few seconds to a minute, so as to remove the odorant mixture from the surface and bulk of the sensor's sensing material.

The period during which the odorant is applied is called the response time of the sensor array. The period during which the washing and reference gases are applied is termed the recovery time.

In this Section, the main gas sensing techniques are described. In addition, the state of art of e-noses in clinical field is reported.

3.2 Gas sensors

Gas molecules interact with gas sensors' sensing element causing a physical and/or chemical change, which is measured as an electrical signal. In Figure 3.2 the main physical changes are listed, as well as the related type of gas sensors, according to the classification reported in [36].

In general, gas sensors' response to odorants is considered as a first order time response. When a gas sensor is exposed to a gas, a rise in its output signal occurs, until the sensor reaches a chemical balance with the gas molecules, which corresponds to the plateau in sensor output. When the odorant is flushed out, the output signal returns to

Chapter 3. Why electrify the...nose? Gas sensors and Electronic-nose systems for breath analysis

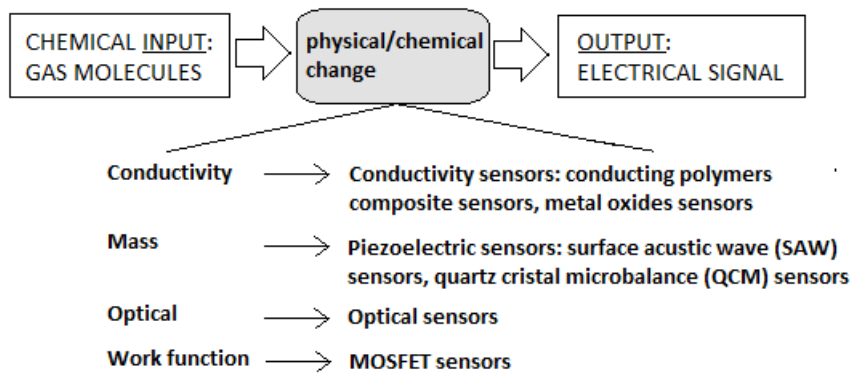


Figure 3.2: The main gas sensors' transduction principles.

its baseline value (see Figure 3.3, adapted from [36]).

Here, we describe some peculiar aspects of the classes of sensors listed in Figure 3.2.

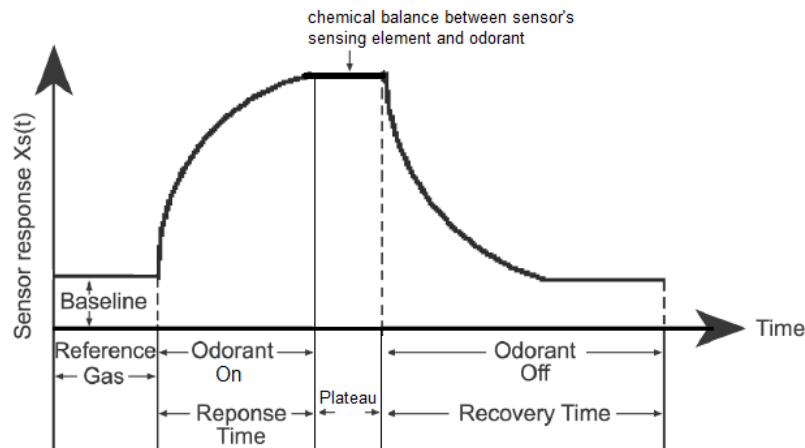


Figure 3.3: Typical gas sensors' output.

3.2.1 Conductivity sensors

They are based on the principle that a change in the properties of the sensing material causes a variation in resistance of the sensor. Figure 3.4 (adapted from [36]) shows a schematic configuration of such type of sensors. The sensing material is placed over the electrodes, through which the variation in resistance is measured. When metal oxides are used as sensing material, very high temperatures are required for making metal oxides-based sensors work correctly. As a consequence, a heater is integrated. Conducting polymer composites, intrinsically conducting polymers and metal oxides are three of the most used classes of sensing materials in conductivity sensors.

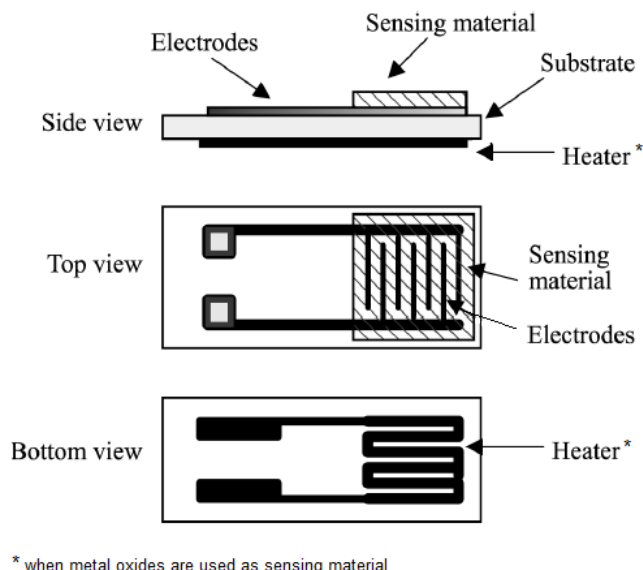


Figure 3.4: Schematic configuration of conductivity gas sensors.

- Conducting polymer composites sensors:** they are based on conductive particles (such as polypyrrole) sprinkled in an insulating polymer matrix [37]. When the sensor is exposed to an odorant, some of the gas, by penetrating the polymer matrix, causes an expansion of the matrix itself. Such expansion of the polymer film reduces the conductive pathways for the charge carriers, thus causing a rise in polymer's electrical resistance.

Response times may vary from few seconds to minutes. The response time depends on several factors, among which: i) rate of diffusion of the vapour into the polymer, ii) nature of polymer, iii) thickness of the polymer film, iv) concentration of gas, v) the partial pressure of the gas at the gas-polymer interface, vi) effects of fillers and temperature [38]. An important factor for the optimization of polymer composites sensor response is the relationship between gas solubility coefficient in the polymer and sensor geometry [39]. For instance, gases with high solubility coefficient have higher affinity to sensors with smaller area. As a consequence, by decreasing the sensor area, the sensitivity towards particular compounds can be improved.

This type of sensors exhibit linear response for several analytes, and also high discrimination can be achieved due to a variety of polymeric materials. In addition, conducting polymer composites sensors show a good repeatability. They are also inexpensive and easy to be manufactured. They can work in conditions of high relative humidity. The signal conditioning circuitry is relative simple (only a resistance is needed).

On the other hand, they are affected by ageing (due to oxidation of the polymer), which causes drift;

- Intrinsically conducting polymers:** they have linear backbones composed of unsaturated monomers, which can be doped as semiconductors or conductors [36]. Polypyrrole, polyaniline, polythiophene are example of conducting polymers. The

Chapter 3. Why electrify the...nose? Gas sensors and Electronic-nose systems for breath analysis

doping of these materials generates charge carriers and alters their band structures, thus increasing the mobility of holes or electrons according to the type of doping (p-doping or n-doping). When the sensor is exposed to odorant, the volatile molecules are absorbed into the polymer matrix, thus causing swelling and altering the electron density on the polymeric chains [37]. As explained for the conducting polymer composites sensors, also in this case sensor's response depends on the diffusion rate of the odorant into the polymer matrix. In general, response times may vary from seconds to minutes [36]. This type of sensors work at room temperature; they have good response to a variety of analytes. Fast responses and rapid recovery times occur in case of polar compounds. On the other hand, poorly understood signal transduction mechanisms, high sensitivity to humidity [37], drift, aging (due to oxidation of the polymer) and difficulties in manufacturing discourage from using such type of sensors;

- **Metal oxides (MOS) sensors:** They have been used more extensively in electronic nose device and are widely available commercially [33, 39]. Popular sensing materials include SnO_2 , TiO_2 , ZnO , In_2O_3 , and WO_3 . In Figure 3.5 the traditional method in the preparation of a SnO_2 sensor is shown.

The gas/semiconductor surface interactions occur at the grain boundaries of the

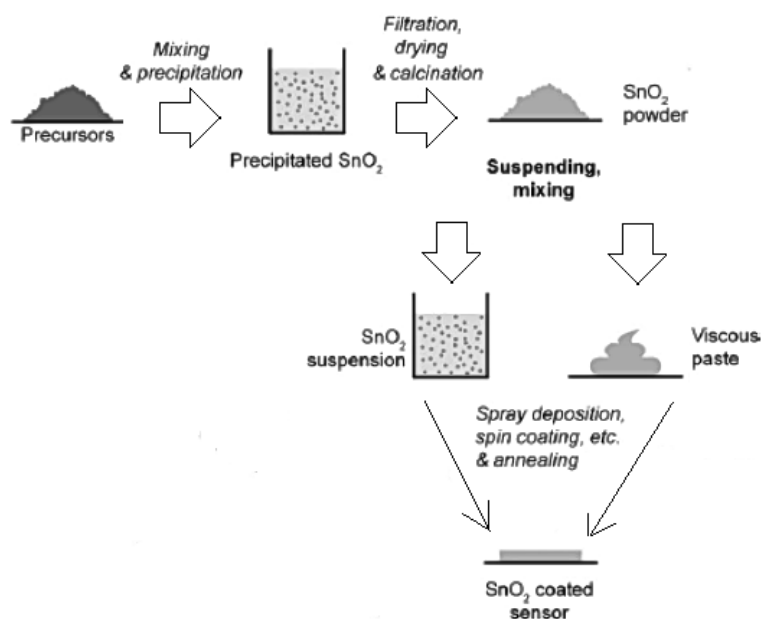


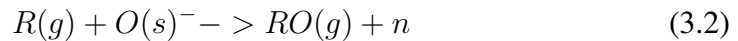
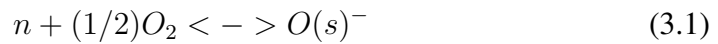
Figure 3.5: Preparation of SnO_2 sensor.

polycrystalline oxide film [40]. They generally include reduction/oxidation processes, adsorption of the chemical species directly on the semiconductor and/or adsorption by reaction with surface states associated with pre-adsorbed ambient oxygen, electronic transfer of delocalized conduction-band electrons to localized surface states and vice-versa, catalytic effects and in general complex surface chemical reactions between the different adsorbed chemical species.

The change in conductance of the oxide is generally proportional to gas concentration. It is a reversible process. The change in the electrical resistance of the

sensor can be explained by the formation of depletion space-charge layers at the surface and around the grains, with upwards bending of the energy bands.

Metal oxides-based gas sensors can be distinguished into n-type and p-type. The n-type sensors respond to reducing gases (such as hydrogen, carbon monoxide, hydrogen sulfide), which react with oxygen and release electrons. In particular, upon exposure to oxygen, the oxygen is chemisorbed onto lattice vacancies in the semiconductor as described in eq. 3.1 (where n is an electron from the conduction band) and in Figure 3.6a). The loss of electrons results in a decrease in conductance and a depletion layer is formed. When the sensor is exposed to an odorant, R , the adsorbed oxygen reacts and is removed from the surface allowing the electrons to flow back into the conduction band. This lowering of the potential barrier and the consequent flow of electrons, leads to a decrease in resistance and a rise in conductivity (eq. 3.2 and Figure 3.6b)).



On the contrary, p-type sensors respond to oxidizing gases (such as oxygen, ni-

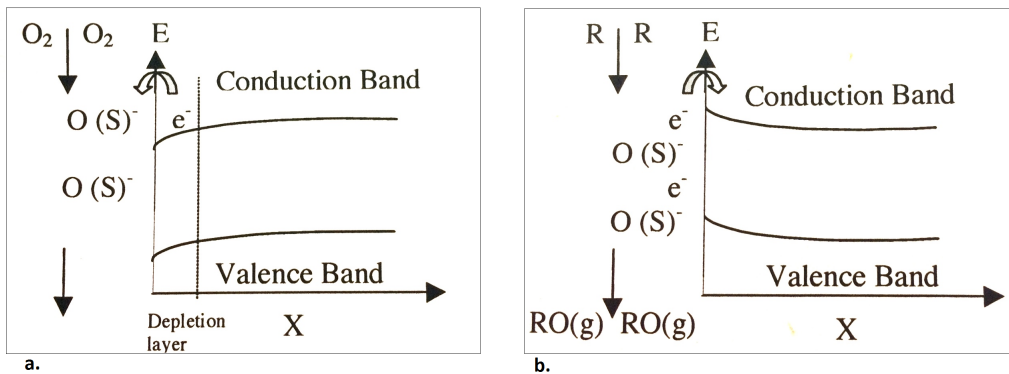


Figure 3.6: Chemical reaction to the boundaries of semiconductor material.

tric oxides), which remove electrons and produce holes, thus producing charge carriers and increasing resistance [36]. The sensitivity of such type of gas sensors depends on the film thickness and on the operating temperature (typically 200-500 °C). Thinner films are more sensitive, but they lead to a quicker sensor saturation, thus reducing sensitivity range. Sometimes catalytic metals are applied on top of oxides (for instance, SnO_2 sensors doped with Cu) in order to improve sensitivity to particular compounds. Typical sensitivities are between 5-500ppm [33]. Metal oxides sensors' response times tend to be very fast: they can reach steady-state in less than 7sec [36]. Indeed, the main advantages of this type of sensors are their fast response and recovery times. In addition they are small, easy to be integrated into the circuitry (that allows to combine in the same device the functions of a sensitive element and control electronics.), relatively inexpensive and easy to be manufactured.

Disadvantages in the use of these sensors are: the need for a heating circuit, poor reproducibility, long-time instability due to ageing which results in a drift of sensor's response (long-time instabilities are of considerable importance for the prac-

tical use of the sensor; pre-ageing thermal treatments and cycle calibration checks have to be carried out in order to avoid the wrong use of the device); non-linear behaviour, it means, the change in sensor response due to a defined change in gas concentration depends generally on the concentration of the gas to be monitored and also on the concentration of other gases (cross-sensitivity effect).

The sensors also respond to water vapour, and, more specifically, to humidity variations [33]. Unfortunately, sensor/water vapour interaction leads to an increase in the sensor's electrical conductance and to a lack of selectivity. Materials with enhanced performance with respect to relative humidity variations have been found: chromium oxide is an example [39].

3.2.2 Piezoelectric sensors

When such type of gas sensors are exposed to a vapour, a change in mass of the piezoelectric coating occurs, due to gas adsorption, resulting in a change in the resonant frequency.

There are two type of piezoelectric sensors that are used in gas sensing: the surface acoustic wave (SAW) sensors, and the quartz crystal microbalance (QCM) sensors.

- **Surface acoustic wave sensors:** They are composed of a sensing membrane placed between an input (emitting) and output (receiving) inter-digital transducers [36]. An alternating current is applied across the input transducer and create a wave which travel along the sensor's surface at an operating frequency between 100 and 400MHz. The interaction between the sensor's sensing membrane and a compatible volatile compound causes an increase in the membrane's mass, which results in a shift of the wave frequency, according to eq. 3.3:

$$\Delta f = \Delta f_p * c_v * K_p / \rho_p \quad (3.3)$$

Where Δf_p is the change in frequency, c_v is the vapor concentration, K_p is the partition coefficient and ρ_p is the density of the used polymer membrane [36, 37]. Sensor sensitivity is defined as ρ_p /ppm of volatile molecule. Polymer-coated SAW sensors have very low detection limits (0.7-4ppm) [36, 37].

Indeed, in general SAW sensors are very sensitive and can detect a broad set of VOCs due to the many types of available sensing coatings. In addition, they have fast response times.

On the other hand, they suffer from poor signal to noise ratio and the circuitry required for their functioning is very complex and expensive [36].

- **Quartz crystal microbalance sensors:** Their working principle is similar to the one of SAW sensors: when the sensing membrane (deposited onto the surface of the piezoelectric quartz crystal) interacts with a compatible analyte, its mass increases, resulting in a shift in three-dimensional wave's resonance frequency (which is normally between 10-30MHz [36]). In this case, the generated wave travels along the entire bulk of the crystal. Higher frequencies and smaller surface area of sensing elements results in a rise in sensitivity.

Such type of gas sensors have high sensitivity for organic vapours and are very selective. In addition, they have fast response times (10sec). Their disadvantages include complex fabrication processes, complex interface circuitry and poor signal-to-noise ratio.

3.2.3 Optical sensors

Many volatile molecules exhibit strong absorption in UV/visible, near infrared (IR) or mid-infrared regions of the electromagnetic spectrum. The absorption lines or bands are specific to each chemical species: this forms the basis for their detection and measurement in the case of optical gas sensing.

Optical gas detection using absorption spectroscopy is based on the application of Lambert-Beer law (eq. 3.4) [41]:

$$I = I_0 * \exp(-\alpha * l) \quad (3.4)$$

Where I is the light transmitted through the gas cell; I_0 is the light incident on the gas cell; α is the absorption coefficient of the sample, which results from the product of the gas concentration and the specific absorptivity of the gas ϵ ; l is the cell's optical path-length (typically in units of cm).

This principle is exploited by using different technological solutions, such as:

- **optical gas cells**, which may be altered to fit a broader variety of applications by using long path cells (to increase the magnitude of the signal according to eq. 3.4), or optical fibres (to deliver light to a sample cell to a remote location), or hollow core optical fibres (to form a long, thin gas cell) [41]. Coupling light in many of these cells is made possible by the use of laser sources, as a significantly great proportion of the light may be collimated in a narrow beam and launched into optical fibre. Two examples of hollow core optical fibre are shown in Figures 3.7 and 3.8. In the first example, the glass fibre is coated with a fluorescent dye encapsulated in a polymer matrix. The odorant interacts with the fluorescent dye and causes changes in dye's optical characteristics, such as intensity, spectrum, lifetime changes and wavelength shift in fluorescence [36]. The sensitivity depends on the type of fluorescent dye or on the mixture of dyes and on the polymer used to support the dye. In particular, the polymer's polarity, hydrophobicity, porosity and swelling tendency are important for sensor's response. Adsorbants, such as alumina, can be added to the polymer in order to lower the limit of detection.
- **non-dispersive sensors**; measurements can be made in the mid infrared (non-dispersive infrared or NDIR), near infrared and UV/visible regions of the spectrum. Sensors that can be built are very compact [41] (NDIR sensors in recent times have reached a standard form factor consisting of a 16mm long, 20mm diameter cylinder). These sensors are cheaper, having few components (a simple microbulb light source, gold coated reflective light path and integrated detector containing two or more filtered detection channels). For some gases, such as CO_2 , NDIR gas sensors are the most suitable technology. In the case of breath analysis, they are the most adopted solution to perform capnography.

Chapter 3. Why electrify the...nose? Gas sensors and Electronic-nose systems for breath analysis

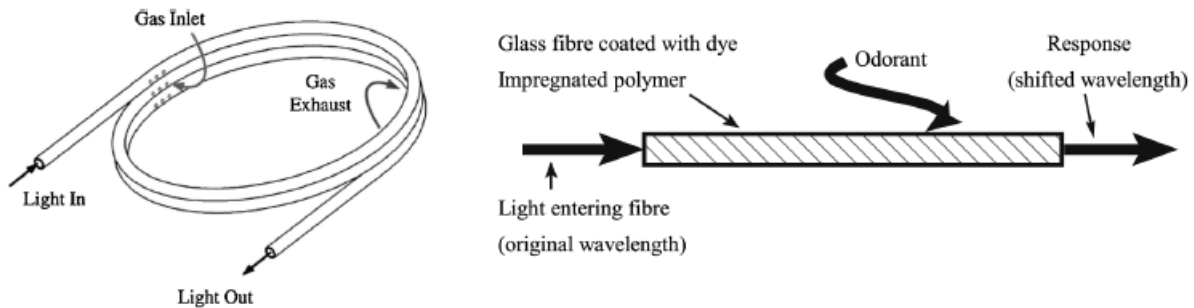


Figure 3.7: Optical gas sensor built by using a hollow core optical fibre.

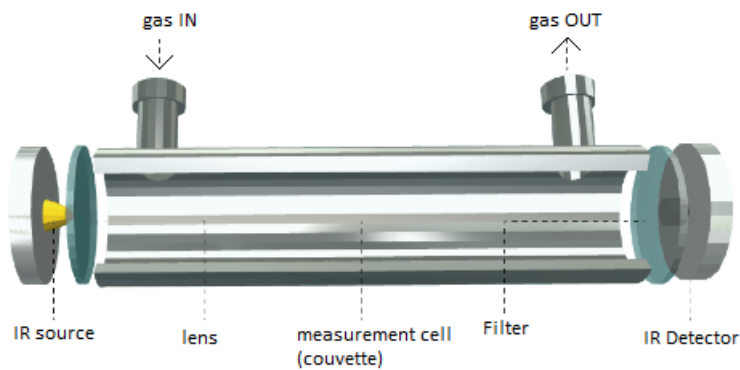


Figure 3.8: Optical gas sensor built by using a hollow core wave-guide and a IR source.

- **compact spectrophotometers and tunable diode laser spectroscopy (TDLS);** in contrast to the non-dispersive techniques, spectrophotometry is dispersive in the sense that the spectrum from a source is dispersed by a wavelength-selective element (such as a grating). The gases whose absorption lines fall within the wavelength of the spectrometer can be detected. UV absorption is the basis of a large number of commercial techniques (see, for instance, <http://aai.solutions/oma-process-analyzer>), which may be also fibre optically coupled so that the electronics can be housed separately from the gas cell. In contrast, the use of the near IR spectrum is limited by the relatively low signal to noise ratios of spectrophotometers compared with alternative methods (NDIR and TDLS). New designs for compact spectrophotometers have resulted from advances in manufacturing methods; the aim is to create systems that are simply, compact and with low power consumption. There has been great progress in the development of small diode array spectrometers able to measure spectra in the UV-visible and near-IR with good spectral resolution sufficient to identify gas species (see, for instance, <https://oceanoptics.com/product-category/maya-series/>). This has been combined with the advances in Si or InGaAs diode arrays using CCD or CMOS technology. Nonetheless, InGaAs arrays are relatively expensive [41] (about 15-16K Euro), indeed alternative solutions that use discrete detectors are adopted, such as in the case of TDLS. TDLS technique provides for an emission wavelength of a narrow linewidth laser

diode which is scanned across an individual gas absorption line at very high resolution [41,42]. Working at such high resolution allows for obtaining a high degree of specificity to the target gas, which can often be achieved for small molecules. Two are the commonly used techniques for TDLS: termed direct spectroscopy (the output of a laser diode is scanned across one or more gas lines in a narrow range, by ramping the laser diode injection current) and wavelength modulation spectroscopy (an ac modulation signal is applied to the laser diode, giving a sinusoidal modulation of the emission wavelength; such methods improves signal to noise ratio).

- **photoacoustic (PAS) sensors** differ in the way that the adsorbed light is detected. In traditional transmission sensors, the level of absorbed light is calculated by comparing the light intensity in the presence/absence of gas absorption, according to eq. 3.4. In photoacoustic sensors, the absorbed light is directly measured: light energy absorbed by the gas is converted to heat; the temperature increase causes the analyte and the surrounding gaseous/liquid/solid matrix to expand. If the light is modulated, the expansion produces pressure that can be detected by a microphone. In addition, to improve sensitivity, microcantilevers have been developed as an alternative to microphones [41,43]. The microcantilevers have very low mechanical compliance and show large deflections in response to pressure waves.

Advantages in the use of optical gas sensors are their fast response (time constant below 1 sec are possible), minimal drift, high specificity and their compactness. If their design is carefully conceived, such sensors may show also zero cross-response to other gases. Because the transduction principle derives from a direct measure of a molecule's physical properties, optical gas sensors' drift is reduced. Although their sophisticated and dedicated circuitry and software increase their costs, optical gas sensors fill a gap between lower cost sensors with limited performance and high-end laboratory equipment.

3.2.4 Metal-oxide-semiconductor field-effect transistor (MOSFET) sensors

They are metal-insulator-semiconductor (MIS) devices and their structure is shown in Figure 3.9, adapted from [36]. When the gate material (usually a catalytic material)

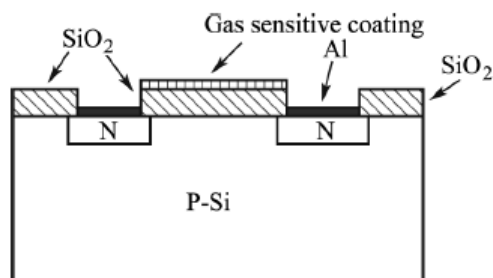


Figure 3.9: Typical MOSFET gas sensor functioning.

interacts with the odorant, the threshold voltage of the MOSFET sensor changes, due to

Chapter 3. Why electrify the...nose? Gas sensors and Electronic-nose systems for breath analysis

the corresponding change in the work functions of the metal and the oxide layers. Such changes in work functions are caused by the polarization of the surface and interface of the catalytic metal and oxide layer when the volatile molecules interact with the catalytically active surface [36]. Also the changes in drain-source current and in the gate voltage can be used as a measure of the interaction with the analyte.

A porous gas sensitive gate is used to facilitate the diffusion of the gas into the sensing material.

The factors that affect the sensitivity of such type of sensors are operating temperature (which is usually between 50 °C and 170 °C), composition and structure of the catalytic material. Temperature is increased to decrease the response (from milliseconds up to 300sec) and recovery times. Typical sensitivities are approximately 0.1ppm [36].

MOSFET gas sensors fabrication reproducibility is quite good and this type of sensors can be integrated into complementary metal-oxide semiconductor (CMOS) technology, resulting in small, low cost sensors.

On the other hand, they can suffer from baseline drift and instability according to the used sensing material.

3.2.5 Electrochemical gas sensors

They exploit the electric charge exchange (resulting in an electric signal) when chemical species react at an electronic conductor/ionic conductor interface. They employ an electrochemical cell consisting of a casing that contains a collection of chemical reactants (electrolytes or gels) in contact with the surroundings through two terminals (an anode and a cathode) of identical composition [44]. For gas sensors, the top of the casing has a membrane which can be permeated by the gas sample (capillary diffusion barrier in Figure 3.10). Oxidization takes place at the anode and reduction occurs at the cathode. A current is created as the positive ions flow to the cathode and the negative ions flow to the anode. Gases such as oxygen, nitrogen oxides, and chlorine, which are electrochemically reducible, are sensed at the cathode while electrochemically oxidizable gases such as carbon monoxide, nitrogen dioxide, and hydrogen sulfide are sensed at the anode.

The output of the electrochemical cell is directly related to the concentration or partial pressure of the gaseous species. Depending on whether the output is an electromotive force (namely an open circuit voltage) or an electrical current, the electrochemical gas sensors can be classified in potentiometric or amperometric.

Solid state electrochemical devices are the most used sensor type for the measurement of oxygen for automotive market where legislation has restricted the permitted emissions levels of carbon monoxide, hydrocarbons and nitrogen oxides. At present, these sensors are commonly produced as macroscopic ceramic devices or, more recently, as miniature thick film devices. The advantages of fuel cell sensors are that they use very little power, are relatively low cost, are ready almost immediately, are more stable over time, rarely give false positive readings.

3.3 Gas sensors and e-noses for breath analysis

Formerly designed for environmental, cosmetic, food industry applications (as shown in Table 3.1), in recent years e-nose technology applications in medical field are grow-

3.3. Gas sensors and e-noses for breath analysis

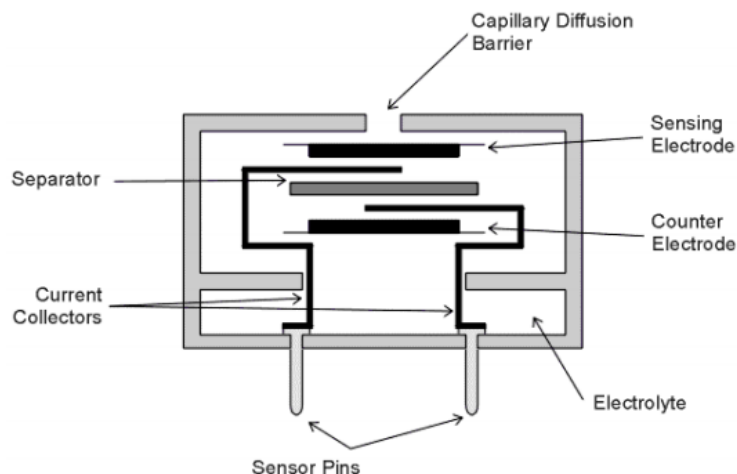


Figure 3.10: Typical electrochemical gas sensor (taken from <https://www.sgxsensortech.com/>)

ing in number.

The earliest studies involving aroma measurements for clinical applications aimed to test the efficacy of using e-nose to diagnose human disease caused by microbial infections [18]. In particular, the capability of e-noses to identify microbes through the detection of VOCs they released in vitro from bacterial plate cultures (or directly from infected tissues) were tested. For instance, Dutta and co-workers used an e-nose based on a sensor array of conducting polymers, the Cyranose 320, to identify three different species of *Staphylococcus aureus* bacteria, responsible for nose, ear and throat infections, in patients [45]. The data were analysed by using PCA, self-organizing map (SOM) and Fuzzy-C Means algorithms. The Cyranose 320 was able to identify the three *Staphylococcus aureus* species with 99.69% accuracy.

Such early investigations of potential e-nose application in medical field led to the realization that their different operating principles associated with their various instrument types and design could be exploited to sample and instantly analyse volatiles molecules directly from patients, thus obtaining many other types of diagnostic information and medical conditions. As a consequence, the range of applications of electronic noses increased and included, for instance, the monitoring of microbial metabolites released from superficial wounds [46], the detection of volatiles associated with upper respiratory tract infections [47], the breath analysis for the detection of lung and other organ-related diseases [48], the analysis of urine and faecal head space for the diagnosis of metabolic disorders and gastrointestinal diseases, respectively [49, 50].

Here the attention is focused on the application of electronic noses in the field of human breath analysis.

An increasing number of studies have shown that breath profiling by e-nose could play a role in the diagnosis and/or screening of various respiratory diseases [51]. In the study conducted by Dragonieri et al. [52] the Cyranose 320 was able to discriminate (with accuracy 100% and 90% respectively) mild and severe **asthmatic patients** from healthy, non-smoking controls. Also the e-nose developed by De Vries et al. [53] and based on metal oxide semiconductor gas sensors was able to distinguish between asthmatics and controls with an accuracy of 87% and an area under the receiver operating

Chapter 3. Why electrify the...nose? Gas sensors and Electronic-nose systems for breath analysis

Table 3.1: Some existing commercial e-noses used for environmental, cosmetic, food industry applications.

Manufacturer	Sensor type	Applications	Dimensions	Costs (Euros)	Website/University
Airsense analysis GmbH	MOS	Food evaluation	Laptop	17000-36000	www.airsense.com
Alpha MOS-Multi Organoleptic System	CP, MOS, QCM, SAW	Quality control of food storage; analysis of perfumes	Desktop	17000- 84000	www.alpha-mos.com
Applied Sensor	MOS, IR MOSFET	Environmental analysis	Laptop		www.ifm.liu.se
Osmetech PLC	CP	Environmental an.; pharmaceutical product evaluation	Desktop	17000-63000	www.osmetech.com
Array Tech	QCM	food analysis			University of Rome, Italy
Bloodhound sensors	CP	Environmental an.; food an.; flavor and fragrance testing	Laptop		University of Leeds, UK
Cyrano Science Inc.	CP	Food quality; chemical analysis; contamination detection	Palmtop	4500	www.cyranosciences.com
Electronic Sensor Technology Inc.	GC, SAW	Food and beverage quality; explosives and drugs detection; environmental an.	Desktop	16500- 23000	www.estcal.com
Forschungszentrum Karlsruhe	MOS, SAW	Fire alarms; automotive appl.; Food quality			www.fzk.de/FZK2/english
HKR-Sensorsystem GmbH	QCM	Food and beverage quality; cosmetics and perfumes quality	Desktop		www.hkr-sensor.de
Illumina	FO	Life sciences; chemical detection; food quality			www.illumina.com
Lennartz Electronic GmbH	MOS, QCM	Food and beverage quality	Desktop	46000	www.lennartz-electronic.de
Microsensor system	SAW	Chemical agent detection; Toxic industrial chemical analysis	Palmtop		www.microsensorsystems.com
OligoSense	CO	Automotive appl.; food analysis			www.oligosense.be
Nordic Sensor Technologies AB	MOS, SAW, QCM	Industrial monitoring	Laptop	33800- 50800	www.nordicsensor.com
Sawtek Inc.	SAW	Toxic gases in chemical atmospheres monitoring	Palmtop	4500	www.microsensorsystem.com

characteristic curve (AUC-ROC) of 0.94 ± 0.15 .

Chronic Obstructive Pulmonary Disease (COPD) is likely to exhibit a specific exhaled VOC profile. Under such hypothesis, Sibila et al. used the Cyrano 320 to differentiate COPD breathprints from healthy controls (with an accuracy of 83% and

3.3. Gas sensors and e-noses for breath analysis

AUC-ROC of 0.93) [54]. Such study was extended by Shafiek and co-workers which used the same e-nose to identify the presence of airway bacterial colonization in clinically stable patients with COPD [55]. Also the Aeonose (a metal-oxide sensors-based e-nose) had good performances in detecting the presence/absence of a viral or bacterial respiratory infection in patients with severe COPD [56].

Exhaled breath of patients with **pulmonary mycobacterium tuberculosis** were differentiated from that of healthy subjects by using a Cyranose 320 [57] (with 72% specificity, 84% sensitivity) and a nano-array system [58].

Many studies aimed to test the ability of e-noses to detect **lung cancer**-related breath-print. Di Natale et al. used a QCM sensor system, coated with different metalloporphyrins, to discriminate the breath of 35 subjects suffering from lung cancer from that of 9 which just had surgical therapy and 18 healthy controls [59]. The e-nose successfully detected 100% of lung cancer patients, 94% of healthy controls and 44% of post-surgery patients. Such approach was confirmed in the studies of Yu et al. [60] and Chen et al. [61]. Other three studies assessed the performances of Cyranose 320: an accuracy of 72% was obtained by Machado et al. [62] in comparing the breath-print of 14 Non-Small Cell Lung Cancer (NSCLC) with that of 37 healthy subjects. Likewise, Bikov et al. [63] involved 27 individuals with NSCLC and 10 controls, showing an accuracy of 70%. The study of Dragonieri et al. [64] showed an accuracy of 80%, with 10 NSCLC subjects and 10 healthy controls. Also a SAW-based e-nose system showed good performance (80% accuracy) in comparing breath profiles of 5 lung cancer patients and 5 controls [65].

The performances of Cyranose 320 were assessed also in the case of **Obstructive Sleep Apnoea Syndrome (OSAS)** [66] and **Pulmonary Sarcoidosis** [67]. In particular in [66], Cyranose 320 was used to discriminate (with a sensitivity of 0.93 and a specificity of 0.7) between OSAS patients and control subjects. In additions, that breath-print patterns differed after 3 months of continuous positive airway pressure (CPAP) therapy from untreated OSAS, with an AUC-ROC of 0.82.

Great progresses have been achieved also in the use of e-noses to diagnose and monitor **diabetes** in clinical patients. Ping et al. [68] developed an electronic nose system based on thin-film sensors coated with SnO_2 , having high selectivity for acetone, the most important volatile biomarker detected in the exhaled breath of diabetic patients. In fact, as demonstrated by the studies conducted by Thati et al. [69] and Righettoni et al. [70], breath acetone was found to be correlated with blood glucose levels (Pearson's 0.98 and Spearman's 0.93 [70]). In particular, in [69], a TGS822 tin oxide (SnO_2) sensor was used to detect acetone in exhaled air, while Righettoni and co-workers [70] developed a portable acetone sensor consisting of flame-made, nanostructured, Si-doped WO_3 sensing films.

As described in chapter 2, acetone contained in our exhaled breath principally derived from the breakdown of body fat. As a consequence, it is expected to be a good indicator of **fat burning**. In [71], Toyooka and co-workers prototyped a portable breath acetone analyser, based on two semiconductor gas sensors with different sensitivity characteristics, for monitoring fat loss. It was found that body fat in subjects with a controlled caloric intake and taking exercise decreased significantly, whereas breath acetone increased significantly.

Also neuro-degenerative disorders such as **Alzheimer's disease**, **Parkinson's disease**

and **Multiple Sclerosis** have each been shown to exhibit a unique VOC profile. Example of VOCs include alkanes, methylated alkanes, and carbon disulfide. In [72] and [73], e-noses with functionalized carbon nanotubes as sensing material and multivariate data analysis are used to characterize such breath profiles.

Guo et al. [17] developed a 12 MOS-based gas sensor array placed in a stainless steel chamber and evaluated the prototyped e-nose system performances in two cases: i) in the first test they used their system to distinguish between pre- and post- treatment breath samples from 52 subjects with end-stage renal failure (accuracy of 80.15% and 82% respectively); ii) in the second experiment, they tested the ability of the system to discriminate between healthy controls and subjects suffering from either **diabetes** (sensitivity 86.97%, specificity 87.57%), **renal disease** (sensitivity 83.96%, specificity 84.16%), or **airway inflammation** (sensitivity 73.79%, specificity 71.58%).

Another study [74] aimed to distinguish, by using the Ciranose 320, the breath of smokers from that of non-smokers. Principal component analysis identified the maximal point of differences between classes. The e-nose correctly identified the smoking status in 37 of 39 overall individuals.

Recently, Nakhleh and co-workers [75] developed an artificially intelligent nano-array based on molecularly modified gold nanoparticles and a random network of single-walled carbon nanotubes for a non-invasive diagnosis and classification of 17 disease (**lung cancer, colorectal cancer, head and neck cancer, ovarian cancer, bladder cancer, prostate cancer, kidney cancer, gastric cancer, Chron's disease, ulcerative colitis, irritable bowel syndrome, idiopathic Parkinson's, atypical Parkinsonism, multiple sclerosis, pulmonary arterial hypertension, pre-eclampsia, and chronic kidney disease**) from exhaled breath. The population included 591 healthy controls and 813 patients suffering from one of the 17 diseases. Cluster analysis was used to classify each breath profile. Blind tests showed that 86% accuracy could be achieved, allowing both detection and discrimination between the different disease conditions. GC-MS analysis was the ground truth.

Together with such widely documented advances in gas sensing and e-noses applications in biomedical field, the high cost of detection-instruments needed for disease diagnosis, the increasing demand for specialized detection instruments, and the increased visibility of biomedical needs [76] led many private biotechnological industry have shifted their research and development departments toward the development of e-nose technology. In addition, with their numerous, diverse and specialized possible applications, e-nose instruments developed for diagnostic medical field are often higher priced and more lucrative for commercial development [18].

In Table 3.2 some of the existing e-noses designed for clinical purpose are listed. For instance, Applied Nanodetectors (www.applied-nanodetectors.com), a company formed in 2004, developed a nano-technology based gas sensor array platform for the monitoring of a set of VOCs in the breath of asthmatic patients. Di Natale and co-workers [59] developed an electronic nose, composed by eight quartz microbalance (QMB) gas sensors, to diagnose lung cancer. COSMED s.r.l. (www.cosmed.com), founded in 1980, is a privately owned company manufacturing cardio-pulmonary, metabolic and body composition diagnostic equipment. Recently, COSMED s.r.l. have introduced *K5*, the 4th generation of a wearable metabolic system. Such device, by monitoring the inhaled oxygen and the exhaled carbon monoxide, is able to provide informations about

3.3. Gas sensors and e-noses for breath analysis

the metabolic expenditure of an athlete during a competition. Bedfont Technical Instruments Ltd. (www.bedfont.com) a company established in 1976 and become, today, the pioneer in breath analysis for medical applications, developed a series of portable device for the monitoring of specific diseases (the *NObreath* provides accurate analysis of airway inflammation for the control of asthma; the *Gastrolyzer* aids in the detection of gastrointestinal disorders and food intolerances) or noxious habits (the *Smokerlyzer*, used for smoking cessation, detects carbon monoxide in smokers' breath). Dräger (www.draeger.com) Alcohol test is based on an electrochemical cell gas sensor and provides a real-time and accurate measure of breath ethanol. BreathDX (www.breathdx.com), a UK-based company founded by Professor Tony Killard, developed AmBeR®[®], a breath ammonia measurement device, based on conductive polymers gas sensors, which can diagnose and manage several disease conditions (among which stomach ulcer, chronic liver disease, metabolic disorders). The eNose company (www.enose.nl) developed Aeonose™, an e-nose based on MOS gas sensors, which can be used for screening on tuberculosis and throat cancer.

In addition, many types of biosensors also are being developed for medical applica-

Table 3.2: Existing commercial e-noses used for breath analysis (Costs: updated to October 2017; websites last visit: March 2018).

Manufacturer	Sensor type	Applications	Dimensions	Costs (Euros)	Website/University
Applied Nanodetectors	Nano-technology based sensors	Asthma monitoring	Palmtop		www.applied-nanodetectors.com
Array Tech	QMB	Lung cancer diagnosis			University of Rome, Italy
Shimadzu Co. Diag-nose	MOS	Tuberculosis diagn.; bowel cancer diagn.; infections in wounds and urinary tract	Desktop		www.nose-network.org
COSMED s.r.l.	GFC, IR	Cardiopulmonary diagn.	Palmtop	34000	www.cosmed.com
Bedfont Scientific Ltd	MOS	Monitoring of <i>CO</i> in smokers; monitoring of <i>H₂</i> in people with lactose intolerance; monitoring of <i>NO</i> in asthmatics	Desktop/ Palmtop	1000- 4800 and more	www.bedfont.com
Breathometer Inc.	Electrochem. cells	Oral health monitoring	Palmtop	93	www.breathometer.com
Draeger	Electrochem. cells	Breath Alcohol test	Palmtop	1590	www.draeger.com
BreathDX	Conducting polymers (polyaniline)	Monitoring of breath ammonia	Desktop/ Palmtop		www.breathdx.com
The eNose company	MOS	Screening on tuberculosis and throat cancer	Desktop/ Palmtop		www.enose.nl

tions, in attempt to reproduce the functioning of the bio-olfactory receptors, and will likely provide another very fruitful area for diagnostic methods development [77]. The mentioned research studies and commercial e-noses cover just a small amount

Chapter 3. Why electrify the...nose? Gas sensors and Electronic-nose systems for breath analysis

of the state of art, that demonstrate the theoretical and practical feasibility of using electronic noses in many medical applications. Nonetheless, some challenges remain, including improving device accuracy, without sacrificing ease of use and costs, which often are still very high, as shown in Table 3.2.

CHAPTER 4

The Wize Sniffer

4.1 The aim of the research

In chapter 4, the potential of breath analysis has been explained. For its unobtrusiveness, breath analysis may play a key role in healthcare diagnostics. Comparing with the traditional clinical techniques, breath analysis is harmless to not only the subjects but also the personnel who collect the sample.

Nevertheless, standard instrumentation for gas analysis (GC-MS, for instance), as well as commercial e-noses, do not facilitate the spread and the use of this technique in clinical field, because of their high costs, their difficulties in using and interpreting the results, and long-time analysis.

My aim was to design and develop a device able to accurately analyse human breath composition and, at the same time, to overcome these limitations of existing instrumentations.

In this regard, another important issue was considered, that is the greater demands on improvements in effectiveness, speed, smartness and lower costs of biomedical instruments for daily healthcare applications [18], resulting from increasing limitations of healthcare financial resources as a consequence of budgetary cuts or constraints and changes in socio-economic factors.

Therefore, my work was focused on the design and development of the so called **Wize Sniffer (WS)**, considering the following requirements [19]:

- ability to analyse a set of breath molecules in real time;
- portability, in order to promote its use not only in laboratory settings;
- use of low-cost technology, in order to encourage its purchase;

Chapter 4. The Wize Sniffer

- ease of use, also for non-specialized personnel, in order to foster its use also in home environment, for instance;
- modular and customizable design, in order to easily change the gas sensors according to the molecules to be detected.

In order to fully exploit the potential of breath analysis, the WS was developed with a view to taking the positive aspects of existing instrumentations, and, at the same time, to overcoming their limitations (see Table 4.1).

Table 4.1: Characteristics of standard instrumentation (GC-MS) and electronic nose systems for breath analysis, and WS requirements

Instrumentation	Portability	Costs	Ease of use	Time of analysis	Sensitivity
GC	Not portable	High (15000 Euro on average)	Only specialists	About 1 hour for each sample	High (up to ppt/ppb)
PTR-MS	Not portable	High (13000 Euro on average)	Only specialists	On-line analysis	High (up to ppt/ppb)
Laser spectroscopy	Not portable	High (15000 Euro on average)	Only specialists	Real time analysis	High (up to ppt/ppb)
Commercial e-noses	portable	10000 Euro on average	Also by non-specialists	Real time analysis	up to ppb
WS requirements	portable	low-cost WS core \leq500 Euro	Also by non-specialists	Real time analysis	ppm/ up to ppb

4.2 Detected molecules

The idea of the Wize Sniffer was born in the framework of SEMEiotic Oriented Technology for Individual's CardioMetabolic risk self-assessment and Self-monitoring (SEMEOTICONS, www.semeoticons.eu) European Project.

The idea behind SEMEOTICONS was to exploit human face as an indicator of individual's health status and translate the semeiotic code of the face into measurements and descriptors automatically evaluated by a computerized application. In particular, the eligible application field was the one of cardio-metabolic diseases prevention, for which healthcare systems are registering an exponential growth of social costs, especially due to expensive diagnostic resources, often improperly prescribed. One of the principal aims of SEMEOTICONS Project was to move the semeiotic analysis from the office of medical doctors closer to individual's normal-life settings and enable normal people to self-assess their personal well-being status, particularly concerning their cardio-metabolic risk.

To this end, SEMEOTICONS designed and constructed an innovative, multi-sensory system, based on multi-spectral cameras and other advanced detection tools, integrated into a hardware platform having the exterior aspect of a mirror: the so-called *Wize Mirror* (WM, see Figure 4.1). The aim of the WM was to detect in human face, all the signs considered as indicators of cardio-metabolic risk [78, 79].

The Wize Sniffer was designed to be a Wize Mirror's tool, in order to analyse user's breath composition and monitor his/her noxious habits for cardio-metabolic risk: smoke, alcohol intake, wrong diet.

Therefore, the WS can help the user to prevent cardio-metabolic risk by detecting in his/her breath the following molecules [20]:

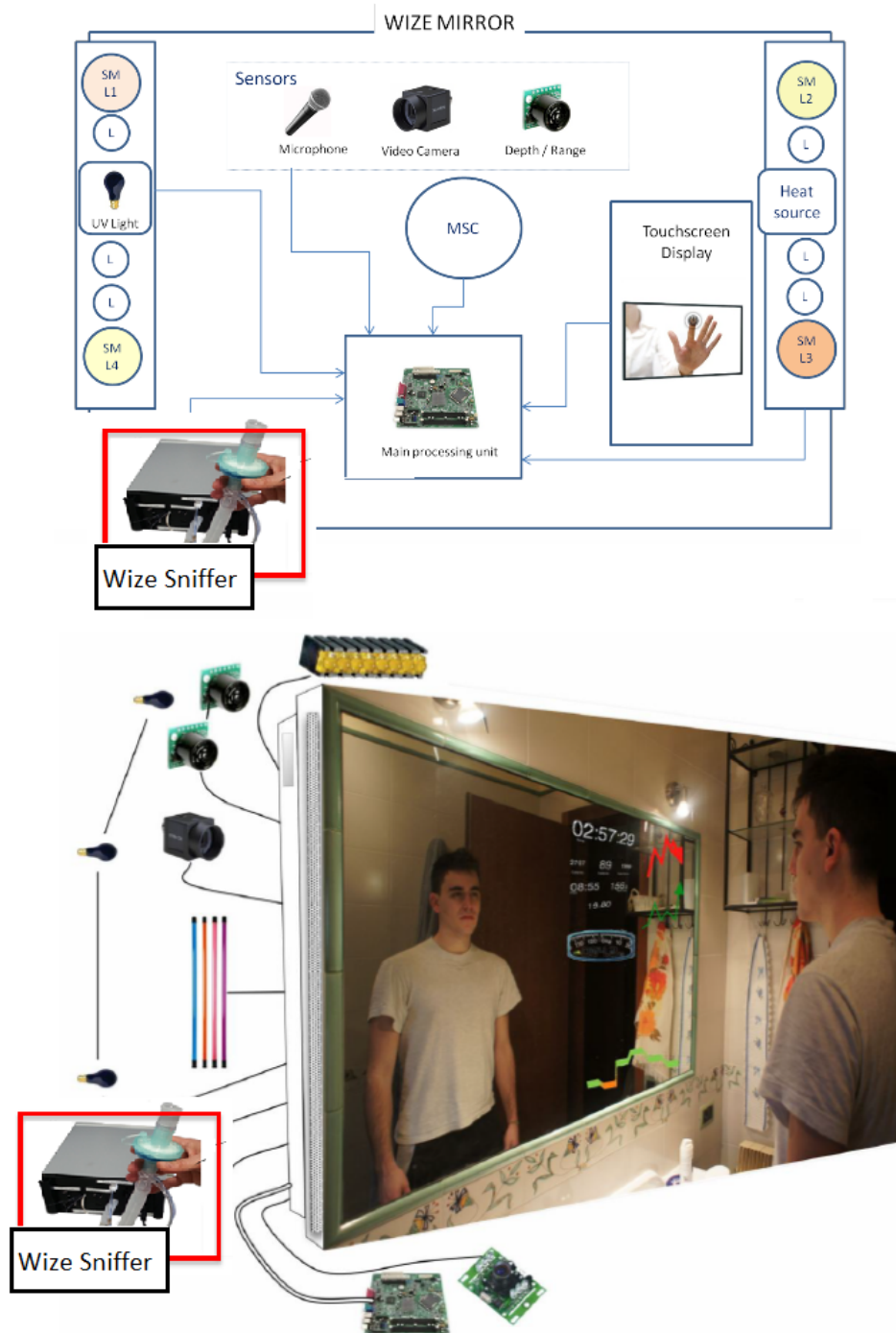


Figure 4.1: Wize Mirror's hardware platform developed in SEMEOTICONS European Project.

- **carbon monoxide (CO):** in human body, it is naturally produced by the action of heme oxygenase on heme when the macrophages of the spleen remove old and damaged erythrocytes from the circulation. CO normal levels in exhaled breath are 2-3.5ppm. It acts as a cellular messenger, as a promoter of neurovascular

growth and functions in vasodilation. Abnormalities in its metabolism have been linked to a variety of diseases, including hypertension.

CO is also the major component present in tobacco fumes (75,95%). Indeed, increasing levels of exhaled CO can be detected in smokers (13.8 - 29ppm).

An increase of CO in blood is very dangerous, as it leads haemoglobin to carry less oxygen through the vessels, because CO usurps the space in haemoglobin that normally carries oxygen, forming carboxyhaemoglobin.

It also increases the amount of cholesterol that is deposited into the arteries;

- **ethanol** (C_2H_6O): Moderate ethanol consumption, in healthy subjects, reduces stress and increases feelings of happiness and well-being, and may reduce the risk of coronary heart disease. Heavy consumption of alcohol, on the contrary, causes addiction and leads to an accumulation of free radicals into the cells, causing oxidative stress.
- **oxygen** (O_2) and **carbon dioxide** (CO_2): Exhaled air has a decreased amount of oxygen and an increased amount of carbon dioxide. These amounts show how much O_2 is retained within the body for use by the cells and how much CO_2 is produced as a by-product of cellular metabolism.
Exhaled O_2 amount is about 13.6%-16%. Mean CO_2 concentration in exhaled breath is about 4% (= 40000ppm).
Lower values of breath O_2 may be due to respiration disorders.
Increased levels of CO_2 can be due also to physical activity, for example. There is a decrease in case of congenital heart disease (for example, cyanotic lesions that result in a bluish-grey discolouration of the skin and in a lack of O_2 in the body). Also individual's breathing rate influences the level of CO_2 in blood and, as a consequence, in exhaled gas. Breathing that is too slow causes respiratory acidosis (that results in an increase of CO_2 partial pressure in blood, which may cause hypertension, build up of heart rate), while breathing that is too rapid leads to hyperventilation, which may cause respiratory alkalosis (that results in decrease of CO_2 in blood; so, it can no longer fulfil its role of vasodilator, resulting in arrhythmias, extra systoles). A way to monitor the carbon dioxide concentration (or partial pressure) is capnography, as previously described in chapter 2. The max value of capnogram correspond to the end of tidal volume of exhaled breath and the steady-state concentrations of each breath;
- **hydrogen** (H_2): it is related to the carbohydrate breakdown in the intestine and the oral cavity by anaerobic bacteria. Its baseline value is about 9.1ppm, but it may vary from an individual to another, especially in case of lactose intolerance;
- **hydrogen sulfide** (H_2S): it is a vascular relax agent; for instance, it has a therapeutic effect in hypertension Its baseline level in human exhaled breath is about 0.33ppm.

4.3 Hardware

As previously reported, the WS was thought to be integrated into the WM. Nevertheless, my idea was to design and develop an instrument which could be used both as a

4.3. Hardware

WM's tool and as a stand-alone device. In collaboration with COSMED s.r.l., I started defining the block diagram and the aspect of the WS, respectively shown in Figure 4.2 and Figure 4.3.

I considered a sampling chamber in which the breath gases would have been col-

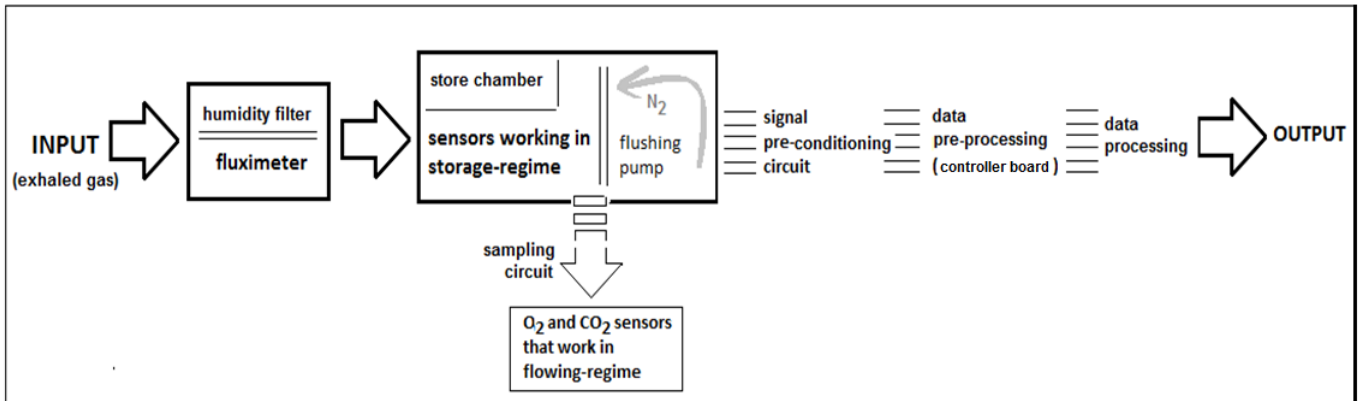


Figure 4.2: WS block diagram.

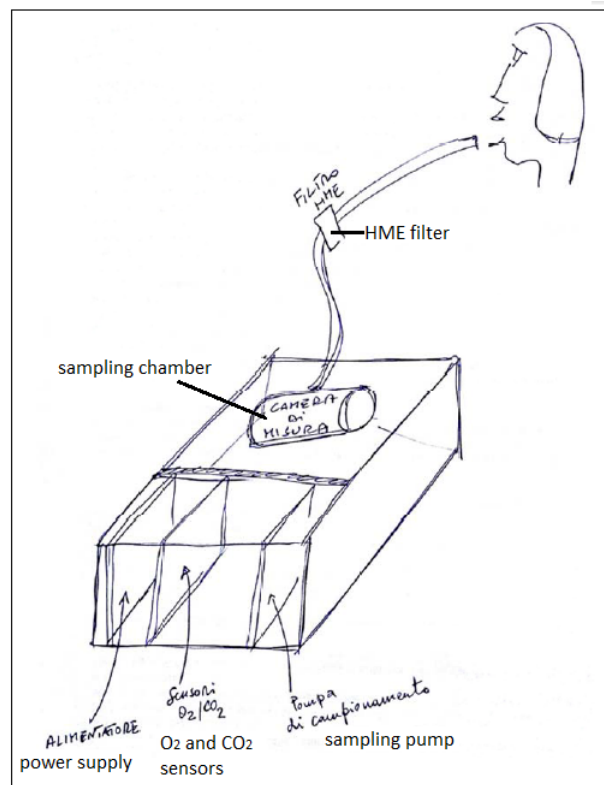


Figure 4.3: Sketch of WS' appearance.

lected. A heat and moisture (HME) filter, made of hygroscopic material, would have been needed to absorb the water vapour present in exhaled breath. A flow-meter would have enabled the exhaled gas volume to be calculated. The gas sensors would have been placed into the gas sampling chamber. In case of faster response time, a sampling pump

would have been needed to inject the sampled exhaled gases to the sensors working in *flowing-regime*. In addition, I included a pre-conditioning module (an *ad-hoc* circuit), to stabilize sensors raw signals. Finally, I considered a controller board to read and pre-processes sensors raw data and a data processing phase to analyse them. In the following sub-sections each part of WS is described in detail.

4.3.1 The core of the WS: the gas sampling chamber and the gas sensor array

The gas sampling chamber was realized in collaboration with COSMED s.r.l., one of the industrial partner of SEMEOTICONS Project.

Its dimensions were fixed at about 600ml, according to the human resting tidal volume¹ [27]. The chamber was made up of acrylonitrile butadiene styrene (ABS), a common thermoplastic polymer, and delrin, which is a type of polyoxymethylene (POM). Such materials were chosen because they do not interfere neither with the target molecules, nor with gas sensors' behaviour

In Figure 4.4a) and b), the rendering of the chamber realized by means of a Computer-Aided Drafting (CAD) software and the 3-D printed chamber are respectively shown. My idea was to realize a modular device: the gas sensors, housed in the chamber's white slots, can be easily changed according to the molecules to be detected.

Regarding the gas sensor array, one fundamental requirement was the use of robust

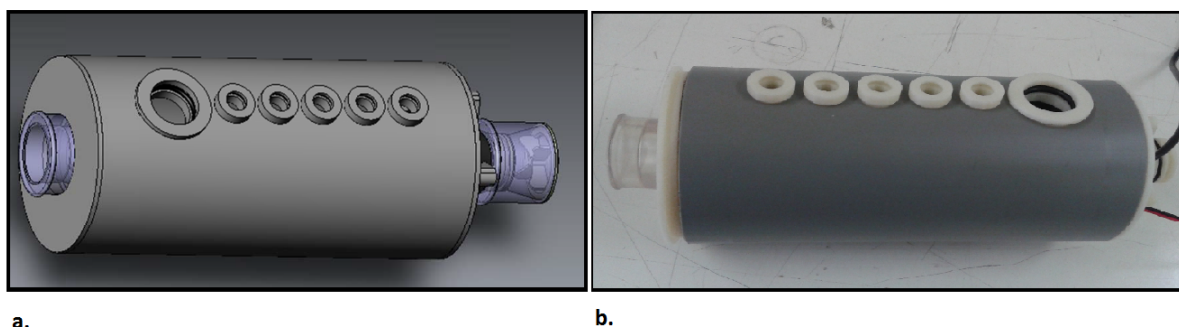


Figure 4.4: The gas sampling chamber. a) its rendering with a Computer-Aided Drafting (CAD) software; b) the 3-D printed chamber.

and low-cost technology. As mentioned in chapter 3, although very sensitive and able to detect very low concentrations, optical gas sensors are expensive and often they cannot be miniaturized. Also CNF-based gas sensors are expensive, especially for their fabrication and manufacturing. SAW and QCM-based gas sensors have very high sensitivity but they need complex circuitry and, in the case of QCM-based gas sensors, they have a poor signal-to-noise ratio. Therefore, my choice was to employ MOS-based gas sensors. They have long life, strong sensitivity, rapid recovery time [19]. In comparison to other types of gas sensors, MOS-based gas sensors' availability and low cost make them the most widely used gas sensors [33].

Within the gas sampling chamber, six Taguchi semiconductor-based gas sensors, manufactured by Figaro Engineering (www.figarosensor.com) were integrated. Beginning

¹The volume of air that enters or leaves during a respiratory cycle is termed *tidal volume*. About 500ml-600ml of air enter during a normal, resting inspiration. On the average, the same volume leaves during a normal, resting expiration. Thus, the resting tidal volume is about 500ml [27].

his research in 1962, Mr. Naoyoshi Taguchi became the first person in the world to succeed in the development of a semiconductor device which could detect low concentrations of combustible and reducing gases when used with a simple electrical circuit [80]. Figaro Inc., a gas sensor company based on metal oxides started by Taguchi in 1968, still stands as one of the world's leading gas sensor manufacturer. In Table 4.2 the employed Taguchi MOS-based sensors are listed. They all are n-type:

Table 4.2: Taguchi MOS-based gas sensors integrated in the WS

Sensor	Detected molecules	Best detection range
TGS2602	hydrogen, ammonia, ethanol, hydrogen sulfide, toluene	1-10ppm
TGS2620	hydrogen, carbon monoxide, ethanol, methane, isobutane	50-5000ppm
TGS821	hydrogen	1-1000ppm
TGS2444	ammonia	10-100ppm
TGS4161	carbon dioxide	350-10000ppm
MQ7	carbon monoxide, hydrogen	1-50ppm

their sensing element is tin-dioxide (SnO_2)-based. Figure 4.5 shows their general structure; in Figure 4.6 their general functioning is reported.

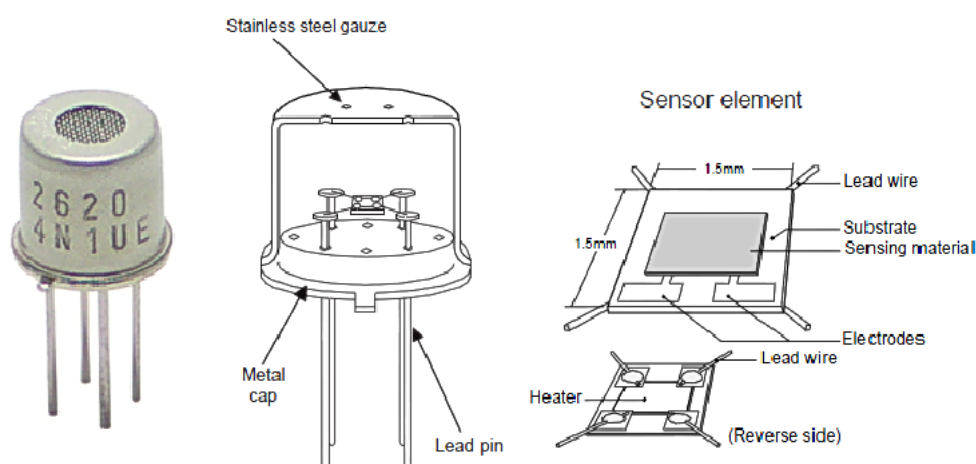


Figure 4.5: Employed Taguchi MOS-based gas sensors' general structure.

A voltage V_c (5V DC) is applied across the sensor sensing element which has a resistance (R_s) between the two electrodes and a load resistor (R_L) connected in series. When the sensor senses gas particles, a change in R_s occurs, that is indirectly measured by taking the voltage value across the load resistance V_{RL} , according to eq.4.1. The environmental conditions such as operating temperature determine the sensing performance and characteristics of such type of gas sensors. The operating temperature influences the receptor function through its effect on the chemical dynamics at gas-solid interface, thus determining important sensing properties such as selectivity, stability, response and recovery times [21]. As a consequence, sensors operating temperature is kept constant by means of a heating circuit (V_H , Figure 4.6).

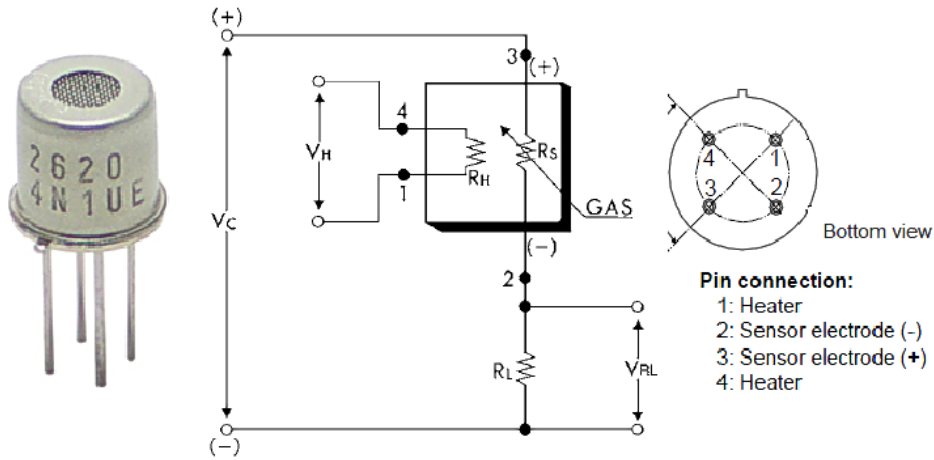


Figure 4.6: Employed Taguchi MOS-based gas sensors' general functioning: the basic measurement circuit.

$$R_s = \frac{V_c - V_{RL}}{V_{RL}} \quad (4.1)$$

An example of Taguchi gas sensors (TGSs) sensitivity characteristics is shown in Figure 4.7. As previously described in chapter 3, in presence of a detectable gas, sensor conductivity increases depending on the gas concentration.

In general, the response of a Taguchi sensor to each gaseous compound have a power

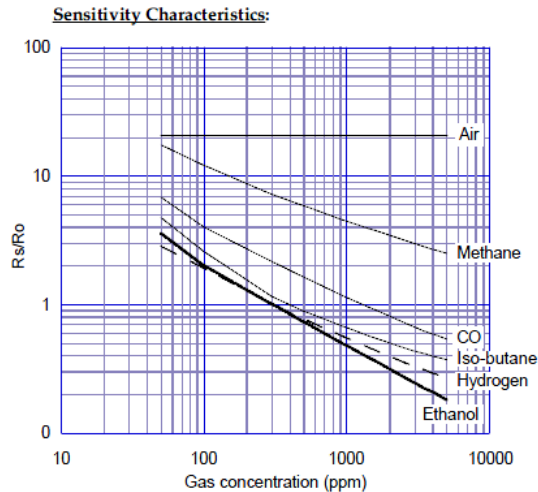


Figure 4.7: An example of sensitivity characteristic of the employed gas sensors. In this case, this is TGS2620 sensitivity characteristic in bi-logarithmic scale. The Y-axis is indicated as sensor resistance ratio between R_s (= sensor resistance in displayed gases at various concentrations) and R_0 (= sensor resistance in 300ppm of ethanol).

law nature. Indeed, in presence of a target volatile molecule, sensor resistance follows the equation 4.2 [81]:

$$R = R_0 * P_{O_2}^\beta * (1 + K_{gas}[gas])^{-\beta} \quad (4.2)$$

Where R_0 is sensor resistance in air and P_{O_2} is the oxygen partial pressure. K_{gas} can be considered as the sensor sensitivity coefficient. In ambient air the equation 4.2 can be simplified as follows:

$$R = R_0 * (1 + K_{gas}[gas])^{-\beta} \quad (4.3)$$

Beyond the non-linear nature of sensors response, represented by the power law exponent β , the equation 4.2 suggests that **oxygen** plays an important role in the detection of gases by the TGSs [81].

The ambient of a metal oxide surface is normally classified as dry or wet, according to the humidity level. As will be discussed, in wet atmosphere, water molecules have a major role and influence on the receptor function, while oxygen plays an important role in dry atmosphere (eq. 4.2). Due to its high electronegativity and lone pairs of electrons, oxygen can be easily adsorbed on the surface of metal oxides. In dry atmosphere, it acts as an electron acceptor, gets ionized and forms an ionic layer on the surface. This helps in sorption of other gas molecules on to the metal oxide surface [21].

Also **humidity** level has a larger influence on Taguchi (and MOS-based in general) gas sensors response [21,82], as the water vapour undergoes dissociative adsorption on metal oxide surfaces and the resultant ions, which are adsorbed on the metal oxide surface, affect the electronic and ionic conducting properties of the semiconducting metal oxides. In many cases, increase of humidity greatly impedes the response of sensor, lowering the sensitivity of the sensing element [83, 84]. It may be due to the change in conductivity from the free electrons produced, or simply by the occupation of the active sites by the adsorbed water molecules. Moreover, a distinction should be done between n-type and p-type-based sensing materials. As shown in Figure 4.8, when humidity increases, resistance of the n-type-based film decreases. Further increase in humidity leads to a drastic decrease in resistance while it slows down at higher humidity level [21].

A relative humidity (RH) around 50-60% is optimum for sensing gases by both n-type

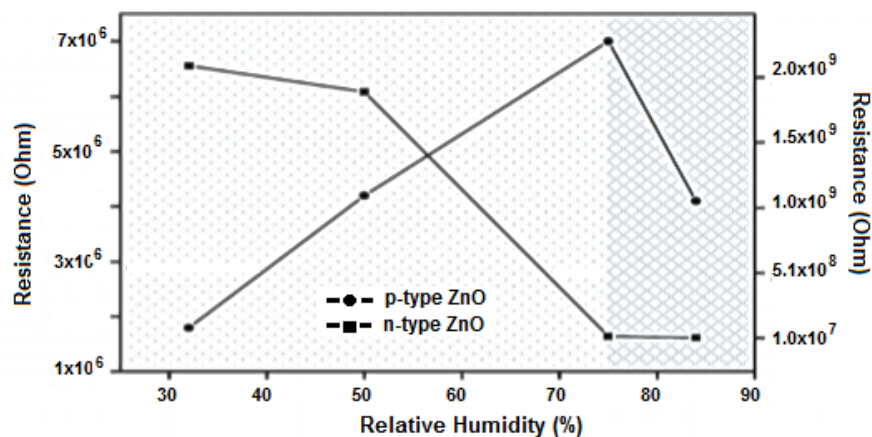


Figure 4.8: Resistance vs. Relative Humidity (RH) for n-type and p-type metal oxide sensing films [21].

and p-type semiconductor films.

In the case of the Wize Sniffer the humidity plays a crucial role, as it deals with human breath that have a 90%RH. Therefore, I deemed it necessary to take steps to manage

this factor and optimize its effects. Firstly, a HME filter, made of hygroscopic material, was put at WS mouthpiece to absorb the majority of the water vapour present in exhaled breath. Secondly, a temperature and humidity sensor (Sensirion SHT11) was integrated within the gas sampling chamber to monitor the variation in humidity (see Figure 4.9). Indeed, by the Sensirion SHT11, I observed that: i) after the integration of the HME filter, the relative humidity in the gas sampling chamber decreased from 90% to 60-70%RH when a breath test was performed; ii) a variation of about +35% occurred while performing a breath test (Figure 4.10).

In order to take into account such variations in relative humidity which may influence

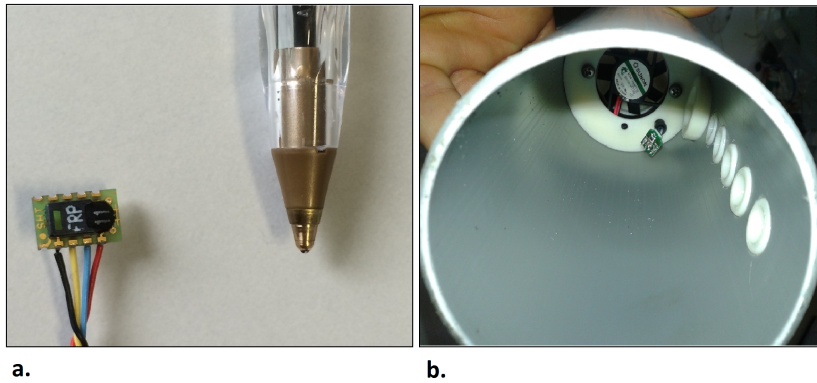


Figure 4.9: Sensirion SHT11 integrated within the sampling chamber.

Taguchi gas sensors behaviour, I i) calculated sensors drift due to variations in humidity; ii) investigated sensors sensitivity in those precise measurement conditions [22] ($30\text{ }^{\circ}\text{C}\pm 7\%$, $70\%\text{RH}\pm 5\%$, the ones that occur in the sampling box during a breath test, as shown in Figure 4.10).

For this purpose, TGS sensors were inserted into a vial (whose volume was 500ml, similarly to the WS gas sampling box), as shown in Figure 4.11. Then, relative humidity into the vial was increased from about 40% up to 65%. Raw sensors output were read by an Arduino Mega2560 connected via serial port to a personal computer. The experimental data were displayed in real time on the computer screen and stored as text files for later processing (which was done by using MATLAB R2014a).

In Figure 4.12, how the humidity strongly affects sensors output (in this case the one of MQ7 gas sensor) is shown. The relationship between humidity and sensors output generally can be modelled by means of a power law (eq. 4.4), as reported also by Barsan and co-workers [85]:

$$V_{out} = f(hum) = a * (hum)^b + c \quad (4.4)$$

where a, b and c are constant.

Calculating sensors humidity drift was useful to potentially compensate it during the data processing. I considered the entire range of humidity variation (40%-65%RH) and then I calculated the slope of the curves. From the slope, drift coefficients were assessed (see Table 4.3) as the decrease in sensors' output (Volt) per unit decrease in humidity, as given in eq. 4.5:

$$S_d = \frac{\Delta V}{\Delta hum} \quad (4.5)$$

4.3. Hardware

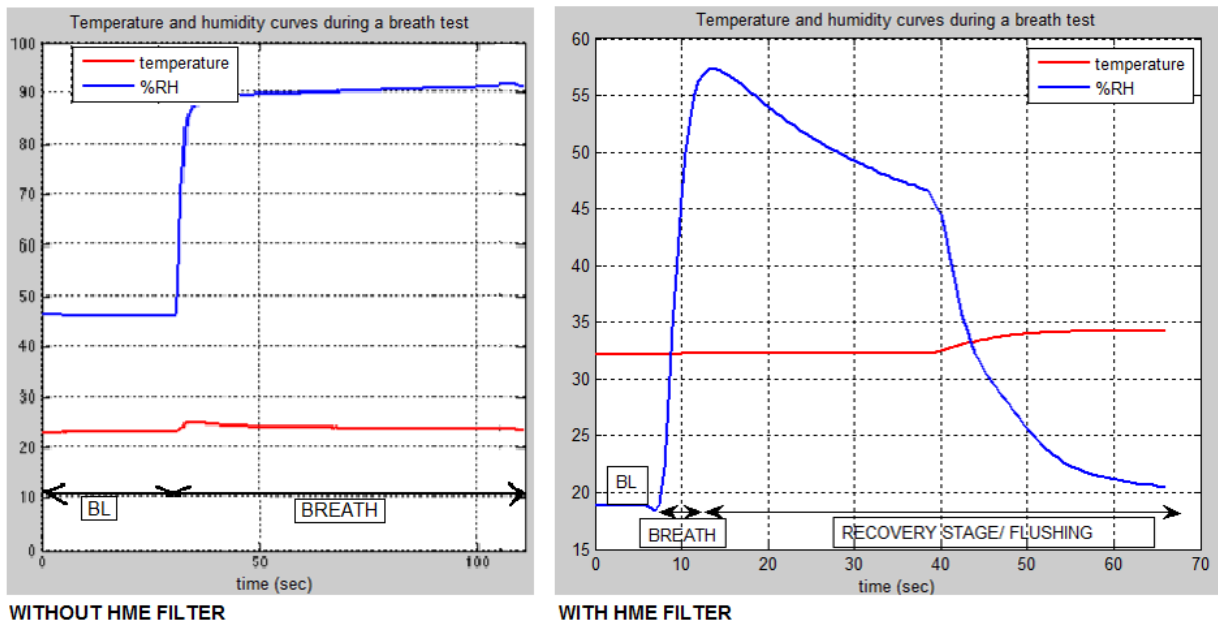


Figure 4.10: By means of Sensirion SHT11, temperature and relative humidity values can be monitored within the gas sampling chamber during a breath test. Without hygroscopic filter on WS mouthpiece, humidity in gas sampling chamber increases up to 90%RH (plot on the left); by putting the HME filter (plot on the right), the humidity increases up to 60%.

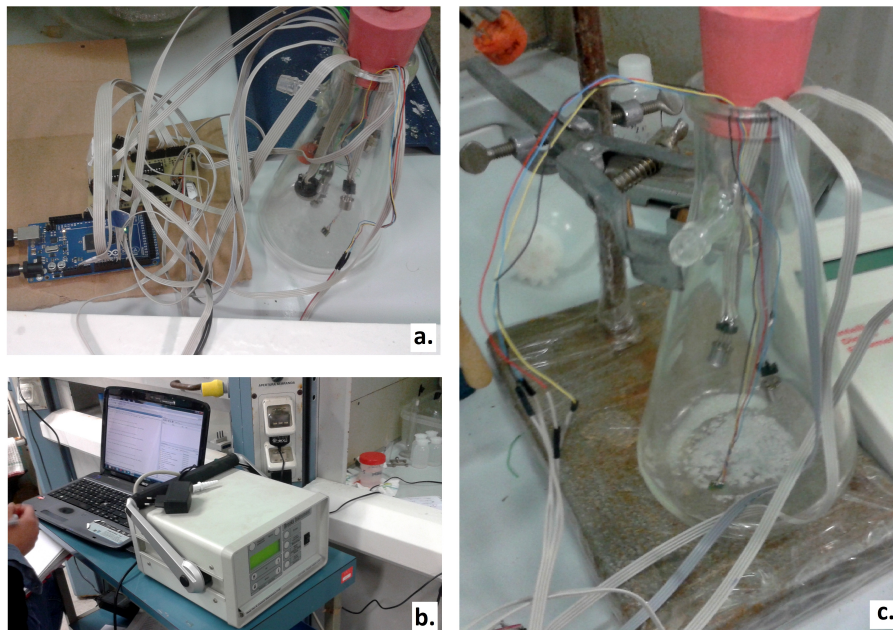


Figure 4.11: Experimental set-up; the data stream from sensors was read by an Arduino Mega2560 board via serial port and displayed in real time on pc screen.

By keeping the humidity constant, sensors output depends on the gas concentration only. For this purpose, as previously mentioned, sensor outputs in response to well-

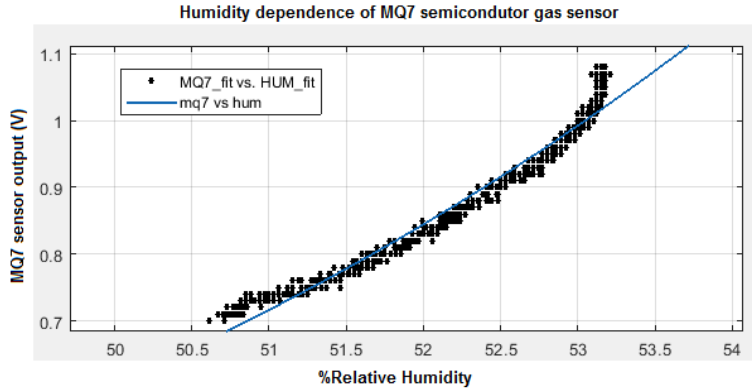


Figure 4.12: MQ7 output when a rise in humidity occurs.

Table 4.3: Sensors drift due to humidity

Sensor	$\Delta V / \Delta \text{hum}$ (mV)
MQ7	296
TGS2620	60
TGS2602	82
TGS821	120
TGS2444	84

known gas concentrations, at a fixed humidity and temperature conditions, were investigated. Also in this case, the used experimental set-up was the one reported in Figure 4.11. The humidity into the vial was kept at 70%RH \pm 5% by means of a saturated solution of *NaCl* placed on the bottom. Measurements were performed only after the sensors were operated at a fixed temperature for several hours (at least 2 hours for warm-up). Then, well-known gas concentrations, were injected and sensors raw output were read by an Arduino Mega2560 connected via serial port to a personal computer. The experimental data were displayed in real time on the computer screen and stored as text files for later processing. Just as example, in Figure 4.13, we can see TGS2620 output when well-known concentrations of carbon monoxide (*CO*), ethanol (*C₂H₆O*) and hydrogen (*H₂*) were separately injected into the vial. The relationship between sensors output and each gas contribution can be modelled by means of the previously reported equation 4.3.

Nevertheless, when a breath analysis is performed, a mixture of gases spreads into the gas sampling box and chemically interacts with the sensors. In this case, the phenomenon known as **cross sensitivity** makes the semiconductor gas sensors non-selective. In addition, the detection threshold (that is, the minimum concentration of gas necessary to a meaningful change in sensors conductivity) depends not only on absolute sensitivity to that particular gas but also on concentrations of other gases, which partially mask the response to the gas of interest [81], as shown in eq. 4.6.

$$\left(\frac{R}{R_0}\right)^{-\frac{1}{\beta}} = \frac{(1 + \sum K_j * [G_j]^{n_j} * K_i * [G_i]^{n_i})}{[O_2]} \quad (4.6)$$

Where $[G]$ represents the gas concentration and n is an integer or fractional integer power. In some cases, for some terms of the summation, there is only one term per gas,

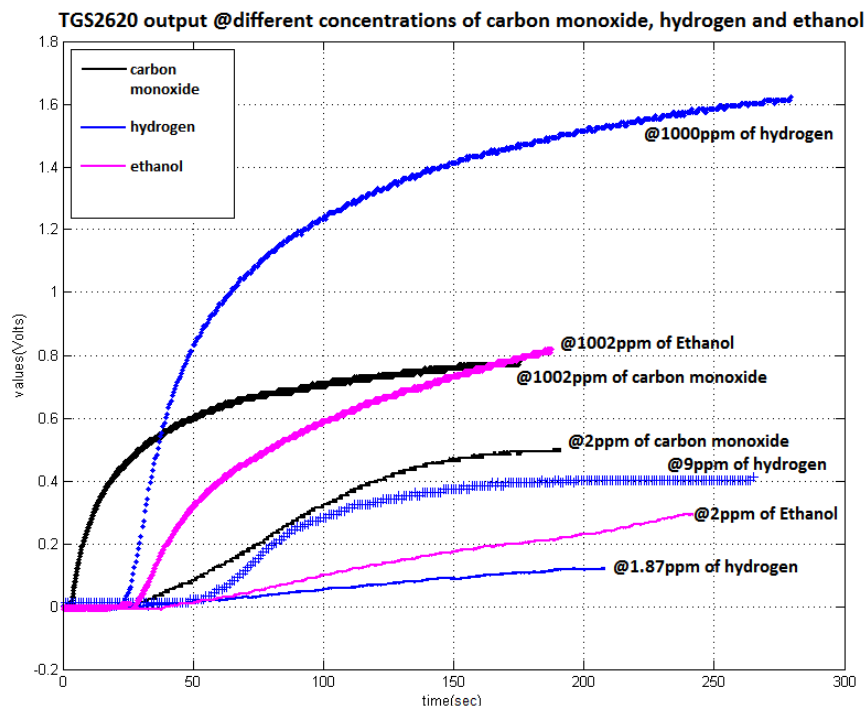


Figure 4.13: TGS2620 output when well-known concentrations of CO , H_2 and C_2H_6O were separately injected into the vial.

for others there is a product of several.

However, because of the multitude of factors involved, understanding the interaction mechanism behind the MOS-based gas sensors' sensing property in general remains an open issue [21].

Also, I tried to investigate the cross sensitivity of Taguchi gas sensors. In Figure 4.14, we can see TGS2620 response when well-known mixed concentrations of the three gases (carbon monoxide, ethanol and hydrogen) were simultaneously injected into the vial. In this way, how the different VOCs add together and influence gas sensors' output (in Volt) can be understood. The single gas contribution can be modelled by a power law similar to the eq. 4.3 but each of them has its "weight" on the overall output, as shown in eq. 4.6.

To sum up, both from the literature and the experimental tests, we can affirm that:

- on one hand, semiconductor gas sensors are affected by different factors, such as:
 - temperature: operating temperature affects the receptor function, as it influences, according to a well-defined functional dependence [81], the power law exponent β . The problem was solved by integrating a heating voltage in the sensors' measurement circuit, in order to keep them at a constant temperature (about 200-500 °C), as suggested by sensors datasheet and shown in Figure 4.6;
 - oxygen partial pressure: oxygen plays an important role in dry atmosphere (as shown in eq. 4.2). In dry atmosphere, it acts as an electron acceptor, forms an ionic layer on the surface and helps in sorption of other gas molecules

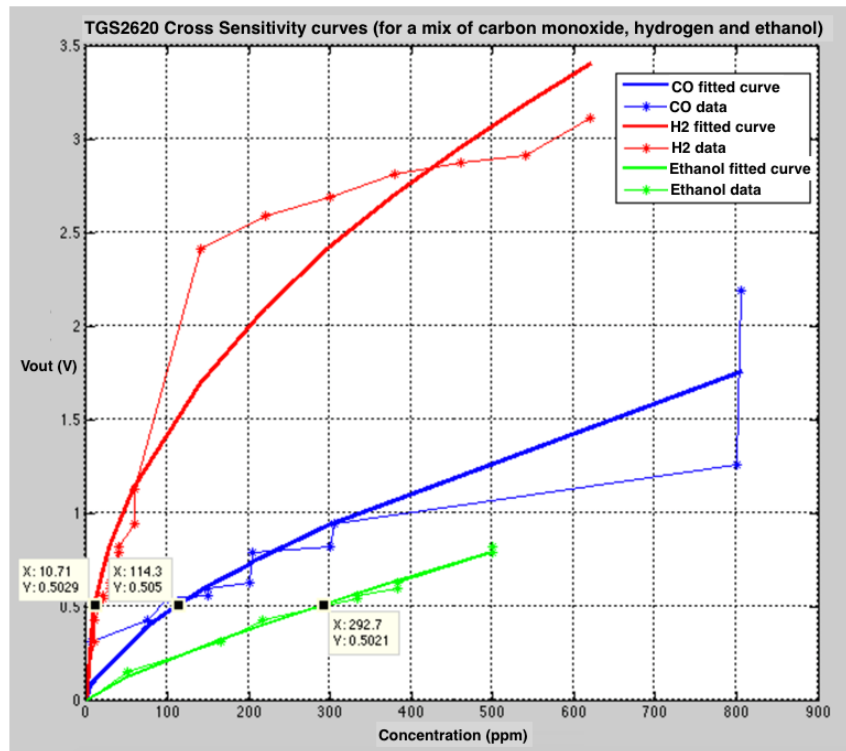


Figure 4.14: TGS2620 output (in Volt) in response to well-known mixed concentrations (ppm) of CO, H₂ and C₂H₆O.

on to the metal oxide surface. In this case, breath tests will be performed in ambient air conditions. As a consequence, oxygen partial pressure will not influence gas sensors' behaviour (eq. 4.3);

- humidity: as shown in Figure 4.12, when humidity increases, resistance of the n-type-based film decreases. To manage humidity influence, I: i) integrated a filter, made of hygroscopic material, at the WS mouthpiece, in order to absorb at least 30-40% of the water vapour present in human exhaled breath; ii) integrated, within the gas sampling chamber, a Sensirion SHT11 in order to monitor the humidity when a breath test is performed and eventually compensate (during the data processing) the resulting sensors drift; iii) investigated sensors sensitivity characteristic in the same measurement conditions (30 °C ± 7%, 70%RH ± 5%) that occur in the sampling box during a breath test;
- cross-sensitivity: as shown in eq. 4.6, the conductivity response depends on a linear combination of individual gas terms, where the effects of one gas can be masked by the combined effects of others. In addition to this "competition" among gases, there is an associative interaction by which the effects of one gas are enhanced by the presence of another. I tried to investigate and understand such type of phenomenon, as shown in Figure 4.14; nevertheless, because of the multitude of factors involved, understanding the interaction mechanism behind this phenomenon remains a challenge. However, as described in chapter 5, pattern recognition techniques allow for overcoming this

problem.

- on the other hand, concerning both the literature and experimental tests, such type of gas sensors show long term stability and reproducibility of gas response [81], great metallurgical and chemical stability of the sensing material [81], high sensitivity towards target gases, short reaction and recovery time, easy calibration. In addition, they are small, compact, durable and inexpensive (about 25-40 Euro).

In Figure 4.15 the gas sampling chamber and the gas sensors are shown.

In addition, in order to facilitate sensors recovery time, a flushing pump was integrated



Figure 4.15: *First prototype of the sampling chamber with gas sensor array.*

on one side of sampling chamber, as shown in Figure 4.16. After each breath test, it can be switched on in order to "purge" the chamber with ambient air and recovery sensors baseline.

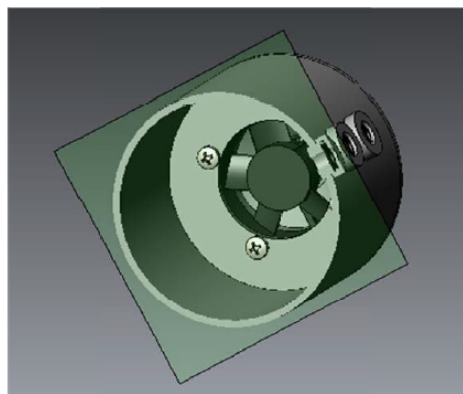


Figure 4.16: *Flushing pump on the one side of the sampling chamber.*

4.3.2 The corrugated tube, the heat and moisture filter and the flow-meter

The exhaled gases reach the gas sampling chamber by means of a corrugated tube made of polyvinyl chloride (PVC), as shown in Figure 4.17. A HME filter, made of hygroscopic material, absorbs the water vapour present in human breath and stifles the

Chapter 4. The Wise Sniffer

bacteria.

A PNT Flow-Ree flow-meter (Figure 4.18) allows to monitor the user's breath flow rate



Figure 4.17: The corrugate tube (made of PVC) with the heat and moisture (HME) filter.

by calculating the pressure difference on its ends by means of a pressure sensor (PCLA Series). The flow-meter and the pressure sensor (measurement range: $0 \pm 10 \text{ ml/sec}$; accuracy after calibration: $\pm 2\%$; accuracy without calibration: $\pm 10\%$; resolution: 1 ml/sec) were provided by COSMED s.r.l.

In Figure 4.19 the PNT Flow-Ree raw curves are shown, both in case of slow blow-

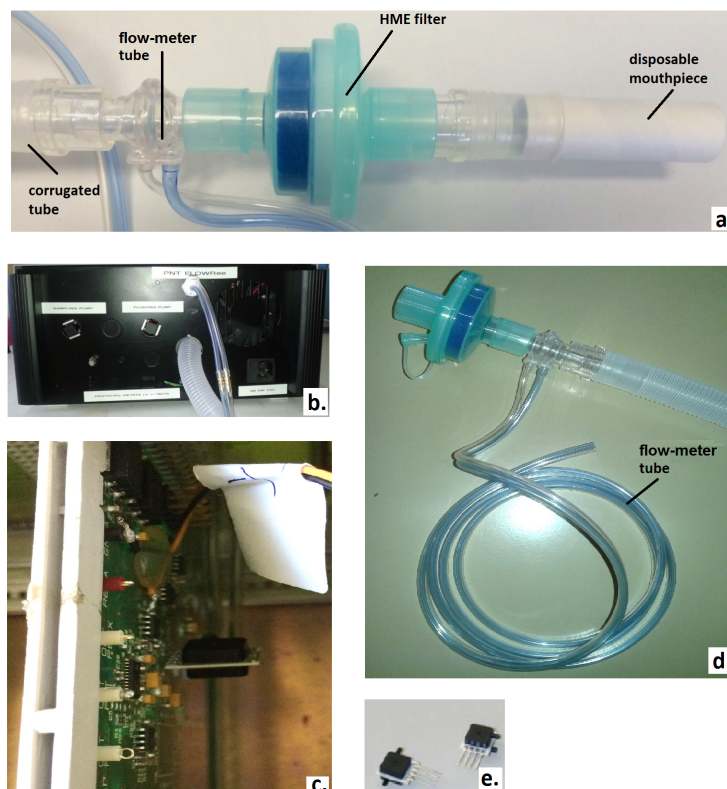


Figure 4.18: a) and d) The disposable mouthpiece, the HME filter, the flow-meter tube and the corrugated tube; b) the connection of the flow-meter to the WS; e) the used pressure sensor (PCLA Series); c) the pressure sensor board integrated into the WS.

ing and in case of fast blowing. Sensors raw output is represented by a voltage; by

means of the sensor in/out characteristic, the user's flow rate and exhaled volume can be calculated.

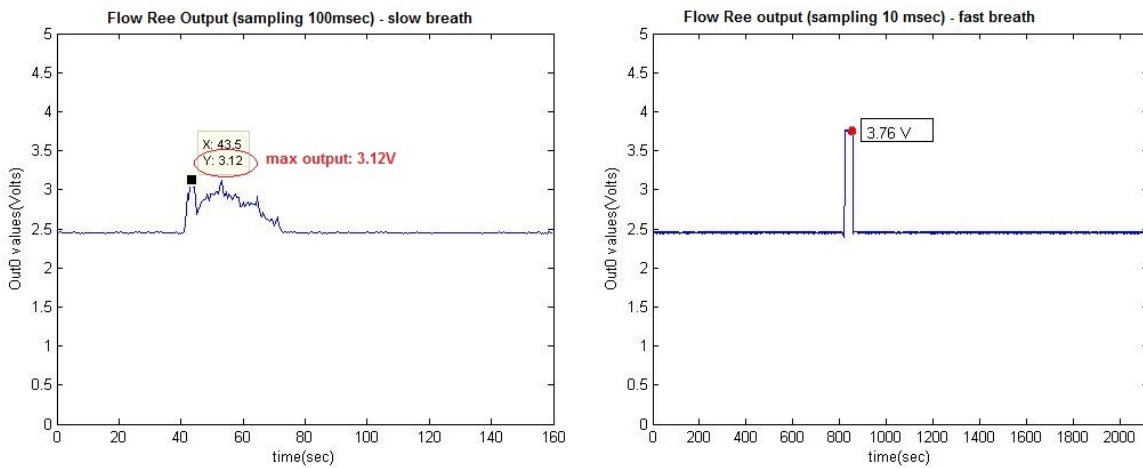


Figure 4.19: PNT Flow-Ree raw data (Volts).

4.3.3 The sampling pump and the CO_2 and O_2 gas sensors

Other two gas sensors were integrated into the WS. Because of their faster response, they work in a *flowing regime*. Indeed, a sampling pump injects, at a fixed rate (120ml/sec), the breath gases stored into the gas sampling box to these sensors. In Figure 4.20 the sampling circuit and the gas sensors are shown.

They allow to monitor exhaled CO_2 and O_2 , as reported in Table 4.4. They were provided and integrated into WS case by COSMED s.r.l..

By the IR1507 sensor, having a faster response than TGS4161 sensor, I intended to

Table 4.4: CO_2 and O_2 sensors characteristics.

Sensor	MOX 20, City Technology
Functioning principle	Electrochemical cell
Target gas	Oxygen
Measurement range	0-1500mBar
Output	0.8-1.25V in air
Response time	<750ms
Sensor	IR1507, Servomex
Functioning principle	NDIR sensor
Target gas	Carbon dioxide
Measurement range	0-40% (40000ppm)
Output	0-4.5V
Response time	100ms

monitor user's capnogram, in order to sample only systemic volatile biomarkers, if needed², and monitor the quality of the breath test.

²as reported in chapter 2, the end-tidal expired gas is collected when the plateau of CO_2 curve is reached. Such method is used if only systemic volatile biomarkers are to be detected, that are those VOCs that have endogenous origins and participate to alveolar exchanges

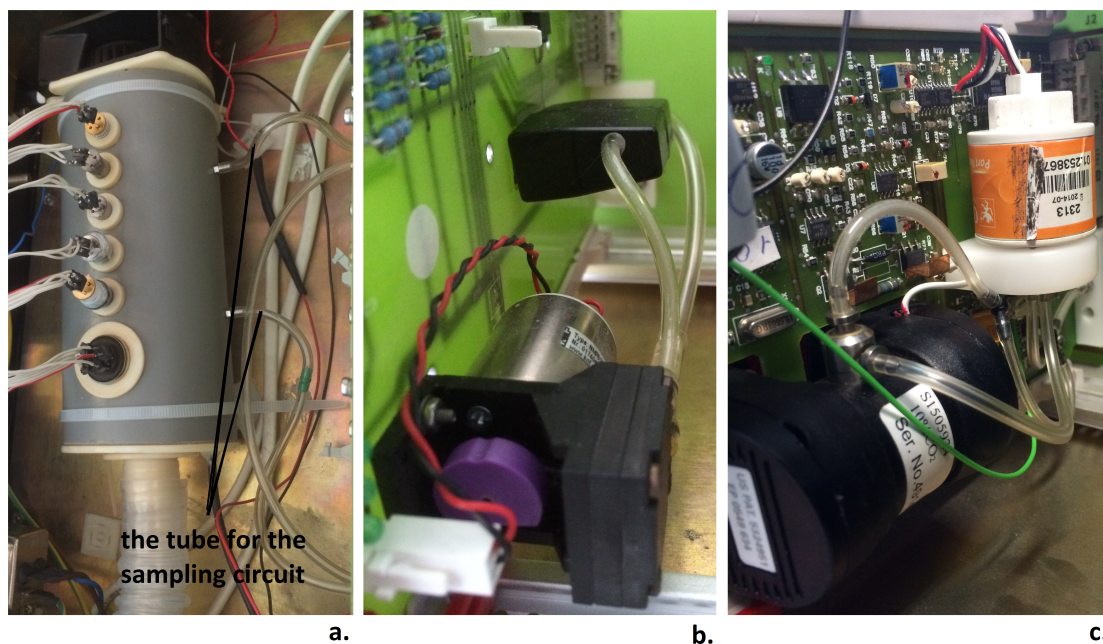


Figure 4.20: a) a tube of small diameter coming out of gas sampling chamber; b) the sampling pump; c) CO_2 and O_2 gas sensors.

4.3.4 The signal conditioning module and Arduino board

I developed a signal conditioning module in order to stabilize and transfer sensors raw signals to the micro-controller board. Its scheme, designed by Eagle CAD, is shown in Figure 4.21.

A series of voltage buffer amplifiers (LM124-N, Texas Instrument) were used to stabilize and transfer sensors raw signal to the micro-controller board. The power circuit and the heating circuit were separated, because the second one requires more current than the first and overloads the 5 V power supply. Two resistances of $10K\Omega$ each were used as pull-up resistances in order to stabilize the clock and the output of the Sensirion SHT11. $15K\Omega$ load resistances R_L were used for TGS sensors measurement circuit. To read sensors output and to pre-process them, a widely employed open-source controller was used: an Arduino Mega2560 with Ethernet module (cost: about 45Euro).

4.3.5 The final hardware configuration

In Figure 4.22 and 4.23 the WS final configuration is shown. Its dimensions are: 30x30x14cm. The case of the device was realized in collaboration with COSMED s.r.l.. The user blows into the corrugated tube made of PVC; a hygroscopic filter absorbs the majority of the water vapour present in the exhaled breath, allowing for reducing the humidity of -30%. A PNT Flow-Ree flow-meter allows for monitoring the user's flow rate and for calculating the exhaled gas volume. Indeed, a measure is considered "valid" if the subject's exhaled volume is at least 600ml. The gases reach the gas sampling chamber, where an array of six semiconductor-based gas sensors are placed. Within the gas sampling box, also a sensor for temperature and humidity (Sensirion SHT11) is placed. In addition, a sampling pump injects, at a fixed rate (120ml/sec), the

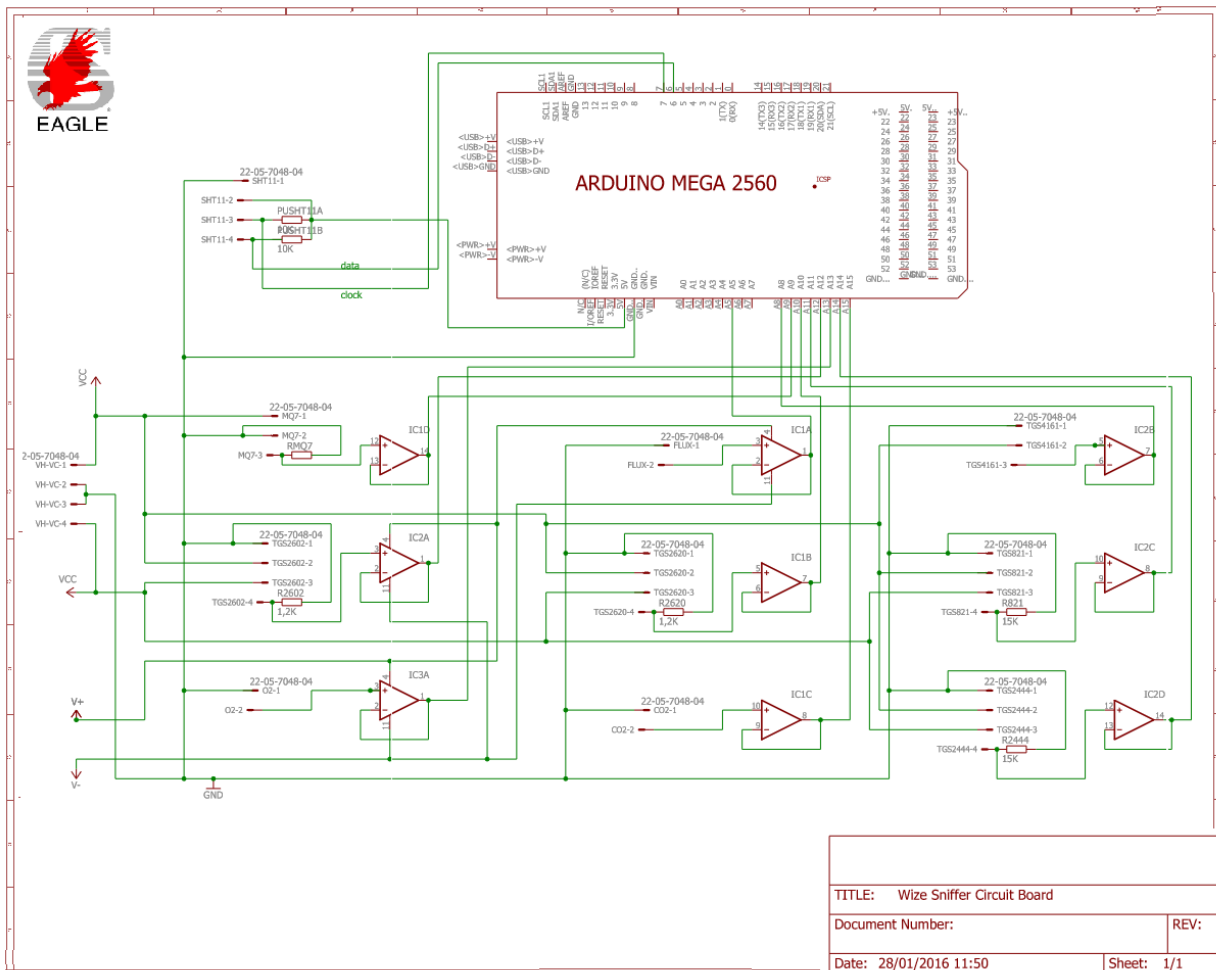


Figure 4.21: WS pre-processing circuit (schematic) designed by Eagle CAD.

sampled exhaled gas to other two sensors which have faster response time and work in *flowing-regime*. They detect oxygen and carbon dioxide and are respectively based on an electrochemical cell and an infrared source. Sensors raw output are pre-processed and stabilised by a signal conditioning module: a series of voltage buffer amplifiers (LM124-N, Texas Instrument) transfers sensors signals from the measurement module to a widely employed open source controller: an Arduino Mega2560. Finally, in order to facilitate sensors recovery time, a flushing pump was integrated on one side of sampling chamber. After each breath test, it can be switched on in order to "purge" the chamber with ambient air and recovery sensors baseline.

As previously reported in subsection 4.3.1 and 4.3.4, WS core (TGS sensors + Arduino board) is entirely based on low-cost technology. Indeed, its total cost is lower than 500 Euro, thus meeting the requirements of Table 4.1. However, in order to have a complete picture of WS cost, all components and labour must be included. This would put the total unit cost at least at 1000-1500 Euro, since most of the components of the device have to be manually assembled. The multiplier for a commercial version is typically 5-10, to cover marketing, support, etc. This would put the WS commercial cost at least



Figure 4.22: The Wize Sniffer while performing a breath test.

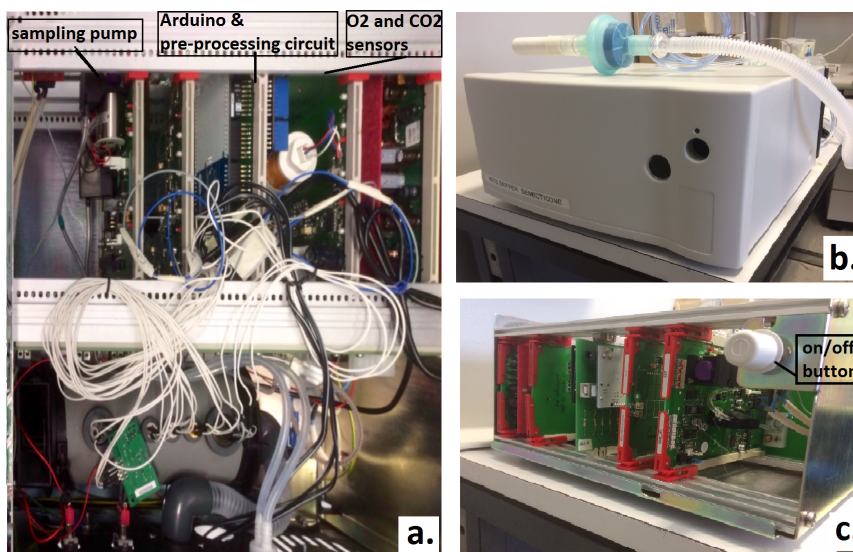


Figure 4.23: Details of Wize Sniffer hardware final set-up: a) internal configuration; the gas sensors in the gas sampling chamber are shown, as well as the sampling pump circuit, the Arduino board and the CO₂ and O₂ gas sensors. b) external configuration; c) WS back side.

5K-15K Euro with considerable opportunities to reduce such prototype cost through economies of scale.

In addition, an Arduino Ethernet module was integrated in order to send breath test results also to a remote healthcare centre, or a personal computer in general, by means of an internet connection. The combination of a localized monitoring using an e-nose and data transmission methods provides a means of extending the effective range within which medical doctors can provide services and offer clinical support.

4.4 Data processing

Signal and data processing constitute a critical step in the development of an electronic nose device capable of detecting, identifying and measuring volatile compounds. Proper processing can improve the robustness of the instrument against the diverse influencing factors, namely, environmental variables, background changes, sensors drift, sensors cross-sensitivity, etc.

The processing of WS raw data is composed of two steps: firstly, sensors output are read and pre-processed by Arduino; a second step of analysis was implemented in MATLAB environment. With the concept of implementing, in future, the whole data processing on Arduino, my aim was to develop a simple and computationally inexpensive method, which was also suitable, smart and robust, to make the Wize Sniffer able to understand individual's cardio-metabolic risk from his/her breath composition.

4.4.1 Data pre-processing

Pre-processing stage is somewhat tied to the underlying sensor technology: therefore it aims, on one hand, at compensating the factors which can influence and affect the measure; on the other hand, it aims at carefully selecting significant descriptive parameters from the sensor array response and preparing the feature vector for further analysis.

I programmed Arduino Mega2560 (with Ethernet module) in order to read and pre-process sensors output in real time. In addition, in order to send breath analysis results also to a remote personal computer, a client-server architecture was implemented. It means that, after performing a test and processing the results, the device, by means of an internet connection and a TCP/IP communication protocol, can send the results to the physician, for instance. Arduino is programmed to execute a daemon on port 23. By implementing a Telnet server, it waits for a command line from the remote personal computer and then can provide the data.

The workflow of the software implemented on Arduino board is shown in Figure 4.25. First, the needed libraries are uploaded (the ones designed to work with the Arduino Ethernet Shield, the ones for reading data from Sensirion SHT11, and finally the ones to compute common mathematical operations and transformations) and the network parameters (for instance, the IP address of Arduino Ethernet shield) are configured, as shown in the first block in the flow-chart in Figure 4.25.

Second, the several variables and vectors are initialized, as well as the Ethernet shield: the server starts listening for clients (block 2 and 3 of the flow-chart).

Then, for each sensor, the output is read every 0.250 sec and saved in a vector. In addition, also temperature and humidity values before and after the breath test are read and saved in a vector (block 4a and 4b of the flow-chart).

By means of flow-meter outputs, the exhaled volume is calculated (block 5). If it is lower than 600ml (that is, gas sampling chamber's volume), the breath test must be repeated because the measure is considered not valid. In this case, the exhaled volume is not sufficient to perform the analysis. Otherwise, if the exhaled volume is greater than 600ml, block 6 and 7 are executed: in these steps, sensor outputs are pre-processed and the drift due to humidity is compensated.

First, the baseline is manipulated. Three baseline manipulation methods are commonly used [86, 87]: i) the *difference* method subtracts the baseline and it is used to eliminate additive drift from sensor response; ii) *relative* manipulation divides by the baseline, remove multiplicative drift and generates dimensionless response; iii) *fractional* manipulation subtracts and divides by the baseline, generating a dimensionless and normalized response. Here, the fractional method for baseline manipulation was used, as it removes both additive and multiplicative errors.

In addition, three features are extracted from each sensor output signal. Several parameters and features can be extracted from sensors output curves to fully characterize them [88, 89]. Feature extraction method is one of the key-points of performance improvement of an e-nose systems, as it is the first step of the sensors signal analysis. The aim of feature extraction is to extract robust information from sensors' response which may represent the different finger-print, or, in this case, breath-print patterns as well as possible. I chose to extract, for each sensor output signal (see Figure 4.24):

- the value at curve plateau ($\Delta X_s(\infty)$), as it better describes the chemical balance between sensors sensing element and target gases, and represents the final steady state feature of the entire dynamic response process [88, 90–92];
- the response time T_r , as it is characteristic of each vapour/sensor pair, concentration independent and shows high repeatability [93]. It is measured from 20 to 75% of $\Delta X_s(t)$;
- the maximum slope of the curve.

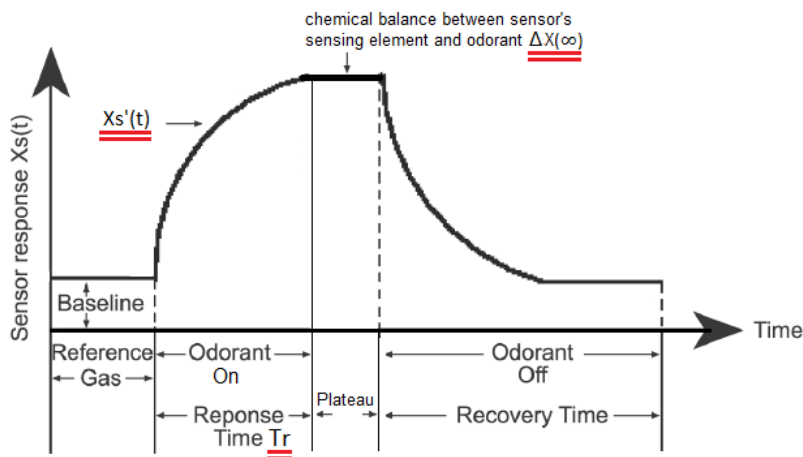


Figure 4.24: The three extracted features from a typical gas sensors output (adapted from [36]).

Finally (block 8), if a client is asking for the results, they are transmitted by means of a TCP/IP protocol and an internet connection.

4.4.2 Data analysis

As previously described, the Wise Sniffer was designed to detect a set of volatile molecules present in human breath and related to the noxious habits for cardio-metabolic

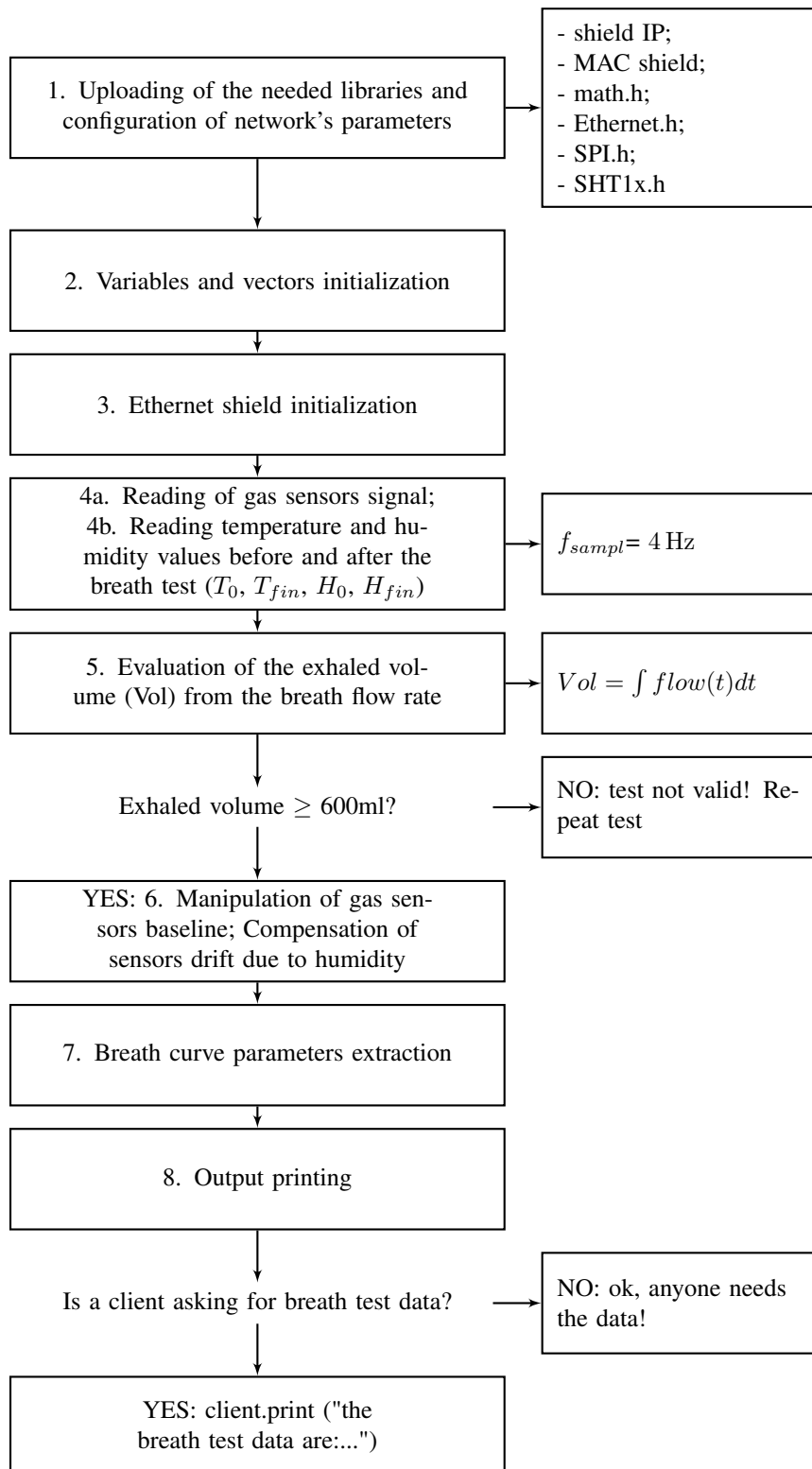


Figure 4.25: Workflow of the software implemented on Arduino Mega2560 board

risk. Indeed, the clinical assumption behind the Wise Sniffer lied in the fact that harmful habits such as alcohol consumption, smoking, unhealthy diets cause a variation in the concentration of a set of molecules (listed in section 4.2) in the exhaled breath.

The scores from clinical questionnaires relative to alcohol consumption (AUDIT test), smoking (Fagerstrom test) and lifestyle in general, were the ground-truth. Therefore, the more dangerous the habits will be, the higher the scores and the higher the cardio-metabolic risk.

For this purpose, my aim was to develop a suitable, smart and robust method for data analysis, to make the Wise Sniffer able to understand individual's cardio-metabolic risk from his/her breath composition. In addition, the developed method was supposed to be also simple and computationally inexpensive, in order to subsequently implement it on WS hardware/software platform. Finally, the result was supposed to be clear, intuitive, easily interpretable not only by expert personnel.

Data pre-processing step returns 3 features for each gas sensor. Once normalized and zero-centred the data, in order to highlight their qualitative aspects, counteract possible fluctuations, and equalize the dynamics of sensors' responses [94], my idea was to firstly reduce the dimensions of the input space, in order to smartly cram the information contained in the data.

Several approaches for dimensionality reduction can be found in literature [86, 88, 94]: i) direct use of subspace projection methods such as PCA (Principal Component Analysis), LDA (Linear Discriminant Analysis), FFT (Fast Fourier Transform), DWT (Discrete Wavelet Transform); ii) curve fitting methods; iii) wave-form descriptors; iv) non-linear subspace projections such as SOM (Self-organizing maps), Sammons mapping; v) clustering in feature space, etc.

Here, two methods for data reduction were taken into account: **Principal Component Analysis (PCA)** and **Independent Component Analysis (ICA)**.

PCA is the most common and computationally inexpensive approach for data reduction. The objective of PCA is to express the information in the variables in the input data matrix by a lower number of variables called *principal components*. It has been successfully applied to analyse response of tin oxide-bases gas sensors [17, 93, 95]. The possibility of a reliable representation of e-nose data in a space of reduced dimensionality lies in the fact that chemical gas sensors always exhibit a certain degree of correlation among them. PCA, by exploiting such correlation, consists in finding an orthogonal basis where the correlation among sensors disappears and the data show the maximum of variance. It is a second-order linear data transformation method, and it assumes that the data follow a Gaussian distribution [94]. Indeed, PCA is performed considering only the second momentum of the probability distribution of the data, as for normally distributed data the covariance matrix ($X^T X$) completely describes zero-centred data. The k -th principal component (PC) is a linear combination of the m features X_{ij} extracted from the n gas sensors. The k -th principal component for the j -th sample can be expressed as follows (eq. 4.7):

$$PC_k = \sum_{i=1}^{m*n} \alpha_{ij} * X_{ij} \quad (4.7)$$

where α_{ij} are the eigenvectors of covariance matrix (or *loadings*) and measure the contribution of each sensor feature to the PCA basis. The new coordinates of each gas

sensor feature vector (a column of X) in the PC base are called *scores*. The percentage of data variance contained in each PC is given by the eigenvalues of covariance matrix. The highest eigenvalues correspond to components defining the directions of highest correlation among sensors. By using only the most meaningful components (that is, explaining the maximum of variance), the noise of the sensors is also removed.

PCA, by exploiting gas sensors cross-correlation, performs well in many cases. This fitted well also in this case, as my dataset resulted from cross-sensitive gas sensors measurements. Nevertheless, PCA assumes that the data follow a Gaussian distribution. This might be a strong limitation: in fact, the joint distribution of gas sensor array measurement data often appears to be non-Gaussian. The measurement related to the same cluster may exhibit a Gaussian distribution, but, in this case, the samples would have been extracted from more than one cardio-metabolic risk class, thus not resulting in a normally distributed data set.

ICA can be viewed as an extension or generalization of PCA, since it is a higher order statistical tool, and it assumes that the data are non-Gaussian in nature [94, 96]. ICA aims to find a coordinate system that makes the original signal from the unknown source as independent as possible, by using higher-order statistics from the probability densities of the data. ICA is a novel method in the analysis of gas sensor array measurement data and seemingly indicates potential to improve the performance of the instrument [92, 97, 98]. ICA fitted well in this case, as breath signals and the environmental ones (noise) get mixed with each other before the chemical interaction with the sensor array. In addition, due to sensors cross-sensitivity effect, the conductivity response depends on a linear combination of individual gas terms, where the effects of one gas can be masked by the combined effects of others. In addition to this "competition" among gases, there is an associative interaction by which the effects of one gas are enhanced by the presence of another. As a consequence, each sensor output is the result of a combination of different gaseous contributions, as shown in eq. 4.8

$$x_t = a_{t1}s_1 + a_{t2}s_2 + a_{t3}s_3 + \dots + a_{tn}s_n \quad (4.8)$$

where s_1, s_2, \dots, s_n are the independent sources which have been mixed together through a linear system and contribute to the sensor response. Their number is not necessarily well defined [92]. For simplicity, the eq. 4.8 can be written also as the mixing model in eq. 4.9:

$$X = A * S \quad (4.9)$$

where A is the mixing matrix containing the elements a_{tj} . This model is called **noise-free ICA model** [92,99], and the estimation of $W = A^{-1}$ is the aim, in order to extract S . Several different algorithms have been proposed in literature to perform ICA [100–103]. I used FastICA algorithm, implemented in MATLAB R2014a environment, as it was very flexible and very accurate. Before ICA is applied, it is usually recommended to remove redundant information in the original data matrix (X in our case) with the help of PCA [92]. In addition, although the traditional procedure is projecting original data to PCA eigen space firstly and processing the mapped new data with ICA secondly [104], I chose to apply ICA directly to the PCA eigen matrix M , to obtain ICA eigen space U and project the original data matrix X to the final ICA eigen space U . This choice was made to reduce the computational cost [105].

In more detail, I chose to firstly extract, zero-centre and whiten PCA eigen matrix

M_c . Whitening of the matrix M_c with zero-mean components usually greatly simplify the application of ICA [92, 97, 100]. Whitening is a process of transforming a matrix linearly so that a new matrix is obtained whose components are uncorrelated and their variances equal unity (see eq. 4.10 and 4.11).

$$E\{M_c M_c^T\} = E D E^T \quad (4.10)$$

$$M_{cw} = E D^{-\frac{1}{2}} E^T M_c \quad (4.11)$$

where M_c is the covariance matrix, E its eigenvectors orthogonal matrix and D its eigenvalues diagonal matrix. The centred and whitened PCA eigen matrix M_{cw} is given by the eq. 4.11. ICA, directly applied to M_{cw} , provides for the new ICA eigen space (eq. 4.12):

$$U = W * M_{cw} \quad (4.12)$$

Where $W = A^{-1}$. Finally, the original data matrix can be directly mapped to the ICA eigen space U , according to the eq. 4.13:

$$Y = X * U^T \quad (4.13)$$

I chose to run the FastICA package using the symmetric approach, wherein all the independent components are simultaneously separated, and the non-linearity function $g(u) = \tanh(u)$.

A first set of normalized and zero-centred breath data were used to compared the performance of PCA and ICA. PC scores were plotted against the subjects' risk score (RS, that means, the sum of the scores of the questionnaires on the noxious habits), as shown in Figure 4.26A. From an exploratory analysis, I saw that except for PC3, the PC scores did not have a sharp increasing or decreasing linear trend with respect to RS, thus not having enough information to contribute to any prediction or classification model [23]. Also individual ICs were plotted against subjects' RS. As shown in Figure 4.26B., in this case sharper linear trends emerged, thus showing enough information to build a prediction model. Thus, from a visual inspection of Figure 4.26A. and B., ICs seemed better candidates for building a model which was able to predict subjects' cardio-metabolic RS form breath data. This result, supported also by the study of Balasubramanian and co-workers [97], lead me to use independent components rather than principal components (although PCA undoubtedly is computationally less expensive than higher order methods [92]) to build a prediction model.

In particular, my idea was to implement regression techniques in order to create a smart, computationally inexpensive, optimized model able to evaluate subjects' cardio-metabolic risk score on the base of their breath composition.

4.4.3 Data handling: development of a Graphical User Interface (GUI)

With a view to a validation campaign, I developed a graphical user interface (GUI) in MatlabR2014 environment in order to acquire data from Arduino and save both raw data and the extracted features in .txt files. Also, the GUI permitted to visualize sensors raw signals in real time to evaluate the quality of each breath test. In Figure 4.27 an example of the GUI is shown. The workflow of the code implemented in Matlab environment for the development of the GUI is shown in Figure 4.28.

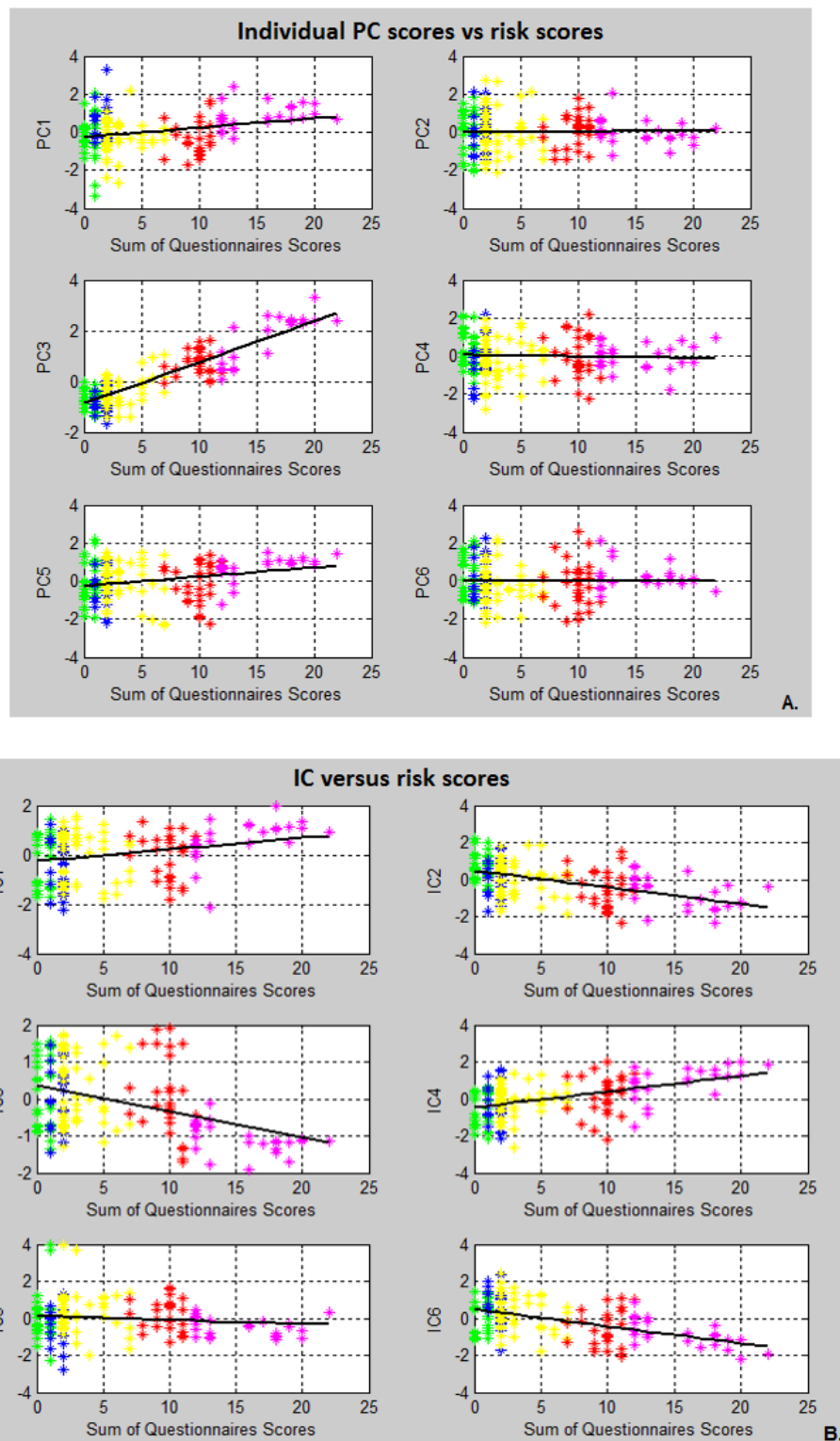


Figure 4.26: A. PC scores against subjects' RS arranged in ascending order; B. IC scores against subjects' RS arranged in ascending order. Green points correspond to no-risk subjects, the blue ones represent low-risk subjects, the yellow ones correspond to medium-risk subjects, the red ones to the high-risk subjects, the magenta ones represent very high-risk subjects.

Chapter 4. The Wise Sniffer

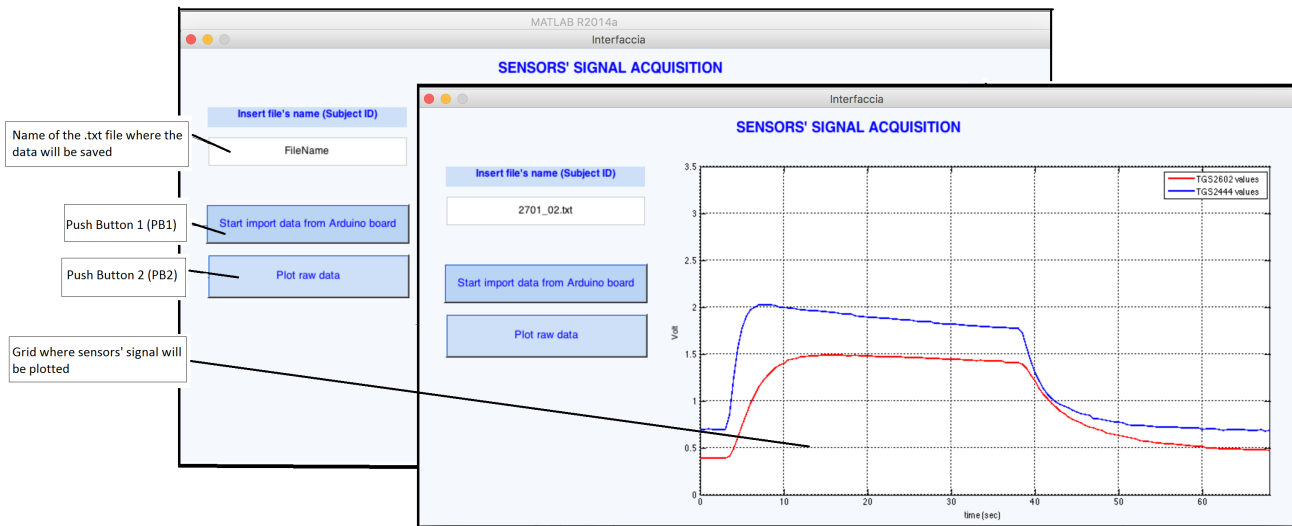


Figure 4.27: The GUI implemented on Matlab to acquire data from Arduino and an example of sensors' signals visualization.

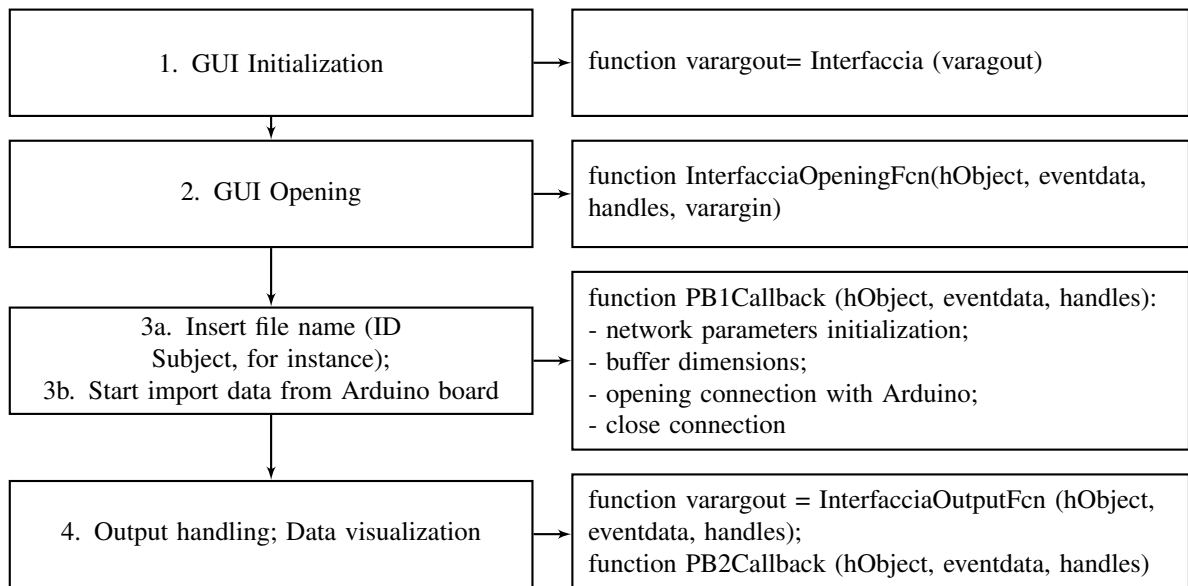


Figure 4.28: Workflow of the GUI

CHAPTER 5

WS validation: self-monitoring the breath for the prevention of cardio-metabolic risk

5.1 Introduction

The developed technological and data analysis methods were validated. The capabilities of the WS in understanding individual's cardio-metabolic risk on the base of his/her noxious habits identified by analysing the breath.

A population of healthy volunteers was involved. All the individuals with chronic illness, neurodegenerative disorders or consuming medication on a regular basis were excluded. As the general goal of SEMEOTICONS Project was focused on preventive medicine, the aim of our validation was not to provide a diagnosis, rather than to identify users' harmful habits, by analysing their breath composition, and help them prevent/reduce the cardio-metabolic risk.

Here, the study, the used test protocol and finally the results are described.

5.2 The data acquisition campaign

The study included 169 volunteers overall, among which 77 subjects involved in SEMEOTICONS validation campaign (held in three clinical research centres: National Research Council, CNR, in Pisa and Milan and Centre de Recherche en Nutrition Humaine, CRNH, in Lyon) and the remaining others involved in the previous acquisition campaigns. The women were 80, the men 89; the mean age range was 30-60 years old. Subjects suffering from comorbid diseases (chronic illness, lung and heart diseases, diabetes, cardiac or renal insufficiency, COPD, celiac disease, neurodegenerative disorders) and/or consuming medication on a regular basis were excluded, also in order not

Chapter 5. WS validation: self-monitoring the breath for the prevention of cardio-metabolic risk

to affect the tests.

The study was approved by the Ethical Committee of the Azienda Ospedaliera Universitaria Pisana, protocol n.213/2014 approved on September 25th, 2014; all patients provided a signed informed consent before enrolment

The volunteers had different habits and lifestyle as shown in Figure 5.1 and 5.2.

They were asked to answer the Alcohol Use Disorders Identification Test (AUDIT)

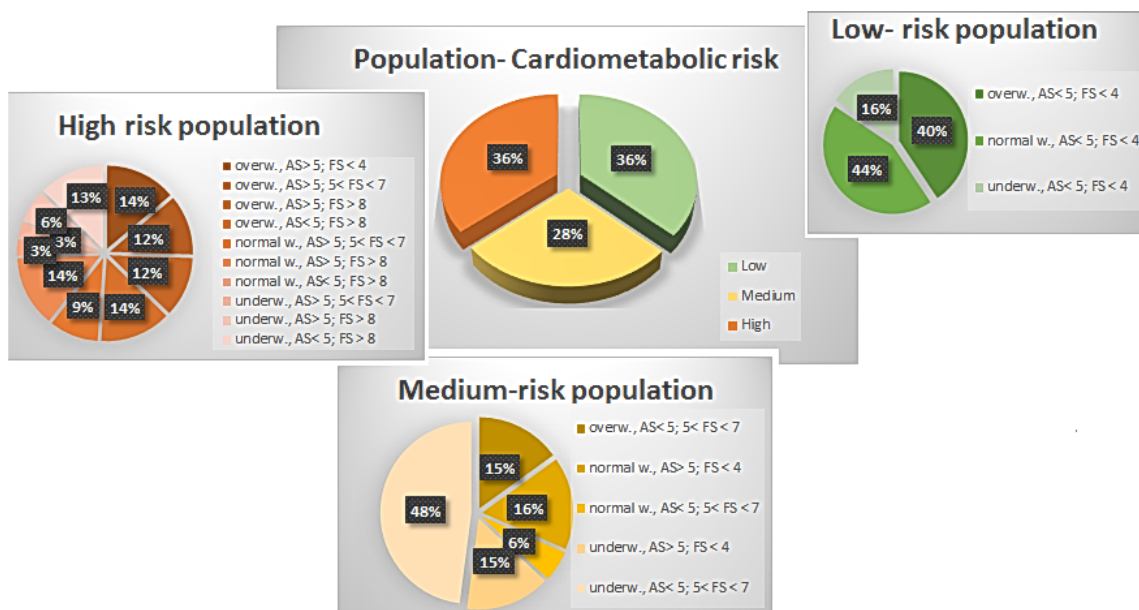


Figure 5.1: The population of volunteers described according to their cardio-metabolic risk level. AS= AUDIT score; FS= Fagerstrom score; overw.= overweight; underw.= underweight; normal w.=normal weight.

and Fagerstrom questionnaire, and another questionnaire about lifestyle in general. The **AUDIT test** was developed in 1987 by the World Health Organization (WHO) to identify risk drinkers. Proposed as an oral interview or written test, also self-administered, consists of 10 items divided into 3 groups with closed answers. Each answer is scored from 0 to 4. With a score ranging from 8 to 14, the subjects has an unsafe consumption, or has or has had alcohol-related problems (although probably he is not physically alcohol-dependent); with a score equal to or greater than 16, the patient has alcohol-related problems and/or is an alcohol-dependent person [106]. In collaboration with the clinicians, I lowered the threshold for the unsafe consumption from 8 to 5, as we did not deal with severe cases. The **Fagerstrom Test** for nicotine dependence is a standard instrument for assessing the intensity of physical addiction to nicotine related to cigarette smoking. It contains six items that evaluate the quantity of cigarette consumption, the compulsion to use, and dependence. Yes/no items are scored from 0 to 1 and multiple-choice items are scored from 0 to 3. The items are summed to yield a total score of 0-10. The higher the total Fagerstrom score, the more intense is the patient's physical dependence on nicotine [107]. On the base of clinicians' suggestions, I divided the total Fagerstrom score in three ranges: 0-4, corresponding to a low nicotine dependence, 5-7, corresponding to a moderate dependence, and ≥ 8 indicating a high/increasing nicotine dependence.

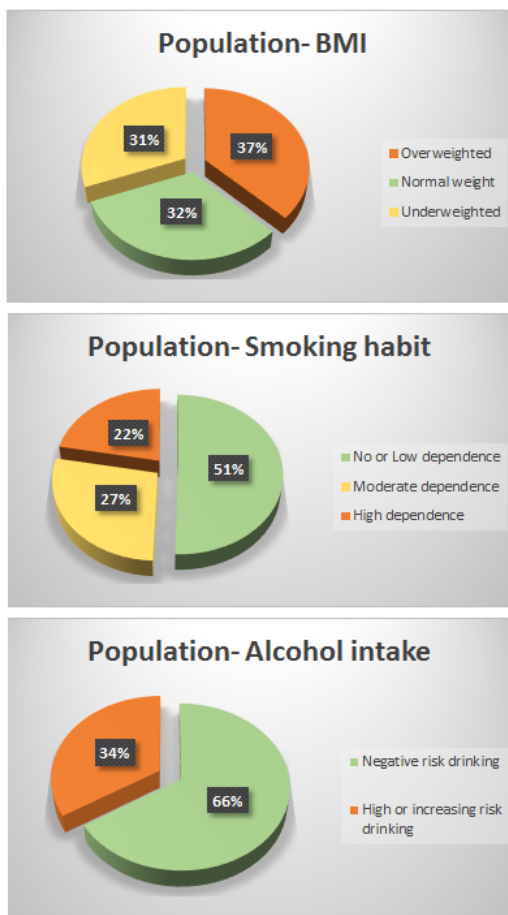


Figure 5.2: *The population of volunteers described according to their habits.*

Therefore, the volunteers were classified in "low-risk population", "medium-risk population" and "high-risk population" on the base of the sum of the scores of the questionnaires, as shown in Figure 5.1. The questionnaires and the relative scores were our ground truth.

Regarding the breath test, a protocol was drawn up. As previously described (chapter 2), standard protocols for breath sampling do not exist. Exhaled breath composition is strongly influenced by breath sampling method [2], as well as by breath flow rate [108], posture [9], ambient air [5], lung volume [109]. In this case, also factors such as BMI, sex, age, subjects' lifestyle might influence the breath composition: for example, alcohol disposal in men is different than the one in women, and, in addition, it may depend on body mass index (BMI) [110], as well.

This led me to the question about which of the different sampling methods (end-tidal sampling, mixed expiratory sampling, time-controlled sampling, described in chapter 2) would have been the most reliable method, able to give the lowest intra- and inter- variability in the measured VOCs concentrations. One of the most frequently used breath sampling method is the **mixed expiratory breath sampling technique** [2, 7, 111], where a volunteer has to breath the whole exhaled volume into a sampling bag. Therefore, I also chose such method of sampling, given, in addition, its easily

Chapter 5. WS validation: self-monitoring the breath for the prevention of cardio-metabolic risk

manageable and cost-efficient applicability. Nevertheless, mixed expired air consists of dead space, transition phase and alveolar phase. The dead space and the transition phase contain breath compounds from the upper airways, whereas the alveolar phase contains the VOCs resulting from alveolar exchanges, which better represent the individual's metabolic conditions. Several studies have demonstrated possible advantages when applying specific manoeuvres, such as breath holding [112], high exhaled volume, lower exhalation flow rate [113–115] and single exhalation [116], which may lead to an increase in alveolar VOCs concentrations in breath samples.

Therefore, considered all these methodological issues about breath sampling, the volunteers were instructed to:

- first, take a deep breath in;
- then, hold the breath for 10 sec;
- finally, breath out once through the mouthpiece trying to keep the expiratory flow low (about 160L/min \pm 10%) and constant, and to completely empty their lungs.

All the participating subjects were under the same conditions of environmental temperature and humidity when breath test was performed, in a seated position (as shown in Figure 5.3), at morning, fasting and several hour after brushing their teeth. A chart containing personal data, clinical and/or surgical records, occasional consumption of medications, height-weight data, body mass index, was drawn up for all subjects. Each volunteer underwent the breath test once. Breath flow rate and breath carbon dioxide were monitored in real time as their profile defines the quality of the breath sample. [6].

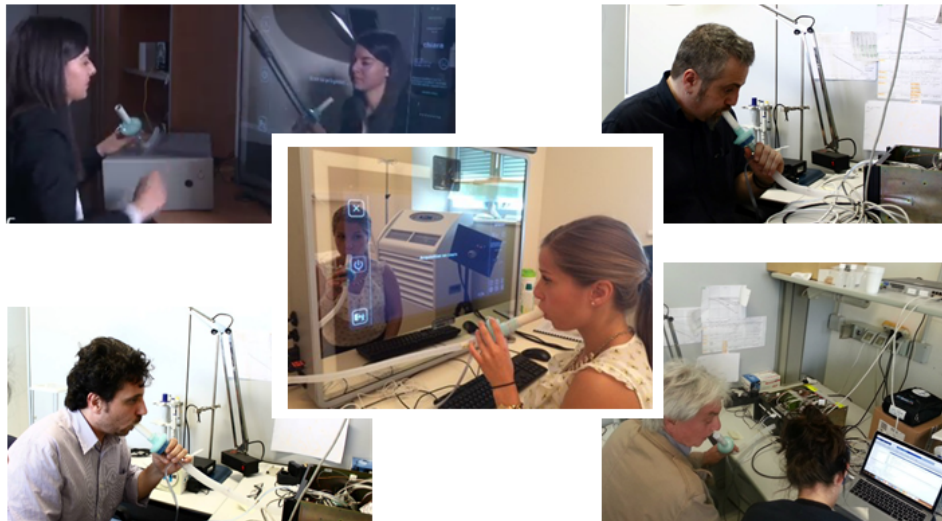


Figure 5.3: *Some of the involved volunteers while performing a breath test.*

5.3 Results and discussion

By means of the Matlab GUI, the breath test data were recorded as text files on a personal computer. Then, the data analysis approach (described in chapter 4) was applied

on such dataset of 169 subjects x 21 gas sensors features.

The prediction model was built by using a sub-group of the calculated independent components. As the data were pre-processed by PCA to reduce information redundancy, I set the number of useful independent components equal to the number (3) of principal components contributing significantly to the explained variance (91.4%), as shown in the screeplot of Figure 5.4.

Then, the data set was split into two data-sets (training data set and validation data set)

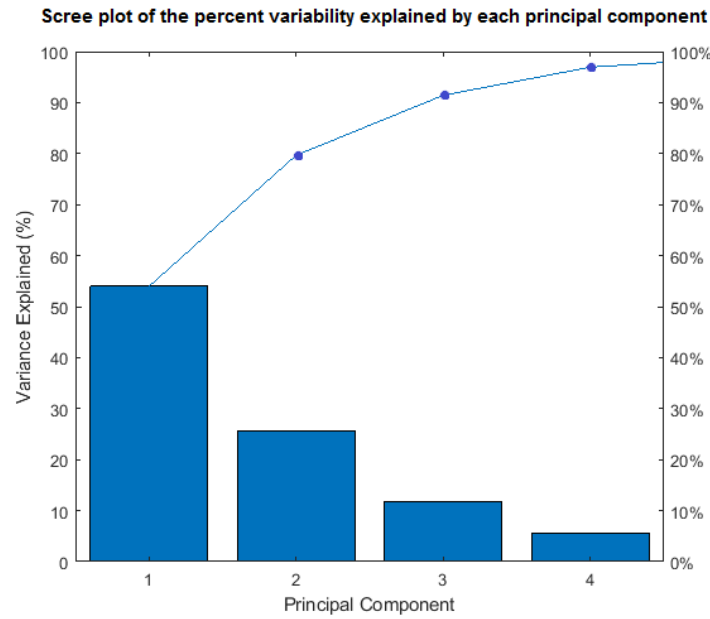


Figure 5.4: The screeplot shows the variance explained by each principal component.

to respectively build and validate the prediction model (eq. 5.1), which was developed in MATLAB R2014 environment.

$$RS_{train} = k + a_1 * IC_{1train} + a_2 * IC_{2train} + a_3 * IC_{3train} \quad (5.1)$$

where $k=64.054$ is the intercept (p-value= $1.01e^{-33}$), $a_1=-1.82$ (p-value= $3.06e^{-16}$), $a_2=-2.47$ (p-value= $3.41e^{-40}$), $a_3=1.23$ (p-value= $1.33e^{-17}$), RS is the subjects' cardio-metabolic risk score, and $IC_{1,2,3}$ the independent components.

The model was able to evaluate individuals' cardio-metabolic risk, on the base of their breath composition, with a prediction accuracy of 79.77% (see Table 5.1).

Table 5.1: Goodness of the model

Parameter	Value
Correlation coefficient between individuals' actual and estimated cardio-metabolic risk score (RS)	0.8976
Prediction accuracy	79.77%
Standard error of prediction (SEP)	1.27
Coefficient of determination (R^2) of the model	0.74

In Figure 5.5 the correlation coefficient (r) between actual and estimated risk scores is reported.

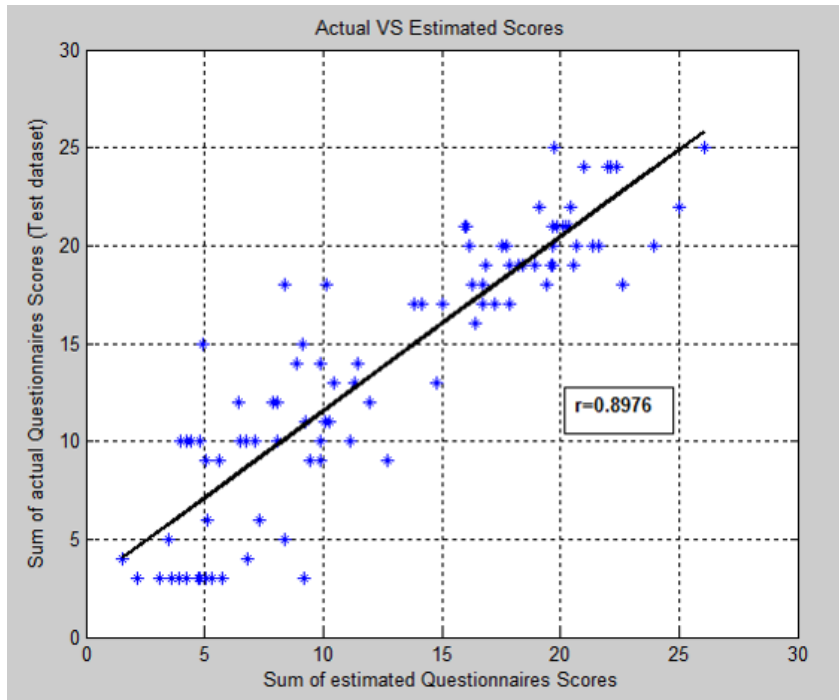


Figure 5.5: Actual risk scores versus predicted ones.

In conclusion, thanks to a simple, computationally inexpensive data analysis method, the Wize Sniffer was able to predict individual's cardio-metabolic risk score from the analysis of his/her breath composition. The easy of use of the Wize Sniffer lies also on the fact that it provides the user with a very easily interpretable outcome and potentially can help him/her to prevent his/her cardio-metabolic risk.

CHAPTER 6

Towards the diagnosis: detection of ammonia in the breath of patients suffering from liver impairment

6.1 Introduction

The liver is the second largest organ in the body and it is responsible for many critical functions. The loss of liver functions can cause significant damage to the body. Chronic liver disease can occur through several mechanisms. A common form of chronic liver disease derives from viral infection (such as Hepatitis B and C) [117, 118]; also high consumption of alcohol can lead to several forms of liver disease including alcoholic hepatitis and alcoholic fatty liver disease [119]. Progression of the disease can lead to the development of cirrhosis, that means, the normal liver cells are replaced by scar tissue that cannot perform any liver function. Cirrhosis may also lead to several complications, among which hepatic encephalopathy.

Hepatic encephalopathy is a neuropsychiatric consequence of advanced chronic liver disease. Although the exact pathogenesis is unknown, accumulation of ammonia from poor hepatic function and portosystemic shunting has been implicated as a primary factor [120]. Clinical testing for hepatic encephalopathy involves evaluation for psychiatric and neuro-muscular impairments, personality changes, disorientation, and asterixis. Biochemical testing may consist of determination of blood ammonia level, though it is not usually used as its accuracy may vary depending on whether venous or arterial blood is tested and on specimen handling, transport, and measurement techniques [121].

In addition, blood ammonia tests for hepatic encephalopathy are invasive, as well as liver biopsy and the majority of clinical testing in case of cirrhosis, and all of them are

Chapter 6. Towards the diagnosis: detection of ammonia in the breath of patients suffering from liver impairment

subject to technical difficulties in measurement.

A simple, non-invasive test, as breath analysis is, to identify chronic liver disease and discriminate among its degree of severity, with particular attention to hepatic encephalopathy, would be a very positive step forward. However, there are few studies on patients with chronic liver disease with e-nose [122].

Given the potential of the WS, and its good performances in monitoring users' breath composition, my idea was to evaluate its discriminative properties in the field of chronic liver impairment. In particular, my aim was to assess the diagnostic capabilities of the WS in:

- detecting ammonia in the breath of patients suffering from chronic liver disease;
- discriminating the several severity degrees of liver impairment on the base of breath ammonia.

A population of 20 patients with chronic hepatitis, 22 with liver cirrhosis, 6 with recent episodes of hepatic encephalopathy and 16 healthy controls were involved. Here, the study, the statistical data analysis and the results are described.

6.2 The liver disease and its progression: from chronic hepatitis to hepatic encephalopathy

The liver plays an important role in many bodily functions from protein production and blood clotting, to cholesterol, glucose (sugar), and iron metabolism. The liver helps fight infections and cleans the blood. It also helps digest food and stores energy for when we need it.

Chronic liver disease can occur through several mechanisms. A common form of **chronic liver disease** derives from viral infection (such as Hepatitis B and C) [117, 118]; also high consumption of alcohol can lead to several forms of liver disease including alcoholic hepatitis and alcoholic fatty liver disease [119]. In the early stage of any liver disease, the liver may become inflamed. It may become tender and enlarged. If the inflammation continues over time, it can start to hurt the liver permanently. Indeed, if left untreated, the inflamed liver will start to scar. As excess scar tissue grows, it replaces healthy liver tissue. This process is called *fibrosis*. Scar tissue cannot do the work that healthy liver tissue can. As more scar tissue builds up, the liver may not work well. Otherwise, the healthy part of the liver has to work harder to make up for the scarred part.

If left untreated, the liver may become so seriously scarred that it can no longer heal itself. This stage – when the damage cannot be reversed – is called **cirrhosis**. Treatments will focus on keeping the condition from getting worse. It may be possible to stop or slow the liver damage. In this stage, the subject may bleed or bruise easily; his/her skin and eyes may take on a yellow colour (a condition called *jaundice*) and itch intensely; water may build up in the legs and/or abdomen. Also, cirrhosis can lead to liver cancer. A frequent complication of liver cirrhosis is portal hypertension, resulting in the diversion of portal blood into the systemic circulation through portosystemic collateral vessels (portosystemic shunting).

In the setting of liver cirrhosis and portal hypertension [123], the presence of neurotoxic substances, including **ammonia**, in the systemic circulation may occur.

In particular, ammonia is produced in the gastrointestinal tract and normally is detoxified in the liver [124]. In case of cirrhosis and portal hypertension, the decrease in mass of functioning hepatocytes and the portosystemic shunting result in i) fewer opportunities for ammonia to be detoxified; ii) diversion of ammonia-containing blood away from the liver to the systemic circulation; iii) accumulation of ammonia in the brain, with multiple neurotoxic effects [120, 125, 126], which may result in **hepatic encephalopathy (HE)**.

Hepatic encephalopathy is defined as a spectrum of neuropsychiatric abnormalities in patients with acute liver dysfunction (after exclusions of brain disease), with a negative impact on survival [127–130]. HE is characterized by personality changes, confusion, disorientation, intellectual impairment and depressed level of consciousness.

It is graded according to the West-Haven classification system [131], from Grade 0 (or minimal HE or subclinical HE), which show an absence of detectable changes in personality or behaviour, but the complex and sustained attention is impaired, to Grade 4 which corresponds to coma.

Minimal HE has attracted increasing attention. Typically, both the patient and those around the patient, including physicians, are not aware that such condition is present. Patients with minimal HE have normal function on standard mental status testing but abnormal psychometric testing. Minimal HE is detected through neurophysiologic tests such as "numbers connecting test" A and B (measuring the speed at which one could connect randomly dispersed numbers 1–20), the "block design test" and the "digit-symbol test" [132]. Nevertheless, such tests can be very time-consuming and cumbersome to perform in the busy physician's office. Other clinical tests include blood ammonia level measurement, but in this case only arterial or free venous blood specimens must be assayed. Blood drawn from an extremity to which a tourniquet has been applied may provide a falsely elevated ammonia level when analysed [121].

Other types of blood tests and imaging studies (computerized axial tomography scan CT, magnetic resonance imaging and ultrasound, US) are helpful in assessing liver function. Liver biopsy may be considered to confirm a specific diagnosis of liver disease. It is the most invasive clinical test in case of liver disease, as under local anesthetic, a long thin needle is inserted through the chest wall into the liver, where a small sample of liver tissue is obtained for examination under a microscope.

6.3 The data acquisition campaign

Given the obtrusivity of the majority of liver function clinical tests, and, in case of minimal HE, the lack of reproducible, reliable, non-invasive tests [120], the use of a simple, non-invasive test, as breath analysis is, to identify chronic liver disease and discriminate among its degree of severity, would be a very positive step forward. Particular attention should be given to the diagnosis of hepatic encephalopathy, which may seriously affect the quantity and the quality of the patients' life, even in patients with minimal HE [133]. In addition, it represents a burden for patients' families [134]. For these reasons, measures for the prevention of HE are needed and it would be important to identify cirrhotics who are at risk of HE by detecting a potential hyperammonemia. In this regard, my aim was to evaluate WS performances in:

Chapter 6. Towards the diagnosis: detection of ammonia in the breath of patients suffering from liver impairment

- detecting ammonia in the breath of patients suffering from chronic liver impairment;
- discriminating the several severity degrees of liver impairment on the base of the detected breath ammonia.

The study included 64 subjects: 20 women (mean age: 52, with a range of 31 to 78) and 44 men (mean age: 55, with a range of 32 to 84)¹, 20 non-cirrhotics with chronic liver disease, 22 cirrhotics, 6 cirrhotics with recent episode of HE and 16 healthy controls. Individuals were defined as healthy subjects if they did not present symptoms and/or signs of either acute or chronic illness, did not have chronic illness, and were not consuming medications on a regular basis.

The diagnosis of cirrhosis was based on liver biopsy or on clinical, biochemical and ultrasonographic findings. Portal-systemic shunts were searched for by US and CT scan. The Child-Pugh and the Model for End-Stage Liver Disease (MELD) scores were calculated.

Blood sample was drawn for each subject for a complete blood count, prothrombin time (PT), bilirubin, international normalized ratio (INR), and liver panel, albumin and creatinine determinations. A chart containing personal data, clinical and/or surgical records, consumption of medications and BMI was drawn up for all subjects.

The presence and the degree of HE were evaluated by focused neurologic exams and psychometric tests, including trail-making test A (TMT-A) and B (TMT-B) and the digit-symbol-test (DST), aiming at evaluating their sustained attention, concentration and intellectual function [136, 137]. Nevertheless, such tests are very time consuming and they may be affected by numerous biases among which subject's vision problems, subject's awe, etc. Exclusion criteria were: alcohol/psychoactive drugs at baseline, neurological disease, lack of compliance with psychometric evaluation. Patients with a history of persistent and recurrent HE defined by two or more than two episodes within the last six months were excluded as these patients are usually treated continuously with lactulose and antibiotics in order to reduce blood ammonia levels.

Also subjects suffering from other chronic illness (cardiac or renal insufficiency, diabetes, COPD, celiac disease) were excluded in order to avoid interference with the test results.

regarding the breath tests, there is no consensus in literature about how measurement of ammonia in exhaled breath should be measured [138]. As a consequence, the protocol for the breath tests was the one described in chapter 5. Indeed, the mixed expiratory breath sampling technique [2, 7, 111] was used, given also its easily manageable and cost-efficient applicability. The volunteers were required to:

- first, take a deep breath in;
- then, hold the breath for 10 sec;
- finally, breath out once through the WS mouthpiece trying to keep the expiratory flow low (about 160L/min \pm 10%) and constant, and to completely empty their lungs.

All the participating subjects were under the same conditions of environmental temperature and humidity when breath test was performed, in a seated position, at morning,

¹Age do not affect the breath ammonia levels, as well as the gender [135].

fasting and several hour after brushing their teeth.

Breath carbon dioxide was monitored in real time (by means of the IR1507 Servomex sensor, see chapter 4), as its profile defines the quality of the breath sample [6], as well as the breath flow rate. The breath ammonia was detected with TGS2444 and TGS2602 semiconductor gas sensors present in WS gas sensor array.

The tests were conducted at the Hepatology Unit of the University Hospital of Pisa, under the supervision of the Director Dr. Maurizia Brunetto. The methods and the protocol were submitted to the Ethical Committee of the Azienda Ospedaliero Universitaria Pisana for approval. All subject provided a signed informed consent before enrolment

6.4 Statistical data analysis and results

By means of the GUI implemented in MATLAB environment, the breath test data were recorded as text files for statistical analysis, for which MATLAB and R (version 3.2.4) environments were used. First, descriptive statistics were used to quantitatively describe and summarizes both breath and clinical data.

In Tables 6.1 and 6.2 the subjects' most important clinical data and the features extracted from TGS2444 and TGS2602 output curves are summarized. For each class of subjects (healthy controls HC, non-cirrhotics with chronic liver disease NC-CLD, cirrhotics CIRRH, and cirrhotics with recent episode of hepatic encephalopathy CHE) the mean value (and the relative confidence interval C.I.) of each parameter is reported.

Table 6.1: The most relevant clinical data from liver function blood tests. For each subjects' class, the mean value of the blood parameter at issue is reported. A value of $p < 0.05$ was considered to be statistically significant.

	n. subj.	Albumin ($\frac{gr}{dl}$) \pm C.I.95%	Bilirubin ($\frac{mg}{dl}$) \pm C.I.95%	Spleen (cm) \pm C.I.95%	PT% \pm C.I.95%
HC	16	4.31 \pm 0.24 <i>p-value:</i> 3.19e-16	0.49 \pm 0.05 <i>p-value:</i> 2.38e-12	9.71 \pm 0.58 <i>p-value:</i> 6.86e-16	99.63 \pm 2.98 <i>p-value:</i> <2.2e-16
NC-CLD	22	4.44 \pm 0.14 <i>p-value:</i> <2.2e-16	0.55 \pm 0.10 <i>p-value:</i> 4.27e-10	11.97 \pm 1.00 <i>p-value:</i> <2.2e-16	95.17 \pm 6.16 <i>p-value:</i> <2.2e-16
CIRRH	24	4.00 \pm 0.23 <i>p-value:</i> <2.2e-16	0.97 \pm 0.23 <i>p-value:</i> 4.89e-09	13.58 \pm 1.02 <i>p-value:</i> <2.2e-16	82.64 \pm 6.17 <i>p-value:</i> <2.2e-16
CHE	6	3.37 \pm 0.38 <i>p-value:</i> 6.64e-07	1.59 \pm 0.73 <i>p-value:</i> 0.001	15.42 \pm 2.86 <i>p-value:</i> 1.187e-05	73.14 \pm 19.01 <i>p-value:</i> 8.17e-05

Albumin is a type of protein made by the liver. It carries vital nutrients and hormones. The typical value for serum albumin in blood is 3.4 to 5.4 gr/dl, as can be observed in Table 6.1 for healthy controls. Low albumin levels can indicate a severe liver impairment, indeed its values decrease especially in cirrhotics and cirrhotics with HE.

Bilirubin is produced in the body when the haemoglobin in old red blood cells is broken down. After circulating in your blood, bilirubin then travels to the liver where it is conjugated and mixed into bile. Normal values of total bilirubin range from 0.3–1.0 mg/dL (see healthy controls in Table 6.1). When the liver can't process the bilirubin in the body, because of an impairment, its values increase.

Chapter 6. Towards the diagnosis: detection of ammonia in the breath of patients suffering from liver impairment

Table 6.2: Mean values of TGS2444 and TGS2602 max value, rising time and maximum slope for each class: healthy controls HC, non-cirrhotics with chronic liver disease NC-CLD, cirrhotics CIRRH and cirrhotics with recent episode of hepatic encephalopathy CHE. A value of $p < 0.05$ was considered to be statistically significant.

	TGS2444 max value (V) ±C.I.95%	TGS2444 T_r (msec) ±C.I.95%	TGS2444 max dV/dt ±C.I.95%	TGS2602 max value (V) ±C.I.95%	TGS2602 T_r (msec) ±C.I.95%	TGS2602 max dV/dt ±C.I.95%
HC	0.39±0.06 <i>p-val.</i> : 1.61e-09	843.75±82.47 <i>p-val.</i> : 8.99e-13	0.06±0.01 <i>p-val.</i> : 6.91e-10	0.33±0.08 <i>p-val.</i> : 6.21e-07	1718.75±569.09 <i>p-val.</i> : 1.12e-5	0.03±0.01 <i>p-val.</i> : 7.36e-4
NC-CLD	0.69±0.13 <i>p-val.</i> : 9.05e-10	1476.19±502.39 <i>p-val.</i> : 5.46e-06	0.08±0.02 <i>p-val.</i> : 1.45e-06	0.57±0.11 <i>p-val.</i> : 2.96e-09	3511.90±460.11 <i>p-val.</i> : 7.97e-13	0.02±0.007 <i>p-val.</i> : 1.16e-06
CIRRH	0.87±0.16 <i>p-val.</i> : 1.45e-11	973.21±189.04 <i>p-val.</i> : 4.21e-11	0.14±0.05 <i>p-val.</i> : 3.69e-06	0.74±0.16 <i>p-val.</i> : 7.23e-10	2794.64±432.76 <i>p-val.</i> : 2.48e-13	0.05±0.03 <i>p-val.</i> : 1.4e-3
CHE	1.12±0.47 <i>p-val.</i> : 1.09e-3	714.28±280.91 <i>p-val.</i> : 7.95e-4	0.20±0.16 <i>p-val.</i> : 2.02e-2	1.02±0.52 <i>p-val.</i> : 3.1e-3	2214.28±909.58 <i>p-val.</i> : 1.00e-3	0.10±0.13 <i>p-val.</i> : 1.06e-1

The possible relationships between splenomegaly (enlarged spleen) and portal hypertension have been analysed in patients with cirrhosis [139]. The increase in spleen size in cirrhotics, as can be observed also in Table 6.1, is followed by an increase in splenic blood flow, which participates in portal hypertension actively congesting the portal system.

Prothrombin is one of the clotting factors made by the liver. Prothrombin time measures how long it takes blood to clot. In case of liver disease, this time increases.

The used Taguchi gas sensors (TGS2444 and TGS2602), as can be observed in Table 6.2, gave good results in detecting breath ammonia. In particular, the sensors maximum output increased with increasing liver impairment, as I expected. Such result can be graphically observed also in Figure 6.1.

Also, in Figure 6.2 the outputs relative to all the WS sensors are shown for three sub-

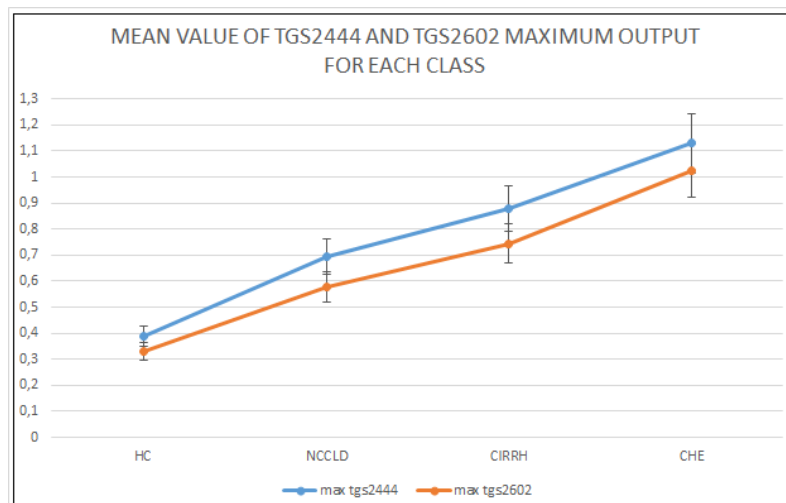


Figure 6.1: Mean values of TGS2444 and TGS2602 maximum outputs relative to healthy control subjects (HC), non cirrhotics- with chronic liver disease (NC-CLD) patients, cirrhotics subjects (CIRRH) and cirrhotic patients with recent episode of hepatic encephalopathy (CHE). Standard deviation (of about 10%) is also shown.

jects taken, just as example, from each class. Visual analysis of these radar-plot profiles

6.4. Statistical data analysis and results

showed a progressive concordant rise in value for TGS2444 and TGS2602 maximum output, from healthy to cirrhotics with HE subjects. However, except for TGS4161 (carbon dioxide sensor) and O_2 sensors which showed a similar profile for all subjects, a change in the whole sensors output pattern was observed. Indeed, cirrhotics with HE showed, in general, a wider radar plot profile.

Regarding the sensors response times, they did not significantly vary due with increased liver impairment. On the contrary, sensors maximum slope (especially for TGS2444) showed a slight increase from healthy controls to cirrhotic with HE.

Then, a bivariate analysis allowed for quantitatively describing the relationship be-

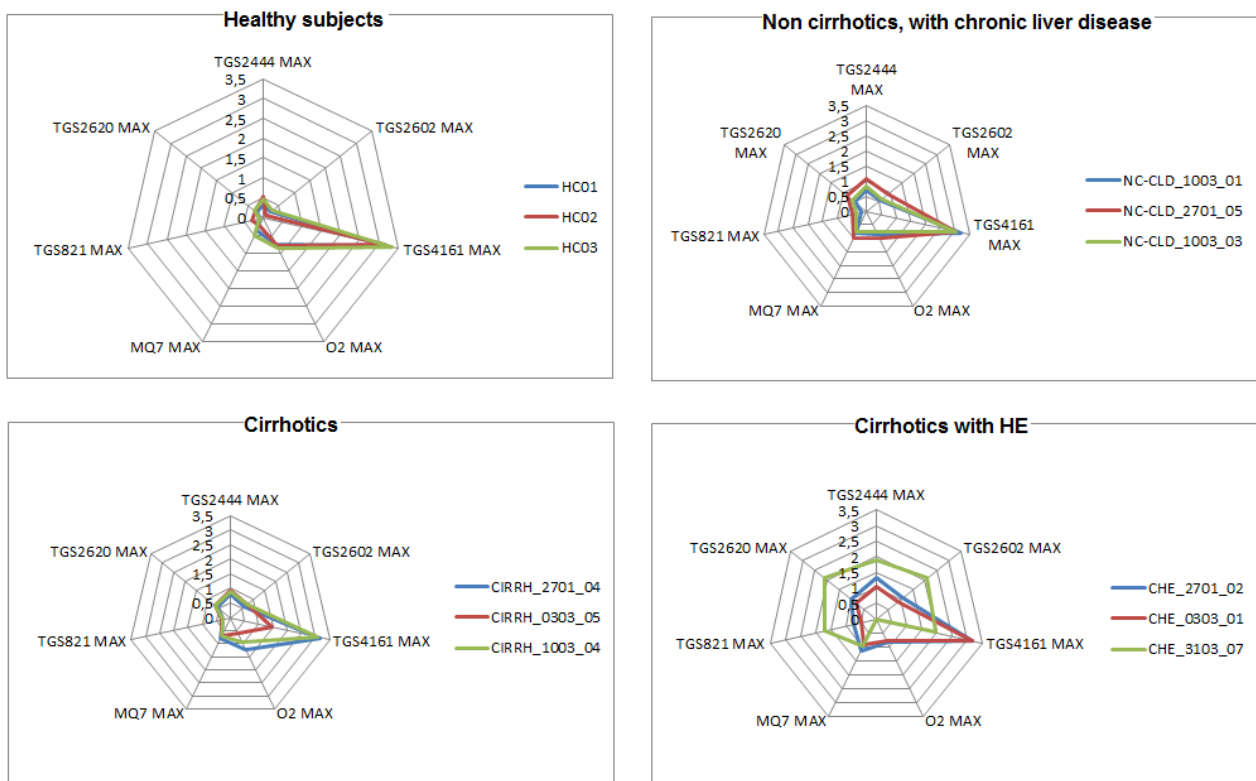


Figure 6.2: Comparison of radar plot profiles relative to healthy control subjects (HC), non cirrhotics with chronic liver disease (NC-CLD) patients, cirrhotics subjects (CIRRH) and cirrhotic patients with recent episode of hepatic encephalopathy (CHE). The radar plots showed a concordant rise in value for TGS2444 and TGS2602 (sensitive to ammonia) maximum output, from HC to CHE subjects. Nevertheless, a change in the whole sensors' outputs pattern was observed. This does not apply to TGS4161- CO_2 and O_2 sensors, which dominate the output pattern in all cases. This led me to think that liver disease does not cause a significant variation in exhaled carbon dioxide and oxygen.

tween breath data and liver function tests. In particular, Pearson's correlation was calculated between the variables.

Spleen dimensions showed significant positive correlation with both TGS2444 and TGS2602 maximum output (Pearson's correlation $\rho = 0.53$ $p\text{-value}^2 = 0.0001939$ and $\rho = 0.42$ $p\text{-value} = 0.001814$, respectively), as shown in Figure 6.3a). Negative correlations were found between prothrombin time and TGS2444 maximum output ($\rho = -0.29$

²A value of $p < 0.05$ was considered to be statistically significant.

Chapter 6. Towards the diagnosis: detection of ammonia in the breath of patients suffering from liver impairment

p -value= 0.02785), TGS2444 maximum slope (ρ = -0.27 p -value= 0.0336), TGS2602 maximum output (ρ = -0.30 p -value= 0.01767), TGS2602 maximum slope (ρ = -0.29 p -value= 0.02057), as shown in Figure 6.3b). Also, TGS2444 maximum output (ρ = 0.40 p -value= 0.01294) and TGS2602 maximum output (ρ = 0.36 p -value= 0,02569) showed positive correlation with serum bilirubin, as shown in Figure 6.3c).

Given firstly sensor outputs coherently increasing with the severity of liver function impairment (Table 6.2) and, secondly, significant correlations between sensor outputs and a set of liver function-related parameters, a further step consisted of evaluating WS diagnostic capability by means of ROC curves analysis. A ROC curve is created by plotting the true positive rate against the false positive rate at various threshold settings. The true-positive rate is also known as sensitivity, recall or probability of detection. The false-positive rate is also known as the fall-out or probability of false alarm and can be calculated as (1 - specificity).

I looked for cut-off values in sensor output features that allowed to differentiate healthy subjects from patients with liver disease, and, among the latter, those with and without cirrhosis. In addition, among the cirrhotics, sensors cut-off values were looked for to differentiate those with and without recent episode of HE (even though the number of CHE was low).

A TGS2444 maximum value of 0.572V permitted to differentiate healthy subjects from patients with liver impairment in general (HC versus LD); indeed, the wider AUC-ROC, as shown in Figure 6.4, was the one relative to TGS2444 maximum output (AUC= 0.867, 95%CI:0.783-0.952, p -value: <0.0001).

Among the patients with liver impairment, the boundary between subjects suffering from chronic liver disease with (CIRRH) and without (NC-CLD) cirrhosis was more difficult to establish. Low values of AUC can be observed for TGS2444 and TGS2602 maximum value. The wider AUC can be observed for TGS2444 maximum slope (AUC= 0.642, 95%CI:0.486-0.798, p -value: <0.037): a value of 0.093 discriminated between cirrhotic and non-cirrhotic with chronic liver impairment patients.

In cirrhotic patients, the boundary between cirrhotic with (CHE) and without (CIRRH) HE was more clear. Indeed, as widely reported before, the hyperammonemia in patients with HE is more pronounced A value of 0.065 for TGS2602 maximum slope (AUC= 0.864, 95%CI:0.662-1, p -value= 0), as well as a value of 0.8 for TGS2602 maximum output (AUC= 0.848, 95%CI:0.649-1, p -value= 0) permitted to differentiate between cirrhotics with and without hepatic encephalopathy.

A summary of these results is reported in Table 6.3.

Table 6.3: *The cut-off sensor features which permitted to discriminate between healthy controls (HC) versus subjects with liver disease (LD); in the population of patients with liver impairment, patients with chronic liver disease with (CIRRH) versus without cirrhosis(NC-CLD); in the population of cirrhotic patients, cirrhotics with (CHE) versus without CIRRH.*

	CUT-OFF	AUC-ROC	p-value	VP	VN	FP	FN	SENS.	SPEC.
HC vs LD	$TGS2444_{max}$ = 0.572	0.867 95%CI:0.783-0.952	<0.0001	37	15	1	11	0.771	0.938
NC-CLD vs CIRRH	$TGS2444_{maxslope}$ = 0.093	0.642 95%CI:0.486-0.798	<0.037	17	13	7	11	0.607	0.650
CIRRH vs CHE	$TGS2602_{max}$ = 0.8	0.848 95%CI:0.848-1	0	5	16	6	1	0.883	0.727

6.4. Statistical data analysis and results

Although this study did not involve measurements of blood-ammonia levels, or even the exact assessment of breath ammonia concentration levels, the WS was able to discriminate well not only between healthy subjects and patients with liver impairment, but also between cirrhotics with and without HE, by using both the dynamic and the steady-state features of a subgroup of sensors selective to ammonia. A larger series of patients may also permit to better define the reference sensors' features and better discriminate between patients with chronic liver impairment with and without cirrhosis. Not only, a larger number of recruited patients, including patients with suspected liver impairment, may allow for confirming such results and for implementing a learning algorithm able to identify the patients, recognize the severity of liver impairment and eventually detect hepatic encephalopathy at its early stage (minimal hepatic encephalopathy, MHE).

This *proof of concept* study also pointed out the unobtrusiveness, the safety and the discriminative properties of WS as a stand-alone device. In addition, its ease of use may permit not only a rapid diagnosis, but also the possibility of self-testing.

Chapter 6. Towards the diagnosis: detection of ammonia in the breath of patients suffering from liver impairment

Most significant correlations calculated between breath data and liver function clinical tests



Figure 6.3: Most significant correlations calculated between breath data (that means, TGS2444 and TGS2602 outputs) and liver function clinical tests. In a), the two scatter plots visually show the relationship between subjects spleen dimensions and ammonia sensors maximum values; In b), the scatter plots visually show the relationship between PT and ammonia sensors outputs (maximum value and maximum slope); In c), the two scatter plots visually show the relationship between subjects bilirubin and ammonia sensors maximum values.

6.4. Statistical data analysis and results

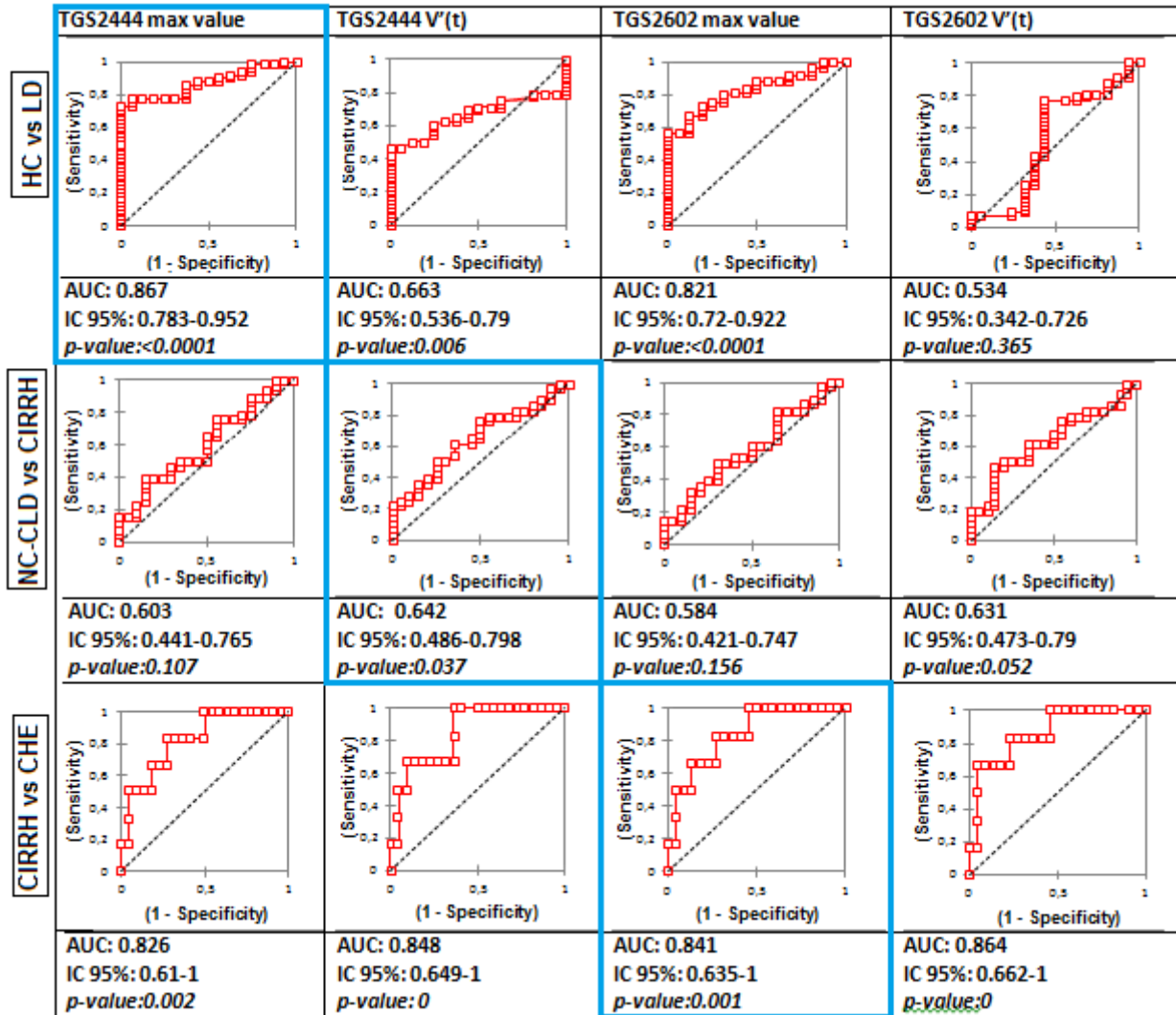


Figure 6.4: Comparison of receiver operating characteristic (ROC) curves for TGS2444 and TGS2602 output features (maximum output and first derivative) in the total evaluated population (first row, healthy subjects versus subjects with liver disease), in the population of patients with liver impairment (second row, patients with chronic liver disease with versus without cirrhosis), in the population of cirrhotic patients (third row, cirrhotics with versus without HE).

CHAPTER 7

Conclusions

The aim of my research activity was to develop a device, for human breath analysis, which could mimic the standard instrumentations (Gas Chromatography, for instance) in their accuracy and sensitivity, and, at the same time, overcome their limitations (high costs, long time analysis, difficulties in using and interpreting the results)

The so called *Wize Sniffer* is **portable** (its dimensions are: 30x30x14cm) and able to analyse breath molecules in **real time**.

Its **core** is entirely **based on low-cost technology**: its core is composed of a commercial, semiconductor-based gas sensor array (25-30Euro each) and a widely employed open source controller, an Arduino Mega2560 (about 45Euro). The majority of semiconductor gas sensors influencing factors were studied, managed and counteracted. Only the phenomenon behind cross-sensitivity remains unclear [21]. Nevertheless, although these sensors may exhibit a sensitivity to a specific analyte lower than that of a selective sensor, due to cross-sensitivity, they are more **versatile in detecting multi-component and complex VOC mixtures**, as breath is.

Indeed, as described in chapter 5, the *Wize Sniffer* was able to detect, in human breath, a set of molecules, that means, a wider number of VOCs, related to the noxious habits for cardio-metabolic risk, and, thanks to a swift, computationally inexpensive data analysis method, it was able to understand users' well-being state and predict their cardio-metabolic risk score. Also, its **easy of use** lies on the fact that it provides the user with a very easily interpretable outcome.

Finally, its **modularity** makes it customizable and adaptable to the use case: in chapter 6, the *Wize Sniffer* gave very good performances also in detecting ammonia in the breath of patients suffering from liver disease and precise cut-off values were found in gas sensor outputs that discriminated the severity of liver impairment on the base of detected ammonia levels.

As described in the first chapter, a number of methodological limitations relative to breath analysis are still matter of debate. First, methodological issues such as sampling set-ups and exhaled breath collection need to be optimized and standardized. Also the architectural principles which e-noses have to be based on should be standardized, in order to obtain compatible signals that may be used and processed by different e-nose systems and shared among physicians all over the world. In addition, subjects- related influencing factors are another source of variation between breathomics studies which still needs to be clarified.

It is evident that a strong cooperation among experts from different fields (engineers, instrument makers, clinicians, breath analysis experts, chemists) is mandatory to look for missing elements in this complex puzzle, from both a physiological and engineering stand point.

My contributions to the research in the field of breath analysis were:

- the development of a portable, low cost, customizable, easy to use device, able to be used in whichever context of use;
- the development of a method to evaluate individual's cardio-metabolic risk from the analysis of his/her breath composition;
- the investigation of the possibility to diagnose liver disease, and evaluate its severity, by detecting breath ammonia and using commercial, semiconductor gas sensors.

Bibliography

- [1] Pereira J. and al. Breath analysis as a potential and non-invasive frontier in disease diagnosis: an overview. *Metabolites*, 5:3–55, 2015.
- [2] Miekisch W., Kischkel S., Sawacki A., Lieban T., Mieth M., and Schubert J. Impact of sampling procedures on the results of breath analysis. *J. of Breath Research*, 2:026007 (7pp), 2008.
- [3] Miekisch M., Schubert J.K. and Noeldge-Schomburg G.F.E. Diagnostic potential of breath analysis- focus on volatile organic compounds. *Clinica Chimica Acta*, 347:25–39, 2004.
- [4] Salvo P. and al. Medical engineering and physics. *IEEE Sensors J.*, 37.
- [5] DiFrancesco F. and al. Implementation of fowler’s method for endtidal air sampling. *Journal of Breath Research*, 2:037009 (10pp), 2008.
- [6] Risby T.H. and Solga S.F. Current status of clinical breath analysis. *Applied Physics B*, 85:421–426, 2006.
- [7] Thekedar B., Oeh U., Szymczak W., Hoeschen C., Paretzke H.G. Influences of mixed expiratory sampling parameters on exhaled volatile organic compound concentrations. *J. of Breath Research*, 5:9pp, 2011.
- [8] Cope K.A., Watson M.T., Foster W.M., Sehnert S.S. and Risby T.H. Effects of ventilation on the collection of exhaled breath in humans. *J. of Applied Physiology*, 96.
- [9] Anthonisen N., Robertson P. and Ross W. Gravity-dependent sequential emptying of lung regions. *Journal of Appl. Physiol.*, 28:589–595, 1970.
- [10] Amann A., Poupart G., Telser S., Ledochowski M., Schmid A. and Mechtcheriakov S. Application of breath gas analysis in medicine. *Int. J. of Mass Spectrometry*, 239:227–233, 2004.
- [11] Pabst F., Miekisch W., Fuchs P., Kischkel S. and Schubert J.K. Monitoring of oxidative and metabolic stress during cardiac surgery by means of breath biomarkers: an observational study. *J. of Cardiothoracic Surgery*, 2:1–8, 2007.
- [12] Thompson D.G. and al. Extra intestinal influences on exhaled breath hydrogen measurements during the investigation of gastrointestinal disease. *Gut*, 26:1349–1352, 1985.
- [13] Montuschi P., Kharitonov S.A. and Barnes P.J. Exhaled carbon monoxide and nitric oxide in copd. *Chest Journal*, 120:496–501, 2001.
- [14] Phillips M., Cataneo R.N., Greenberg J., Grodman R. and Salazar M. Breath markers of oxidative stress in patients with unstable angina. *Heart Disease*, 5:95–99, 2003.
- [15] Gouma P., Kalyanasundaram K., Yun X., Stanacevic M. and Wang L. Nanosensor and breath analyzer for ammonia detection in exhaled human breath. *IEEE Sensors J.*, 10.
- [16] Risby T.H. Volatile organic compounds as markers in normal and diseased states. *Disease Markers in Exhaled Breath: Basic mechanisms and clinical applications ed N Marczin and M Yacoub (NATO ASI Series)*, pages 113–122, 2002.
- [17] Guo D., Zhang D., Li N., Zhang L., Yang J. A novel breath analysis system based on electronic olfaction. *IEEE Transaction on Biomedical Engineering*, 57:2753–2763, 2010.

- [18] Wilson A.D. and Baietto M. Advances in electronic-nose technologies developed for biomedical applications. *Sensors*, 11:1105–1176, 2011.
- [19] Germanese D., Righi M., Magrini M., Guidi M., D’Acunto M. and Salvetti O. A device for self-monitoring breath analysis. *Proceeding of the Seventh International Conference on Sensor Device Technologies and Applications - SENSORDEVICES2016, July 24-28- Nice, France*, pages 77–82, 2016.
- [20] Germanese D. et al. A low cost, portable device for breath analysis and self-monitoring, the wise sniffer. *De Gloria A. (eds) Applications in Electronics Pervading Industry, Environment and Society. ApplePies 2016. Lecture Notes in Electrical Engineering*, 409:51–57, 2017.
- [21] Shankar P., Bosco J. and Rayappan B. Gas sensing mechanism of metal oxides: The role of ambient atmosphere, type of semiconductor and gases - a review. *ScienceJet*, 4, 2015.
- [22] Germanese D., D’Acunto M., Magrini M., Righi M., Salvetti O. A low cost technology-based device for breath analysis and self-monitoring. *Proceedings of the Second International Conference on Advances in Signal, Image and Video Processing, SIGNAL2017 - Barcelona, Spain, May 22-25*, pages 8–13, 2017.
- [23] Germanese D., D’Acunto M., Magrini M., Righi M. and Salvetti O. Cardio-metabolic diseases prevention by self-monitoring the breath. *Sensors and Transducers Journal*, 215:19–26, 2017.
- [24] Dweik R. and Amann A. Exhaled breath analysis: the new frontier in medical testing. *J. of Breath Research*, 2:030301, 2008.
- [25] Pauling L., Robinson A.B., Teranishi R., Cary P. Quantitative analysis of urine vapor and breath by gas-liquid partition chromatography. *Proc. Natl. Acad. Sci. U S A*, 68:2374–2376, 1971.
- [26] Fenske J.D. and Paulson S.E. Human breath emission of vocs. *J. of the Air and Waste Management Association*, 49:594–598, 1999.
- [27] Shier D., Butler J. and Lewis R. *Hole’s human anatomy and physiology-11th ed.* Mc Graw Hill, 2007.
- [28] Zevin S., Saunders S.G., Gourlay S.G., Jacob P. and Benowitz N.L. Cardiovascular effects of carbon monoxide and cigarette smoking. *Journal of the American College of Cardiology*, 38:1633–1638, 2001.
- [29] Bikov A. et al. Exhaled breath volatile alterations in pregnancy assessed with electronic nose. *Biomarkers*, 16:476–484, 2011.
- [30] Kim K.H., Jahan S.A. and Kabir E. A review of breath analysis for diagnosis of human health. *Trends in Analytical Chemistry*, 33:8pp., 2012.
- [31] Phillips M. and Greenberg J. Method for the collection and analysis of volatile compounds in the breath. *J. Chromatogr. Biomed. Appl.*, 8:242–249, 1991.
- [32] Giardina M. and Olesik S.V. Application of low-temperature glassy carbon-coated macrofibers for solid-phase microextraction analysis of simulated breath volatiles. *Anal Chem.*, 75:1604–161, 2003.
- [33] Nagle H.T., Gutierrez-Osuna R. and Schiffman S.S. The how and why of electronic noses. *IEEE Spectrum*, 35:22–31, 1998.
- [34] Persaud K. and Dodd G.H. Analysis of discrimination mechanisms of the mammalian olfactory system using a model nose. *Nature*, 299:352–355, 1982.
- [35] Turner A.P.F. and Magan N. Electronic noses and disease diagnostic. *Nature Reviews Microbiology*, 2:161–166, 2004.
- [36] Arshak K., Moore E., Lyons G.M., Harris F. and Clifford S. A review of gas sensors employed in electronic nose applications. *Sensor Review*, 24:181–198, 2004.
- [37] Albert K.J. and Lewis N.S. Cross reactive chemical sensor arrays. *Chem. Rev.*, 100:2595–626, 2000.
- [38] George S.C. and Thomas S. Transport phenomena through polymeric systems. *Progress in Polymer Science*, 26:985–1017, 2001.
- [39] Briglin S.M., Freund M.S., Tokumaru P. and Lewis N.S. Exploitation of spatiotemporal information and geometric optimization of signal/noise performance using arrays of carbon black-polymer composite vapor detectors. *Sensors and Actuators B: Chemical*, 82:54–74, 2002.
- [40] Capone S. et al. Solid state gas sensors: State of the art and future activities. *Journal of Optoelectronics and Advanced Materials*, 5:1335–1348, 2003.
- [41] Hodgkinson, J. and Tatam, R.P. Optical gas sensing: a review. *Meas. Sci. Technol.*, 24:59pp., 2013.
- [42] Schiff, H.I., Mackay, G.I. and Bechara, J. *The use of tunable diode laser absorption spectroscopy for atmospheric measurements.* Air Monitoring by Spectroscopic Techniques, ed. M.W. Sigrist, 1994.

Bibliography

- [43] Karioja, P. and al. Ltc based differential photo acoustic gas cell for ppm gas sensing. *Proc. of SPIE Photonics Europe, Brussel, Belgium, 7726:77260H*, 2010.
- [44] Moos R., Sahner K., Fleischer M., Guth U., Barsan N., Weimar U. Solid state gas sensor research in germany-a status report. *Sensors*, 9:4323–65, 2009.
- [45] Dutta R., Morgan D., Baker N., Gardner J.W., Hines E.L. Identification of staphylococcus aureus infections in hospital environment: electronic nose based approach. *Sens. Actuat. B*, 109:335–362, 2005.
- [46] Bailey L., Pisanelli A. and Persaud K. Development of conducting polymer sensor arrays for wound monitoring. *Sens. Actuat. B: Chem.*, 131:5–9, 2008.
- [47] Thaler E.R. The diagnostic utility of an electronic nose: rhinologic applications. *Laryngoscope*, 112:1533–1542, 2002.
- [48] Persaud K.C. Medical applications of odor-sensing devices. *Internatl. J. Low. Extrem. Wounds*, 4:50–56, 2005.
- [49] Garner C.E. et al. Volatile organic compounds from feces and their potential for diagnosis of gastrointestinal disease. *FASEB J.*, 21:1675–1688, 2007.
- [50] Guernion N., Ratcliffe N.M., Spencer-Phillips P.T., Howe R.A. Identifying bacteria in human urine: Current practice and the potential for rapid, near-patient diagnosis by sensing volatile organic compounds. *Clin. Chem. Lab. Med.*, 39:893–906, 2001.
- [51] Dragonieri S., Pennazza G., Carratu P., Resta O. Electronic nose technology in respiratory diseases. *Lung*, 195:157–165, 2017.
- [52] Dragonieri S. et al. An electronic nose in the discrimination of patients with asthma and controls. *J. of Allergy Clin. Immunol.*, 120:856–862, 2007.
- [53] de Vries R. et al. Integration of electronic nose technology with spirometry: validation of a new approach for exhaled breath analysis. *Journal of Breath Research*, 9:046001, 2015.
- [54] Sibila O. et al. Identification of airway bacterial colonization by an electronic nose in chronic obstructive pulmonary disease. *Respir. Med.*, 108:1608–1614, 2014.
- [55] Shafiek H. et al. Using the electronic nose to identify airway infection during copd exacerbations. *PLoS ONE*, 10:e0135199, 2015.
- [56] van Geffen W.H., Bruins M., Kerstjens H.A. Diagnosing viral and bacterial respiratory infections in acute copd exacerbations by an electronic nose: a pilot study. *Journal of Breath Research*, 10:036001, 2016.
- [57] van der Schee M.P. et al. Diagnostic value of exhaled breath analysis in tuberculosis. *Am. J. Respir. Crit. Care Med.*, 185:a6510, 2012.
- [58] Nakhleh M.K. et al. Detecting active pulmonary tuberculosis with a breath test using nanomaterial-based sensors. *Eur. Respir. J.*, 43:1522–1525, 2014.
- [59] Di Natale C. et al. Lung cancer identification by the analysis of breath by means of an array of non-selective gas sensors. *Biosens Bioelectron*, 18:1209–1218, 2003.
- [60] Yu H. et al. Detection volatile organic compounds in breath as markers of lung cancer using a novel electronic nose. *Proc. IEEE Sens.*, 2:1333–1337, 2003.
- [61] Chen X. et al. A study of an electronic nose for detection of lung cancer based on a virtual saw gas sensors array and imaging recognition method. *Meas. Sci. Technol.*, 16:1535–1546, 2005.
- [62] Machado R.F. et al. Detection of lung cancer by sensor array analysis of exhaled breath. *Am. J. Respir. Crit. Care Med.*, 171:1286–1291, 2005.
- [63] Bikov A. et al. Expiratory flow rate, breath hold and anatomic dead space influence electronic nose ability to detect lung cancer. *BMC Pulm Med*, 14, 2014.
- [64] Dragonieri S. et al. An electronic nose in the discrimination of patients with lung cancer and copd. *Lung Cancer*, 64:166–170, 2009.
- [65] Chen X. et al. A non-invasive detection of lung cancer combined virtual gas sensors array with imaging recognition technique. *Conf. Proc. IEEE Eng. Med. Biol. Soc.*, 6:5873–5876, 2005.
- [66] Greulich T. et al. Detection of obstructive sleep apnoea by an electronic nose. *Eur. Respir. J.*, 42:145–155, 2013.
- [67] Dragonieri S. et al. An electronic nose discriminates exhaled breath of patients with untreated pulmonary sarcoidosis from controls. *Respir Med.*, 107:1073–1078, 2013.

- [68] Ping W., Yi P., Haibao X., Farange S. A novel method for diabetes diagnosis based on electronic nose. *Biosens. Bioelectron.*, 12:1031–1036, 1997.
- [69] Thati A., Biswas A., Chowdhury S.R. and Sau T.K. Breath acetone-based non-invasive detection of blood glucose levels. *Int. J. on Smart Sensing and Intelligent Systems*, 8:1244–1260, 2005.
- [70] Righettoni M., Schmid A., Amann A., Pratsinis S.E. Correlations between blood glucose and breath components from portable gas sensors and ptr-tof-ms. *J. of Breath Research*, 7:037110 (9pp), 2013.
- [71] Toyooka T., Hiyama S. and Yamada Y. A prototype portable breath acetone analyzer for monitoring fat loss. *J. of Breath Research*, 7:036005 (8pp), 2013.
- [72] Tisch U. et al. Detection of alzheimer's and parkinson's disease from exhaled breath using nano-material-based sensors. *Nanomedicine*, 8:43–56, 2013.
- [73] Ionescu R. et al. Detection of multiple sclerosis from exhaled breath using bilayers of polycyclic aromatic hydrocarbons and single-wall carbon nanotubes. *ACS Chem. Neurosci.*, 2:687–693, 2011.
- [74] Cheng Z.J., Warwick G., Yates D.H. and Thomas P.S. An electronic nose in the discrimination of breath from smokers and non-smokers: a model for toxin exposure. *J. of Breath Research*, 3:036003 (5pp), 2009.
- [75] Nakhleh M.K. et al. Diagnosis and classification of 17 diseases from 1404 subjects via pattern analysis of exhaled molecules. *ACSNano*, 2016.
- [76] Wilson A.D. and Baietto M. Applications and advances in electronic-nose technologies. *Sensors*, 9:5099–5148, 2009.
- [77] Röck F., Barsan N., Weimar U. Electronic nose: current status and future trends. *Chem. Rev.*, 108:705–725, 2008.
- [78] Colantonio S. et al. A smart mirror to promote a healthy lifestyle. *Biosystems Engineering, Special Issue: Innovations in Medicine and Healthcare*, 138:33–43, 2015.
- [79] Henriquez P. et al. Mirror mirror on the wall... an unobtrusive intelligent multisensory mirror for well-being status self-assessment and visualization. *IEEE Transactions on Multimedia*, 19:1467–1481, 2017.
- [80] Taguchi N. Gas detecting device. *US Patent 3, 695, 848*, 1972.
- [81] Clifford P.K. and Tuma D.T. Characteristics of semiconductor gas sensors i. steady state gas response. *Sensors and Actuators*, 3:233–254, 1982.
- [82] Ho Sohn J., Atzeni M., Zeller L., Pioggia G. Characterisation of humidity dependence of a metal oxide semiconductor sensor array using partial least squares. *Sens. and Actuat. B*, 131:230–235, 2008.
- [83] Wang C., Yin L., Zhang L., Xiang D. and Gao R. Metal oxide gas sensors: Sensitivity and influencing factors. *Sensors*, 10:2088–2106, 2010.
- [84] Qi Q. et al. Electrical response of sm_2o_3 -doped sno_2 to c_2h_2 and effect of humidity interference. *Sens. and Actuat. B*, 134:36–42, 2008.
- [85] Barsan, N. and Weimar, U. Understanding the fundamental principles of metal oxide based gas sensors; the example of co sensing with sno_2 sensors in the presence of humidity. *Journal of Physics: Condensed Matter*, 15:813–839, 2003.
- [86] Gutierrez-Osuna, R. Pattern analysis for machine olfaction: A review. *IEEE Sensors Journal*, 2:189–202, 2002.
- [87] Gutierrez-Osuna, R and Nagle, H.T. A method for evaluating data pre-processing techniques for odor classification with an array of gas sensors. *IEEE Trans. Syst. Man Cybern. B*, 29:626–632, 1999.
- [88] Yan J. and al. Electronic nose feature extraction methods: A review. *Sensors*, 15:2784–27831, 2015.
- [89] Eklov T., Martensson P. and Lundstrom I. Enhanced selectivity of mosfet gas sensors by systematical analysis of transient parameters. *Analytica Chimica Acta*, 353:291–300, 1997.
- [90] Setkus A., Olekas A., Senuliene D., Falasconi M., Pardo M., Sberveglieri G. Analysis of the dynamic features of metal oxide sensors in response to spme fiber gas release. *Sens. Actuators B Chem.*, 146:539–544, 2010.
- [91] Zou X., Zhao J., Wu S. and Huang X. Vinegar classification based on feature extraction and selection from tin oxide gas sensor array data. *Sensors*, 3:101–109, 2003.
- [92] Kermit M. and Tomic O. Independent component analysis applied on gas sensor array measurement data. *IEEE Sensors Journal*, 3:500–511, 2003.

Bibliography

- [93] Llobet E., Brezmes J., Vilanova X., Sueiras J.E. and Correig X. Qualitative and quantitative analysis of volatile organic compounds using transient and steady-state responses of a thick-film tin oxide gas sensor array. *Sensors and Actuators B*, 41:13–21, 1997.
- [94] Di Natale C., Martinelli E., D'Amico A. Pre-processing and pattern recognition methods for artificial olfaction systems: a review. *Metrology and Measurement Systems*, 12:3–25, 2005.
- [95] Gardner J.W. Detection of vapours and odours from a multisensor array using pattern-recognition. part 1. principal component and cluster analysis. *Sensors and Actuators B.*, 4:109–115, 1991.
- [96] Naik G.R. and Kumar D.K. An overview of independent component analysis and its applications. *Informat-ica*, 35:63–81, 2011.
- [97] Balasubramanian S., Paniraghi S., Logue C.M., Doetkott C., Marchello M., Sherwood J.S. Independent component analysis-processed electronic nose data for predicting salmonella typhimurium populations in contaminated beef. *Food Control*, 19:236–246, 2008.
- [98] Di Natale C., Martinelli E., D'Amico A. Counteraction of environmental disturbances of electronic nose data by independent component analysis. *Sensors and Actuators B*, 82:2009–2025, 2002.
- [99] Jutten C. and Herault J. Blind separation of sources, part i: An adaptive algorithm based on neuromimetic architecture. *Signal Processing*, 24:1–10, 1991.
- [100] Hyvarinen A., Karhunen J. and Oja E. *Independent Component Analysis*. John Wiley and Sons, 2001.
- [101] Bell A.J. and Sejnowski T.J. An information-maximization approach to blind separation and blind deconvolution. *Neural Computation*, 7:1129–1159, 1995.
- [102] Hyvarinen A. The fixed-point algorithm and maximum likelihood estimation for independent component analysis. *Neural Processing Letters*, 10:1–5, 1999.
- [103] Cardoso J. High-order contrasts for independent component analysis. *Neural Computation*, 11:157–192, 1999.
- [104] Hyvarinen A. and Oja E. Independent component analysis: algorithms and applications. *Neural Network*, 13:411–430, 2000.
- [105] Yan W., Tang Z., Wei G. and Yang J. An electronic nose recognition algorithm based on pca-ica preprocessing and fuzzy neural network. *Proceeding of the 14th International Meeting on Chemical Sensors-IMCS2012-May2012, Nuremberg, Germany*, pages 1227 – 1230.
- [106] Babor T.F., Higgins-Biddle J.C., Saunders J.B. and Monteiro M.G. *AUDIT - The Alcohol Use Disorders Identification Test. Guidelines for Use in Primary Care, Second Edition*. World Health Organization- Department of Mental Health and Substance Dependence, 2001.
- [107] Heatherton T.F., Kozlowski L.T., Frecker R.C. and Fagerstrom K.O. The fagerstrom test for nicotine dependence: a revision of the fagerstrom tolerance questionnaire. *Br. J. Addict*, 86:1119–27, 1991.
- [108] Jones J. and Clarke S. Effect of expiratory flow rate on regional lung emptying. *Clin. Sci.*, 37:343–356, 1969.
- [109] Jones J. The effect of pre-inspiratory lung volumes on the result of the single breath o₂ test. *Respiratory Physiology*, 2:375–85, 1967.
- [110] Maudens K., Patteet L., van Nuijs A., Van Broekhoven C., Covaci A. and Neels H. The influence of the body mass index (bmi) on the volume of distribution of ethanol. *Forensic Sci Int.*, 243:74–78, 2014.
- [111] Thekedar B., Szymczak W., Hollriegl V., Hoeschen C. and Oeh U. Investigations on the variability of breath gas sampling using ptr-ms. *J. of Breath Research*, 3:027007, 2009.
- [112] Larstad M., Toren K., Bake B. and Olin A. Determination of ethane, pentane and isoprene in exhaled air-effects of breath-holding, flow rate and purified air. *Acta Physiol.*, 189:87–98, 2007.
- [113] Anderson J.C., Lamm W.J.E. and Hlastala M.P. Measuring airway exchange of endogenous acetone using a single-exhalation breathing maneuver. *J. of Applied Physiology*, 100:880–889, 2006.
- [114] Hlastala M.P. and Anderson J.C. The impact of breathing pattern and lung size on the alcohol breath test. *Ann. Biomed. Eng.*, 35:264–272, 2007.
- [115] Jones A.W. Quantitative measurement of the alcohol concentration and the temperature of breath during a prolonged exhalation. *Acta Physiol. Scand.*, 114:407–412, 1982.
- [116] George S.C., Babb A.L. and Hlastala M.P. Dynamics of soluble gas exchange in the airways: Iii. single-exhalation breathing maneuver. *J. of Applied Physiology*, 75:2439–49, 1993.

- [117] Benova L., Mohamoud Y., Calvert C. and Abu-Raddad L.J. Vertical transmission of hepatitis c virus: systematic review and meta-analysis. *Clinical Infectious Diseases*, 59:765–73, 2014.
- [118] Komatsu H. Hepatitis b virus: where do we stand and what is the next step for eradication? *World journal of gastroenterology*, 20:8998–9016, 2014.
- [119] Suk K.T., Kim M.Y. and Baik S.K. Alcoholic liver disease: treatment. *World journal of gastroenterology*, 20:12934–12944, 2014.
- [120] DuBois S. et al. Breath ammonia testing for diagnosis of hepatic encephalopathy. *Digestive Diseases and Sciences*, 50:1780–784, 2005.
- [121] Yurdaydin C. Blood ammonia determination in cirrhosis: Still confusing after all these years? *Hepatology*, 38:1308–1309, 2003.
- [122] De Vincentis A. et al. Breath-print analysis by e-nose for classifying and monitoring chronic liver disease: a proof-of-concept study. *Scientific Reports*, 6:1–9, 2016.
- [123] Riggio O. et al. High prevalence of spontaneous portal-systemic shunts in persistent hepatic encephalopathy: a case-control study. *Hepathology*, 42:1158–1165, 2005.
- [124] Hibbard, T. and Killard, A.J. Breath ammonia analysis: Clinical application and measurement. *Critical Reviews in Analytical Chemistry*, 41:21–35, 2011.
- [125] Stahl J. Studies of the blood ammonia in liver disease. its diagnostic, prognostic and therapeutic significance. *Ann. Inter. Med.*, 58:1–24, 1963.
- [126] Hibbard, T. and Killard, A.J. Breath ammonia levels in a normal human population study as determined by photoacoustic laser spectroscopy. *Journal of Breath Research*, 5:1–19, 2011.
- [127] Patidar K.R. and Bajaj J.S. Covert and overt hepatic encephalopathy: diagnosis and management. *Clin. Gastroentrol. Hepatol.*, 13:2048–2061, 2015.
- [128] Bajaj J.S. et al. Review article: the design of clinical trials in hepatic encephalopathy - an international society for hepatic encephalopathy and nitrogen metabolism (ishen) consensus statement. *Aliment. Pharmacol. Ther.*, 33:739–747, 2011.
- [129] Bustamante J., Rimola A., Ventura P.J., Navasa M., Cirera I. and Reggiardo V. Prognostic significance of hepatic encephalopathy in patients with cirrhosis. *J. of Hepatology*, 30:890–895, 1999.
- [130] Riggio O. et al., A model for predicting development of overt hepatic encephalopathy in patients with cirrhosis. *Clinical Gastroenterology and Hepatology*, 13:1346–1352, 2015.
- [131] Cash W.J., McConville P., McDermott E., McCormick P.A., Callender M.E. and McDougall N.I. Current concepts in the assessment and treatment of hepatic encephalopathy. *QJM-An International Journal of Medicine*, 103:9–16, 2010.
- [132] Weissenborn K., Ennen J.C., Schomerus H., Rückert N. and Hecker H. Neuropsychological characterization of hepatic encephalopathy. *J. of Hepatology*, 34:768–773, 2001.
- [133] Groeneweg M. et al. Subclinical hepatic encephalopathy impairs daily functioning. *Hepatology*, 28:45–49, 1998.
- [134] Bajaj J.S. et al. The multidimensional burden of cirrhosis and hepatic encephalopathy on patients and caregivers. *Am. J. Gastroenterol.*, 106:1646–1653, 2011.
- [135] Brooks S.M., Haight R.R. and Gordon R.L. Age does not affect airway ph and ammonia as determined by exhaled breath measurement. *Lung*, 184:195–200, 2006.
- [136] Conn H. Trailmaking and number-connection tests in the assessment of the mental state in portal systemic encephalopathy. *Dig. Dis.*, 22:541–550, 1977.
- [137] Bowie C.R. and Harvey P.D. Administration and interpretation of the trail making test. *Nature Protocol*, 1:2277–2281, 2006.
- [138] Adrover R., Cocozzella D., Ridruejo E., Garcia A., Rome J. and Podestà J.J. Breath-ammonia testing of healthy subjects and patients with cirrhosis. *Dig. Dis. Sci.*, 57:189–195, 2012.
- [139] Bolognesi M., Merkel C., Sacerdoti D., Nava V. and Gatta A. Role of spleen enlargement in cirrhosis with portal hypertension. *Dig. Liver Dis.*, 34:144–150, 2002.